Small-scale turbulence; theory, phenomenology and applications

Physical models for small-scale structures

D.I. Pullin

Graduate Aeronautical Laboratories

California Institute of Technology

Cargèse, August 13-26, 2007

Philip Saffman, Tom Lundgren, Paul O'Gorman

Overview

- Motivation; what can we predict (postdict?)

- Structure-based models of turbulent small scales

- Hills spherical vortex
  - *Longitudinal velocity structure functions*

- Generalized 2-Co-ordinate 3comPonent models (2C-3P)
  - *Burgers vortex tube/sheet*
  - *Stretched spiral vortex (Lundgren)*

- Stretched spiral vortex model of turbulent small scales
  - *Velocity (energy) spectrum*
  - *Scalar (variance) spectrum*
  - *Velocity-gradient/vorticity statistics (1-point)*
  - *Longitudinal velocity structure functions (2-point)*

Modeling Turbulence small scales

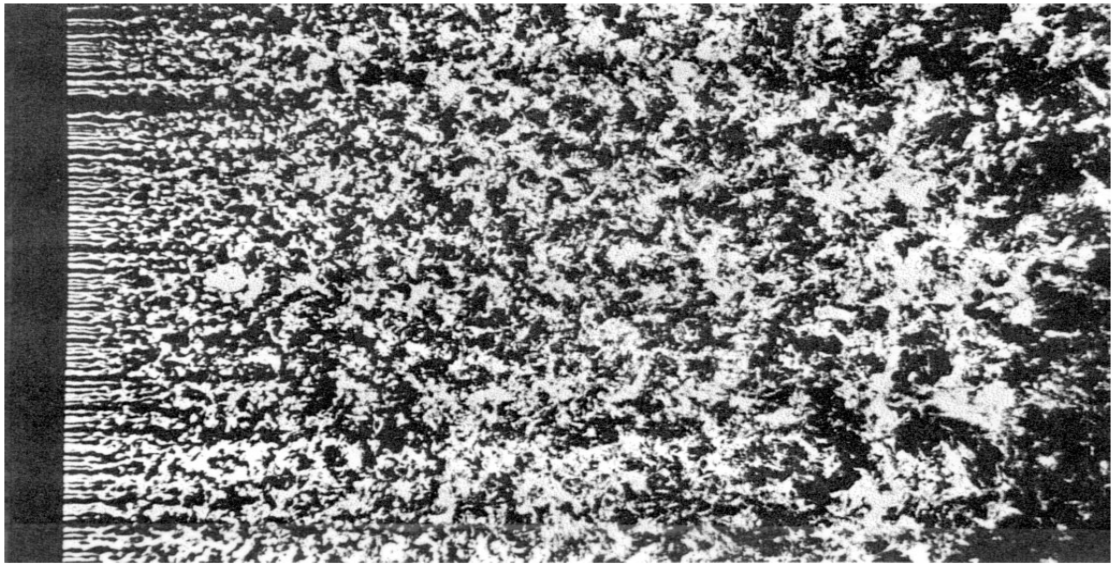

Turbulence forming and decaying downsteam of a grid placed normal to the stream. Corke & Nagib.

Modeling Turbulence small scales

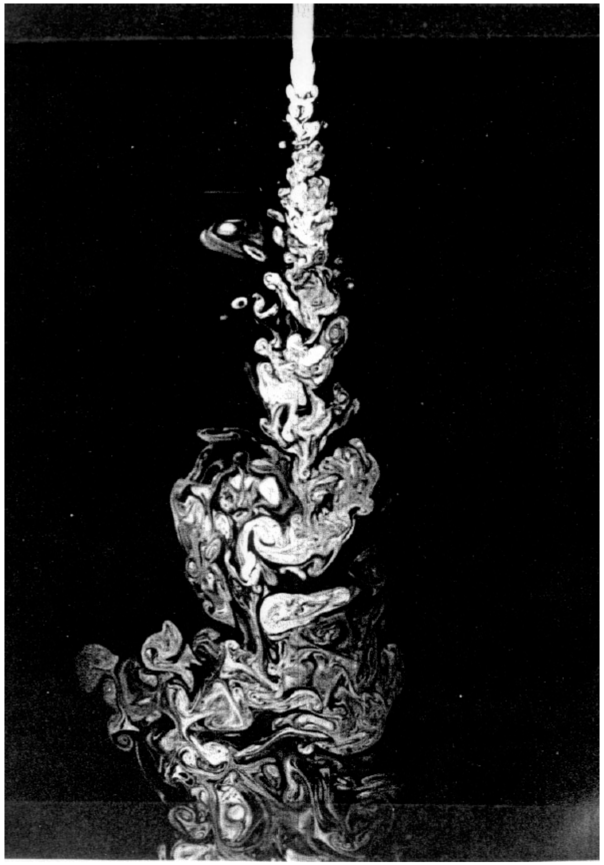

Laser induced fluorescence showing mixing in a turbulent jet.
Dimotakis, Lye & Papantoniou (1981)

Modeling Turbulence small scales

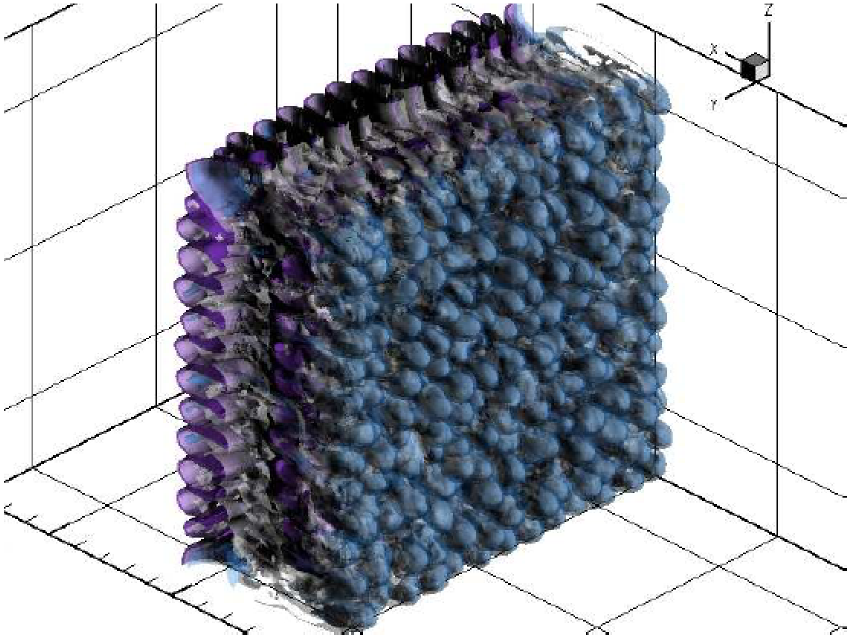

Mixing region in Richtmyer-Meshkov instability

Modeling Turbulence small scales

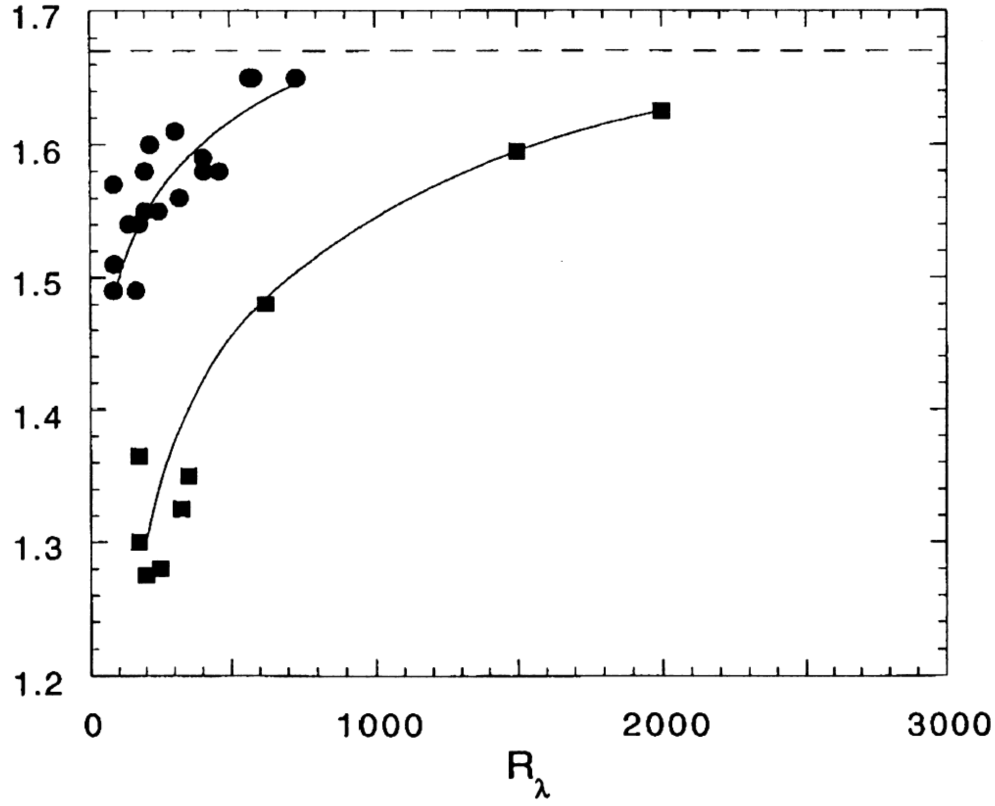

Spectral slope vs Re_λ. • - grid turbulence, (Warhaft, 2000).
■ - Shear turbulence, (Sreenivasan, 1996).

Modeling Turbulence small scales

How does one build ``useful'' analytical models of turbulence small scales?

- Construct general analytical solution of initial-value problem for 3D Navier Stokes equations
  - *Hard (no one has yet done this)!*
  - *May not be very useful for turbulence prediction; one would still need to perform relevant statistics (e.g. Burgers equation)*
- Strong phenomenology. E.G. model turbulence small scales by fractals, fractal systems
  - *No connection with NS dynamics*
  - *Different model for each application*
  - *SGS models for LES (Meneveau, Burton & Dahm)?*
- Structure-based physical models (weak phenomenology)
  - *May be tractable but is there sufficient physics?*
  - *Are assumed structures observed?*
  - *Still need to do statistics*

Structure-based models of turbulence fine scales

- Vortex blobs: Hill's spherical vortex; Synge & Lin (1943), Aivazis, 1997
- 2-Co-ordinate, 3-comPonent (2C-3P) model
  - *Burgers vortex; Burgers (1948), Townsend (1951, Chen, Kambe (1990s)*
  - *Stretched-spiral vortex; Lundgren (1982), Pullin & Saffman (1993), Gilbert (1994,..), Pullin & Lundgren (2001), Okitano (2005)*
- One-point structure tensors; Reynolds and Kassinos (1995)
- Rapid distortion theory; Leonard (2000)

Hills Spherical Vortex; Singe & Lin (1943)

- Model turbulence by ensemble of translating Hills spherical vortices
- Main idea:
  - *Fix two points in space separated by distance r*
  - *Calculate contribution to longitudinal, latitudinal structure functions contributed by HSV of given size, position, and orientation*
- Perform statistics over size, position, orientation with assumed distributions
- Vortices do not interact with each other! Local dynamics.

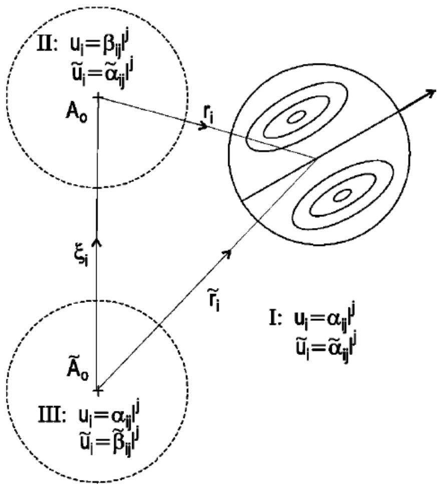

FIG. 1. Case 1: When the vortex diameter is less than the distance between points A_0 and $\tilde{A}_0$, the volume can be partitioned into three distinct regions depending on the relative position of the vortex and the two points.

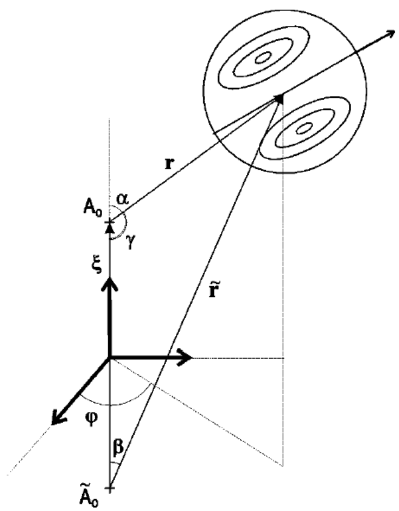

FIG. 3. The toroidal coordinate system. Each point in space is specified by $r=\|\mathbf{r}\|$, $\tilde{r}=\|\tilde{\mathbf{r}}\|$, and the polar angle φ.

Hills Spherical Vortex; Aivazis (PF, 1997)

- Distributions:
  - *Uniform in space, orientation (isotropy)*
  - *Lognormal in size (radii) (Kolmororov, Yaglom)*
  - *Turbulence of vortex blobs. Does not model breakdown process*
- One-parameter model

$$\zeta(u,\sigma)=\begin{cases}\dfrac{(2\pi)^{-1/2}}{\sigma u}\exp\left[-\dfrac{1}{2}\left(\dfrac{\log(u)}{\sigma}\right)^2\right] & (a>0)\\ 0 \quad (a\leqslant 0),\end{cases}$$

$u=a/a_0$, a_0 is a length scale

σ is a dimensionless variance

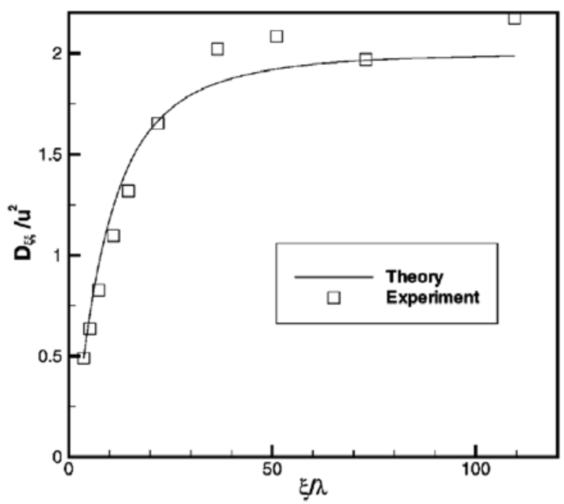

FIG. 7. Normalized second order longitudinal velocity structure function vs normalized separation, Eq. (5.29). Experiment, Tabeling *et al.* (Ref. 17).

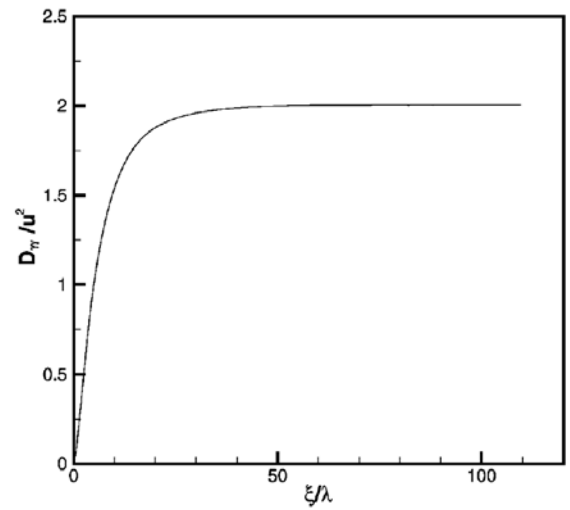

FIG. 8. Normalized second order transverse velocity structure function vs normalized separation, Eq. (5.29).

Higher-order velocity structure functions

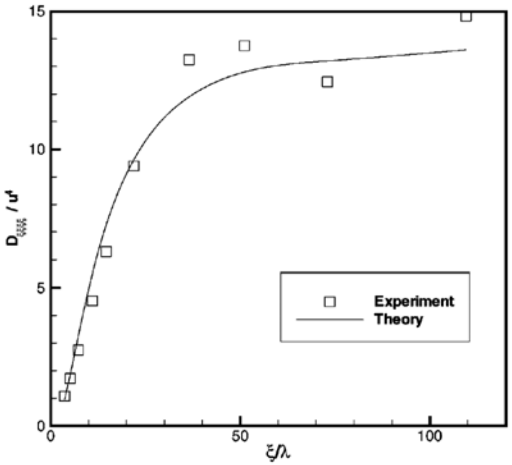

FIG. 9. Fourth order normalized longitudinal velocity structure function vs normalized separation, Eq. (5.36). Experiment, Tabeling *et al.* (Ref. 17).

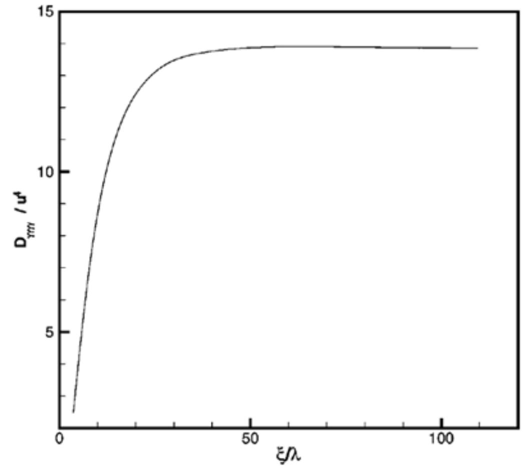

FIG. 10. Fourth order normalized transverse velocity structure function vs normalized separation, Eq. (5.37).

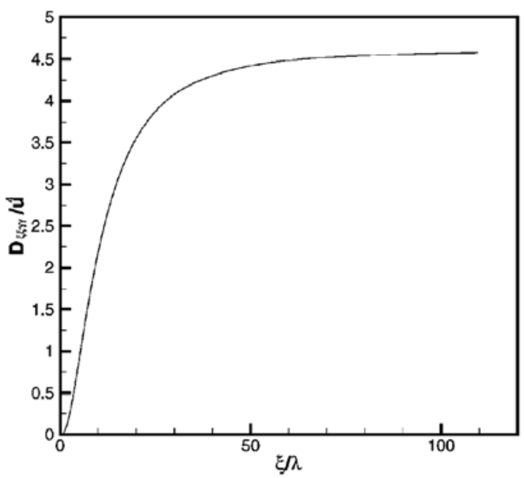

FIG. 11. Fourth order mixed structure function vs normalized separation

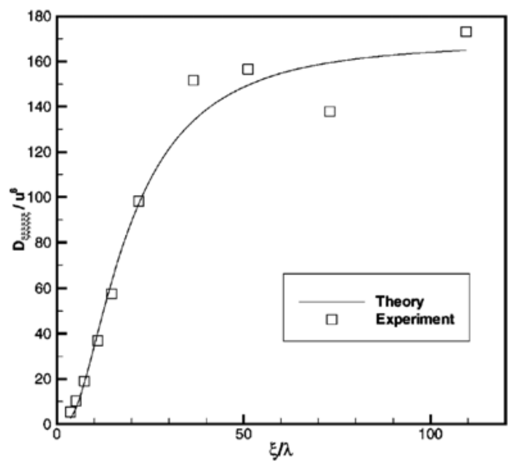

FIG. 12. Sixth order longitudinal velocity structure function. Experiment, Tabeling *et al.* (Ref. 17).

Evidence for existence of tube-like structures

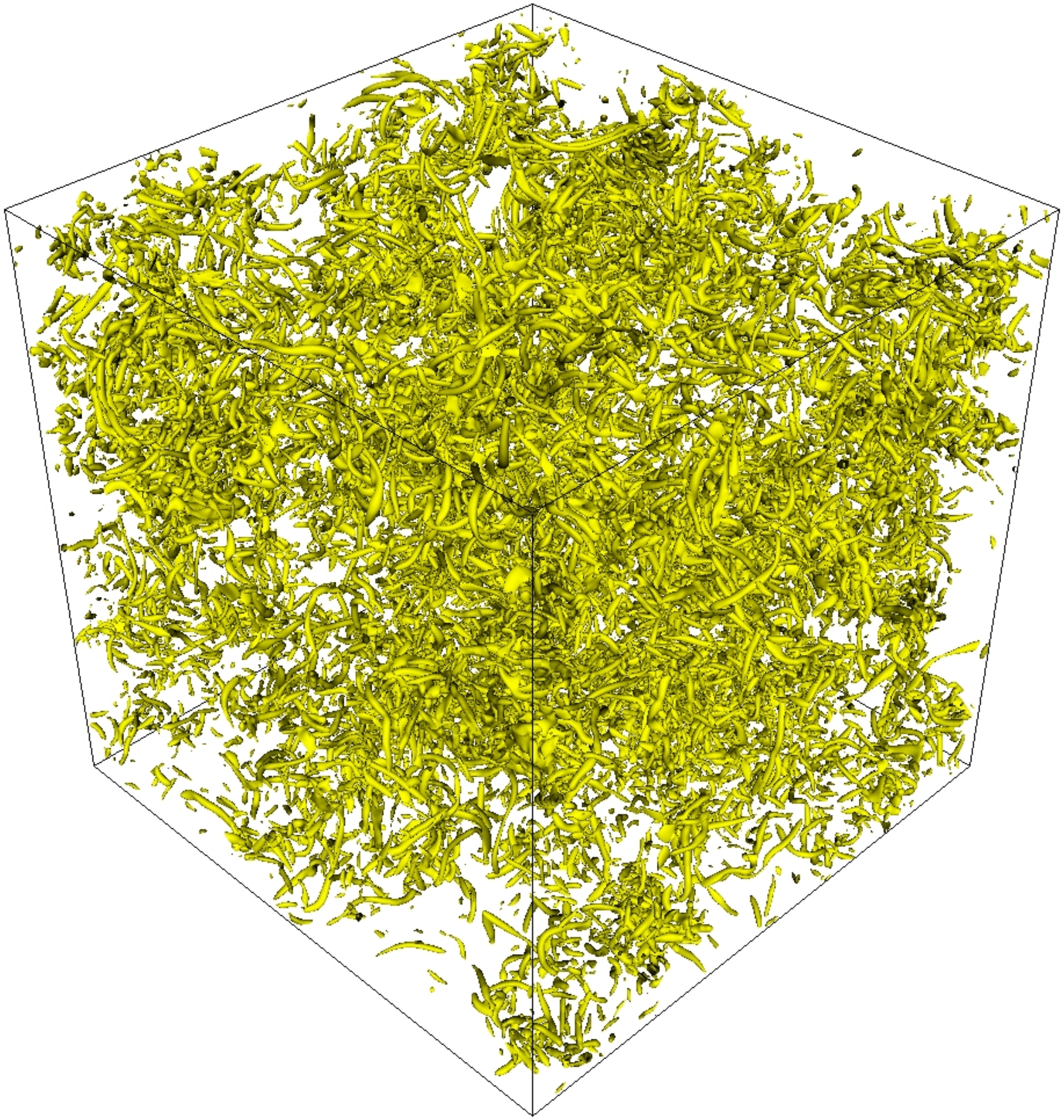

- Ashurst et al (1987)
- Jimenez et al (1993)
- Horiuti DNS data; scale 4

Evidence for existence of tube-like structures

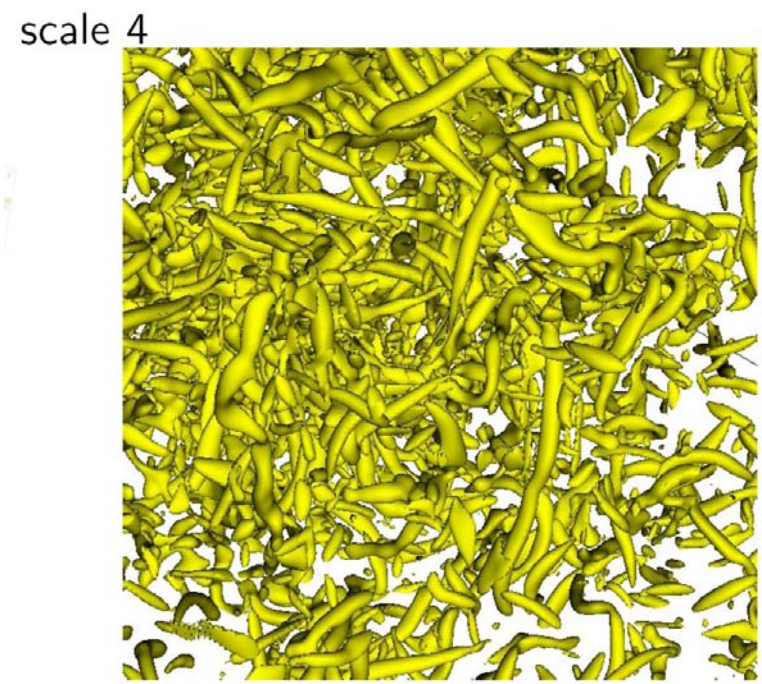

Horiuti DNS data; scale 4 (detail)

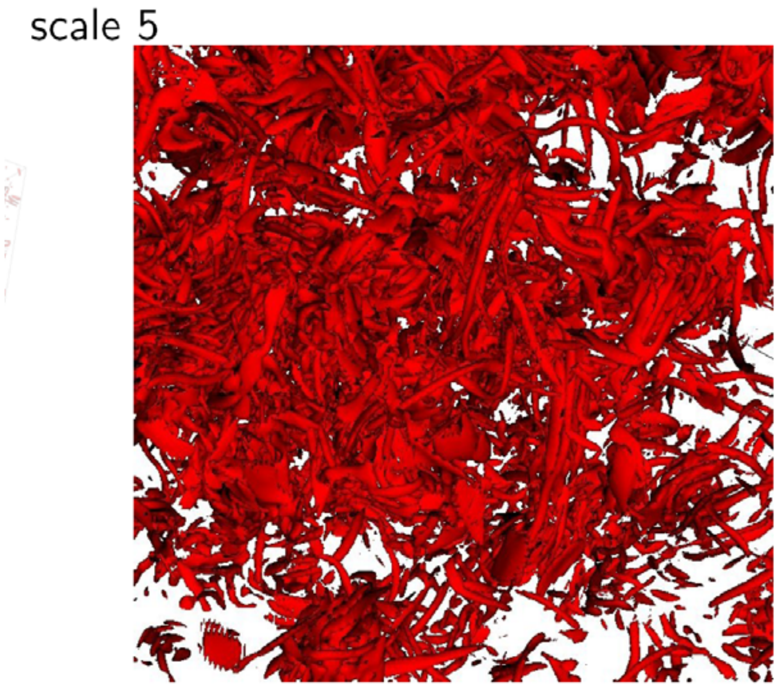

Horiuti DNS data; scale 5 (detail)

Evidence for existence of spiral structures

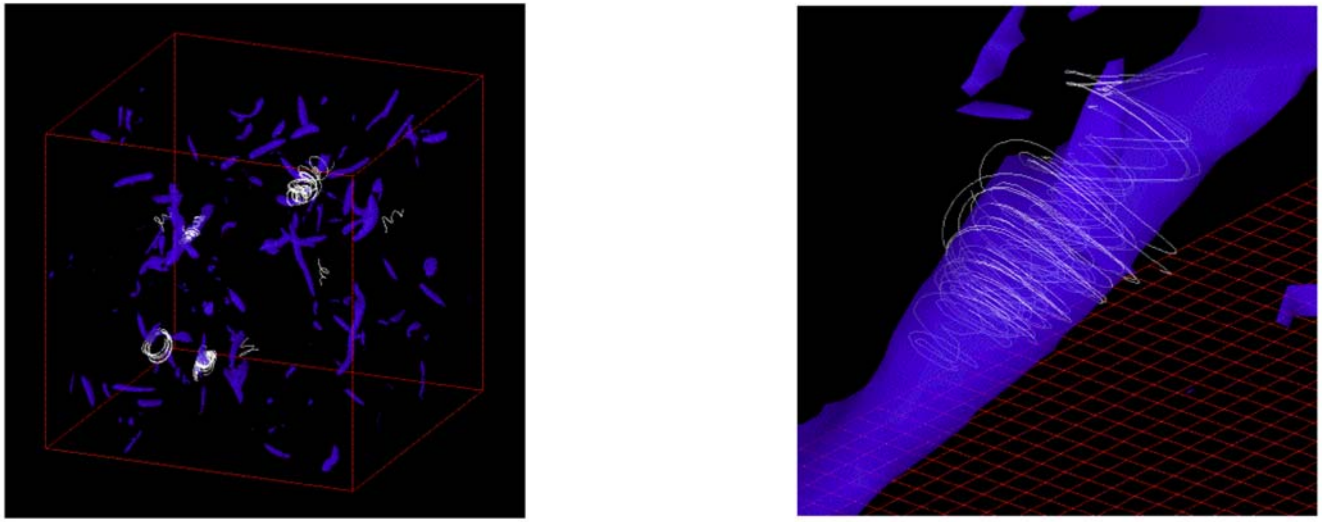

Vortices/particle paths in turbulence. DNS, $R_\lambda = 60$ (Flohr 2002)

- Also: experimental/DNS sightings; Porter *et al.* (1998), Kida & Miura (2000), Brun & Jiménez (2001) [tubes]

Generalized 2C-3P models

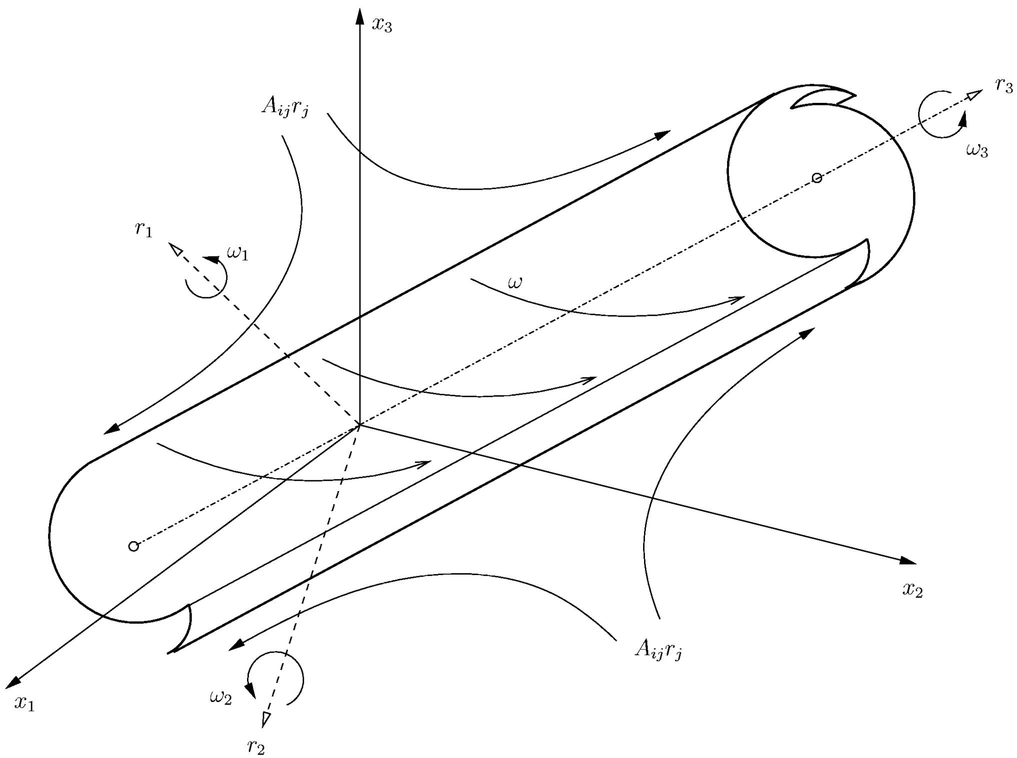

- *Coluar vortex embedded in time varying linear velocity field (outer flow)*
- *velocity field produced by vortex ``cylindrical'': 2-co-ordinate, 3 component*

Generalized 2C-3P models

- *Columnar vortex embedded in time varying linear velocity field (outer flow)*
- *velocity field produced by vortex ``cylindrical'': 2-Co-ordinate, 3 comPonent (2C-3P)*

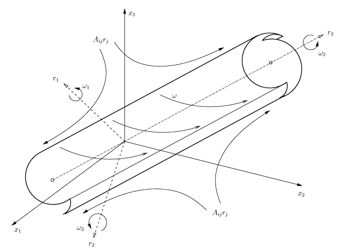

$$\tilde{q}_i = \tilde{A}_{ij}(t)x_j \equiv \tilde{S}_{ij}(t)x_j + \tilde{Q}_{ij}(t)x_j$$

$$\zeta_i(\mathbf{r},t) = \tilde{\xi}_i - 2\Omega_i + \omega_i\,,$$

$$v_i(\mathbf{r},t) = \tilde{A}_{ij}r_j - \varepsilon_{ijk}\Omega_j r_k + u_i$$

$\tilde{Q}_{ij}(t) = \frac{1}{2}\varepsilon_{ijk}\tilde{\xi}_k(t)$ *(Rotation tensor; outer flow)*

$\tilde{S}_{ij}(t)$ *(Rate of strain tensor; outer flow)*

$\tilde{\xi}_i(t)$ *(Uniform background vorticity, outer flow)*

$$\frac{\partial}{\partial t}(v_i + \varepsilon_{ijk}\Omega_j r_k) + v_j\frac{\partial v_i}{\partial r_j} + 2\varepsilon_{ijk}\Omega_j v_k = \frac{\partial P^*}{\partial r_i} + \nu\nabla^2_{r_i} v_i$$

$$\frac{\partial}{\partial t}(\tilde{\zeta}_1 + 2\tilde{\Omega}_i) + v_j\frac{\partial\tilde{\zeta}_i}{\partial r_j} = (\tilde{\zeta}_j + 2\Omega_j)\frac{\partial v_i}{\partial r_j} + \nu\nabla^2_{r_i}\zeta_i$$

Generalized 2C-3P models

$$\Psi = \Psi(r_1, r_2, t),$$
$$u_i = u_i(r_1, r_2, t),$$
$$\omega_i = \omega_i(r_1, r_2, t),$$

(Definition of 2C-3P)

$$u_i = \varepsilon_{ijk} \frac{\partial \Psi_k}{\partial r_j}, \quad \frac{\partial \Psi_i}{\partial r_i} = 0, \quad \omega_i = -\nabla_{r_i}^2 \Psi_i$$

(Vector potential)

$$\Omega_1 = -\widetilde{A}_{23}$$
$$\Omega_2 = \widetilde{A}_{13}$$
$$\Omega_3 = -\widetilde{A}_{12}$$

$$\Longrightarrow \quad \frac{\partial e_i}{\partial t} = e_j \widetilde{A}_{ij} - e_i e_k e_j \widetilde{A}_{kj}$$

(Evolution of vortex axes)

Generalized 2C-3P models

- *Axial vorticity equation (plus 2 other vorticity equations):*

$$\frac{\partial \hat{\omega}_3}{\partial t} + \left(\tilde{S}_{11}\, r_1 + \frac{\partial \Psi_3}{\partial r_2}\right) \frac{\partial \hat{\omega}_3}{\partial r_1} + \left(2\tilde{S}_{12}\, r_1 + \tilde{S}_{22}\, r_2 - \frac{\partial \Psi_3}{\partial r_1}\right) \frac{\partial \hat{\omega}_3}{\partial r_2}$$

$$= \quad 2\, \tilde{S}_{13}\, \hat{\omega}_1 + 2\, \tilde{S}_{23}\, \hat{\omega}_2 + \tilde{S}_{33}\, \hat{\omega}_3 + \nu\, \nabla^2_{r_i}\, \hat{\omega}_3$$

$$\hat{\omega}_3 = \omega_3(r_1, r_2, t) + \tilde{\xi}_i(t)$$

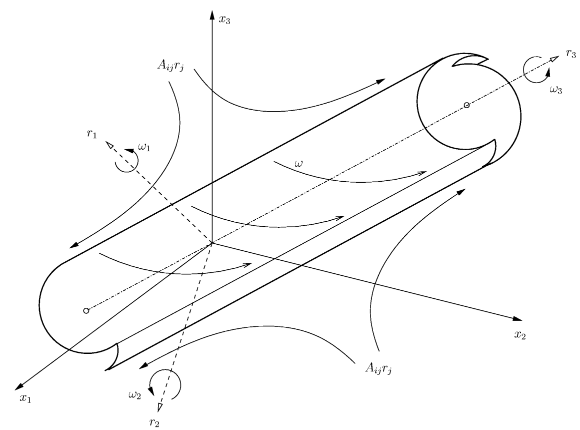

- *Many special cases possible: e.g.*

$$\omega_1 = \omega_2 = 0 \ \text{ at } t = 0, \qquad \tilde{\xi}_i = 0$$

$$\frac{\partial \omega_3}{\partial t} + \left(\tilde{S}_{11} r_1 + \frac{\partial \Psi_3}{\partial r_2}\right) \frac{\partial \omega_3}{\partial r_1} + \left(2\tilde{S}_{12} r_1 + \tilde{S}_{22} r_2 - \frac{\partial \Psi_3}{\partial r_1}\right) \frac{\partial \omega_3}{\partial r_2} = \tilde{S}_{33}\omega_3 + \nu \nabla^2_{r_i} \omega_3$$

- *Describes Burgers vortex sheet and tube. Stretched-spiral vortex*

Stretched-Vortex Models of Turbulent Fine Scales

- Townsend (1951), Lundgren (1982), Pullin& Saffman (1993), Pullin & Lundgren (2001)
- Turbulence consists of an ensemble of stretched ``vortex tubes'' (cylindrical 2C-3P) structures
- Vortex tube axis direction random on unit sphere (isotropy)
- Mutual vortex-vortex interaction not modeled
- At each time t, each tube is a different point in its unsteady evolution
- Turbulence statistics:
  - *<volume integral> = <time integral> over lifetime of tube (ergodic hypothesis)*
  - *Average over all vortex axis orientation*
- Class of tractable models

Burgers vortex tube (Burgers, 1948)

- Steady axisymmetric solution of axial vorticity equation

$$\omega_0(r) = \frac{a\Gamma_0}{4\pi\nu}\exp\left(-\frac{r^2 a}{4\nu}\right)$$

- Energy (velocity) spectrum for turbulence modeled by an ensemble of Burgers vortices (Townsend, 1951)

$$\frac{E}{(\epsilon\nu^5)^{1/4}} = \frac{2C}{k\eta}\exp(-2Ck^2\eta^2)$$

- No cascade dynamics or inertial range

Spiral-vortex models (2C-3P)

- *Several Generic Spiral types*

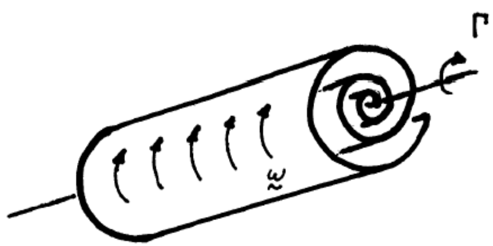

Pearson-Abernathy/Moore spiral

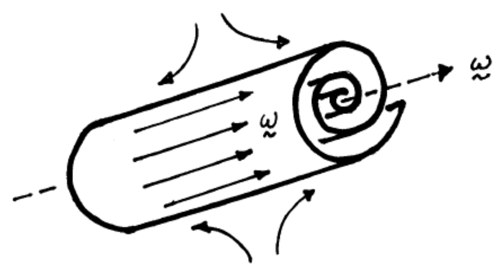

Lundgren spiral

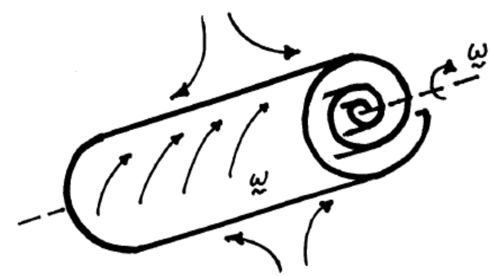

"Mixed" spiral

Stretched-spiral Vortex (Lundgren, 1982)

- Asymptotic solution of Navier-Stokes equations

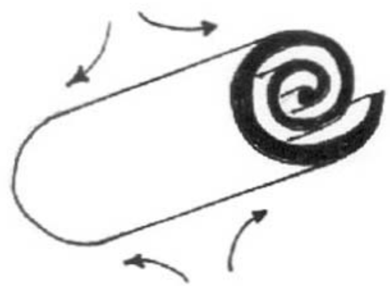

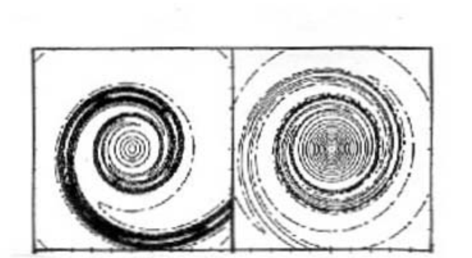

t_1 $\qquad$ $t_2 > t_1$

$$\tilde{\omega}_3(r,\theta,t) = \mathrm{e}^{at} \sum_{\infty}^{\infty} f_n(r)\, \mathrm{e}^{in[\theta-\Omega(r)\,t]-\nu\, n^2 \Lambda(r)^2\, t^3/3}$$

- Velocity (energy) spectrum $E(k) \sim k^{-5/3}$

Stretched-spiral vortex; velocity (energy) spectral dynamics

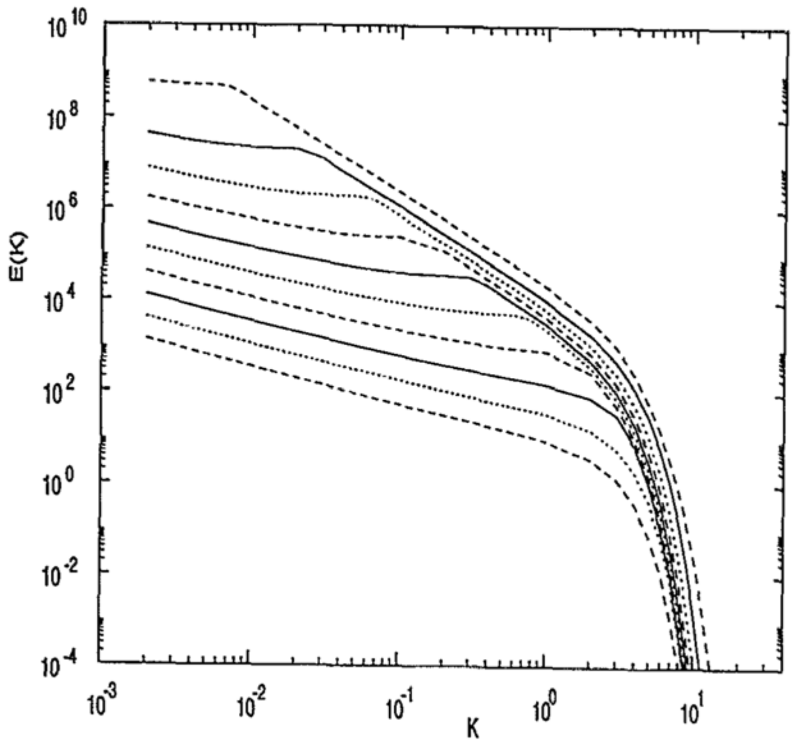

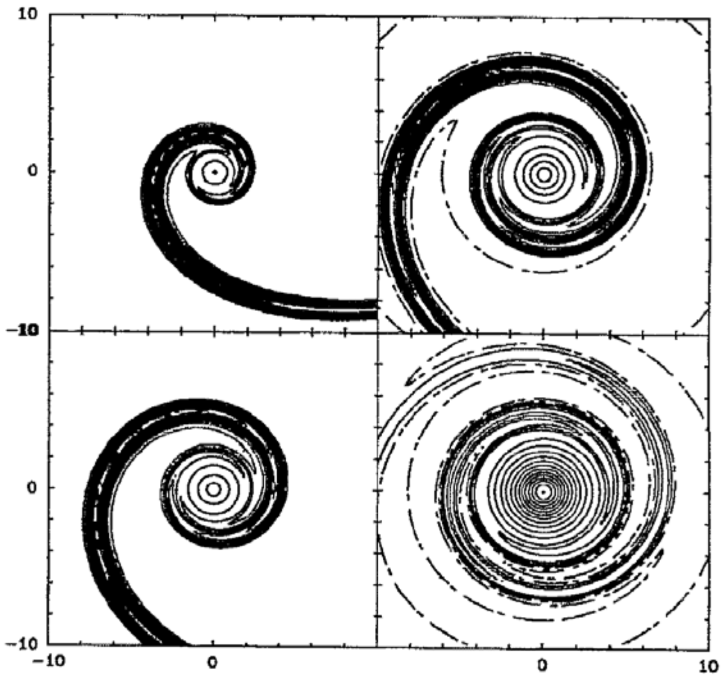

- *Time-evolving spectrum*
- *Early time; k^(-2) (sheet-like)*
- *Late time: k^(-1) (tube like)*
- *k^(-5/3) is time average*

- *time increasing, top-> bottom, left-> right*
- *Sheet-> tube transition*
- *Cascade is extraction of energy from outer linear flow*

Phenomenology of scalar spectra

- Obukov-Corrsin spectrum

$$E_c(k) \sim \epsilon_c\, \epsilon^{-1/3}\, k^{-5/3}, \qquad L^{-1} << k << \left(\frac{\nu^3}{\epsilon}\right)^{-1/4}$$

- Batchelor spectrum

$$E_c(k) \sim \epsilon_c\, \nu^{1/2}\, \epsilon^{-1/2}\, k^{-1}, \qquad \left(\frac{\nu^3}{\epsilon}\right)^{-1/4} << k << \left(\frac{D^2\, \nu}{\epsilon}\right)^{-1/4}$$

- Range of scales

$$\frac{L}{\left(\frac{D^2\, \nu}{\epsilon}\right)^{1/4}} \sim Re^{3/4}\, Sc^{1/2}, \qquad Sc = \frac{\nu}{D} \quad \text{(Schmidt number)}$$

Scalar transport equation

- Scalar convected and diffused within stretched vortex

- Solve axial vorticity equation and passive scalar convection/diffusion equation inside stretched vortex

Axial vorticity

$$\frac{\partial \tilde{\omega}_3}{\partial t} + \frac{1}{\rho}\left(\frac{\partial \tilde{\psi}_3}{\partial \theta}\frac{\partial \tilde{\omega}_3}{\partial \rho} - \frac{\partial \tilde{\psi}_3}{\partial \rho}\frac{\partial \tilde{\omega}_3}{\partial \theta}\right) = \nu \nabla_2^2 \tilde{\omega}_3, \qquad \nabla_2^2 \tilde{\psi}_3 = -\tilde{\omega}_3$$

Passive scalar

$$\frac{\partial c}{\partial t} + \frac{1}{\rho}\left(\frac{\partial \tilde{\psi}_3}{\partial \theta}\frac{\partial c}{\partial \rho} - \frac{\partial \tilde{\psi}_3}{\partial \rho}\frac{\partial c}{\partial \theta}\right) = D \nabla_2^2 c$$

Solution of Transport Equation

- $\tilde{\omega}_3$, $\tilde{\psi}_3$ obtained from solution of axial vorticity equation. E.G. diffusing line vortex, Burgers vortex, stretched-spiral vortex
- Two-time analysis

Fast time variable $\quad \Omega\tau,$

Slow time variables $\quad T_\nu = (\nu\,\Lambda^2)^{1/3}\tau$

$\qquad T_D = (D\,\Lambda^2)^{1/3}\tau, \qquad \Lambda = \frac{d\Omega}{d\rho}$

- Seek solution of form

$$\tilde{\psi}_3 = \tilde{\psi}^{(0)}(\rho, T_\nu) + \tau^{-2} \sum_{-\infty, n\neq 0}^{\infty} \tilde{\psi}_n^{(2)}(\rho, T_\nu)\, \exp\left(i\, n(\theta - \Omega\,\tau)\right) + ..$$

$$c = \sum_{-\infty}^{\infty} \left(\phi_n^{(0)}(\rho, T_\nu, T_D) + \tau^{-1}\, c_n^{(1)}(\rho, T_\nu, T_D) + ..\right) \exp\left(i\, n(\theta - \Omega\,\tau)\right)$$

Evolution of scalar field inside vortex

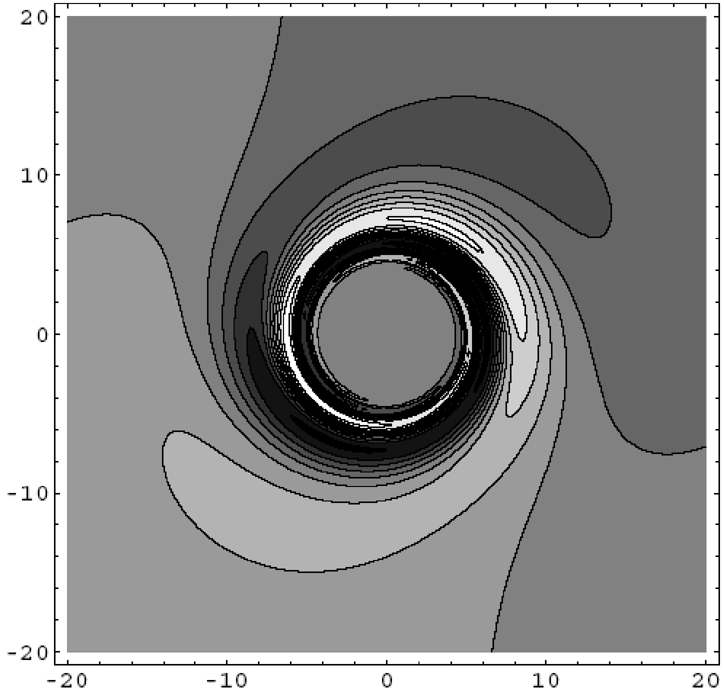

“Wrapping” of a linear scalar field by a diffusing line vortex.

$a = 0$ (no axial stretching). $\Gamma_0/(2\,\pi\,\nu) = 1000$.

Scalar variance spectrum

$$E_c(k) \;=\; E_c^{(0)}(k) \quad + \quad E_c^{(1)}(k)$$

- $E_c^{(0)}(k)$ component

$$E_c^{(0)}(k) = \frac{2}{3}\, a^{-1}\, \epsilon_c^{(0)}\; k^{-1}\; \exp\left(-\frac{2\, D\, k^2}{3\, a}\right)$$

- $a = \frac{1}{\sqrt{15}} \left(\frac{\epsilon}{\nu}\right)^{1/2} \to \mathcal{A} = 2\sqrt{15}/3, \qquad \eta_b = \left(\frac{D^2\, \nu}{\epsilon}\right)^{1/4}$

$$E_c^{(0)}(k) = \mathcal{A}\, \nu^{1/2} \epsilon^{-1/2}\, \epsilon_c^{(0)}\; k^{-1}\; \exp\left(-\mathcal{A}\, k^2\, \eta_b^2\right)$$

- $E_c^{(1)}(k)$ component

$$E_c^{(1)}(k) \;=\; \mathcal{C}_1(k)\, k^{-5/3}\, \exp\left(-\frac{D\, k^2}{3\, a}\right)$$

Scalar Variance Spectrum

- Initial structure

$$\omega_3(r,\theta,0) = 2f_0\, g(r)\sin(2\theta), \qquad c(r,\theta,0) = 2\,c_0\, g(r)\cos\theta$$

- $E_c = E_c^{(0)} + E_c^{(1)}$, strain : $a = \left(\frac{\epsilon}{15\nu}\right)^{1/2}$

$$E_c^{(0)} = 2.58\,\epsilon_c\,\nu^{1/2}\,\epsilon^{-1/2}\,k^{-1}\exp(-2.58 S_c^{-1}\,(k\eta)^2)$$

$$E_c^{(1)} = \frac{4.71}{(\Gamma/\nu)^{1/3}}\epsilon_c\;\epsilon^{-1/3}\,k^{-5/3}\,\exp(-2.58\,(2 + S_c^{-1})\,(k\eta)^2)$$

Scalar Variance Spectrum

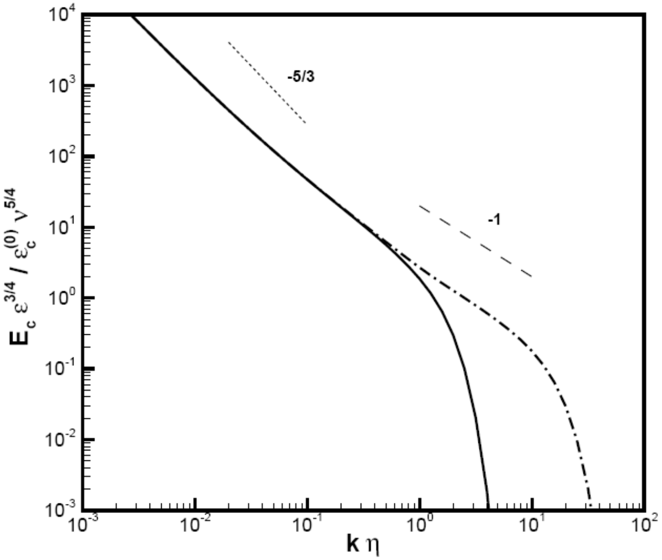

3-D Scalar spectrum. $Sc = 7$. $Sc = 700$. $\frac{\Gamma}{\nu} = 10^3$

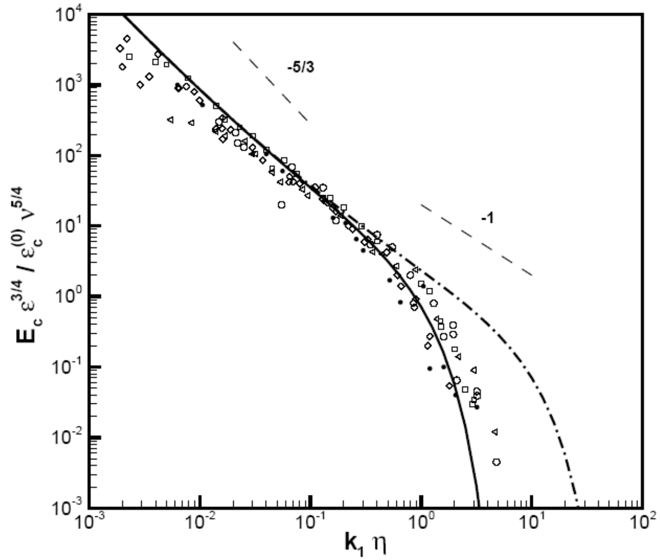

1-D Scalar spectrum. $Sc = 7$. $Sc = 700$. $\frac{\Gamma}{\nu} = 10^3$
Symbols, Data, Gibson & Schwarz (1963)

Modeling Turbulence small scales

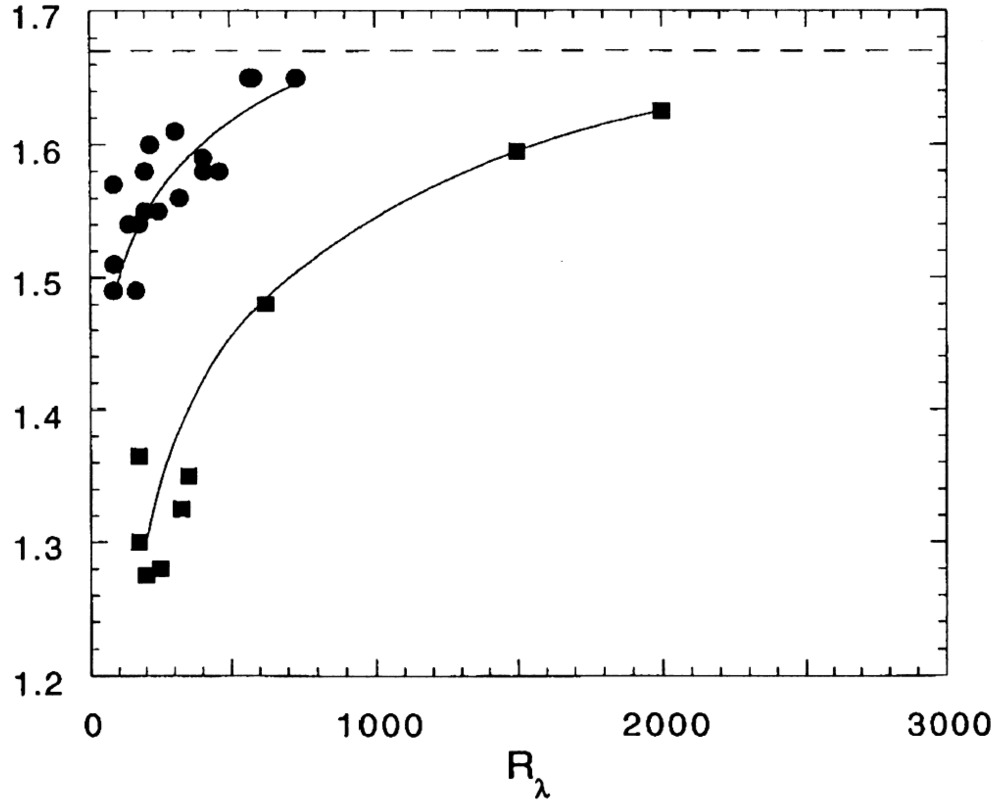

Spectral slope vs Re_λ. • - grid turbulence, (Warhaft, 2000).
■ - Shear turbulence, (Sreenivasan, 1996).

Velocity-Scalar co-spectrum

- Velocity field $u(x, t)$, scalar field $c(x, t)$
- Velocity-scalar cross-spectrum $C_{uc}(k)$ measures velocity-scalar correlations
- Important for small-scale turbulent transport of scalars, SGS scalar-flux models
- Homogeneous turbulence in presence of mean scalar gradient
- $C_{uc}(k) \sim k^{-7/3}$, Lumley (1967)

Velocity-Scalar co-spectrum
(P. O'Gorman)

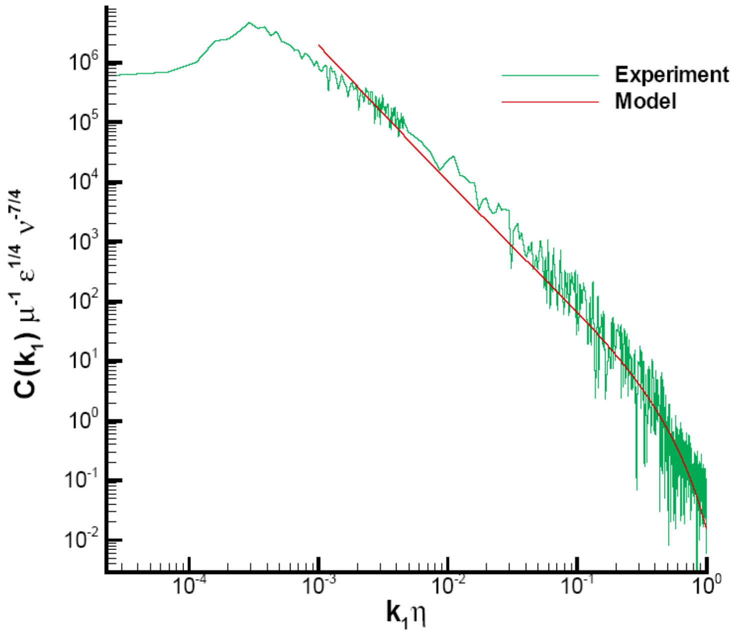

Cospectrum of u_3 and c. Expt.; Mydlarski and Warhaft (1998)

Spectral Exponents

Quantity	SSV		"Classical"	
velocity	$-5/3$		$-5/3$	Kolmogorov
pressure	$-7/3$		$-7/3$	Obukov
scalar	-1		-1	Batchelor
scalar	$-5/3$		$-5/3$	Obukov-Corrsir
scalar-velocity	$-5/3$,	$-7/3$	$-7/3$	Lumley
(vorticity)^2	0		?	

Spectral exponents postdicted by stretched-spiral vortex

Velocity-gradient and vorticity statistics

- *Fix point and direction in space (relative to lab axes)*
- *Assume isotropy*
- *Calculate longitudinal velocity gradient at point within vortex structure in terms of local principal rates of strain*
- *Average over Euler angles (vortex axis) and vortex cross-section in space, from known internal vortex structure (SSV)*

$$\left\langle \left(\frac{\partial u}{\partial x}\right)^n \right\rangle = \frac{1}{4\pi} \int_0^{2\pi} \int_0^{\pi} (e_1 \sin^2\phi \cos^2\chi + e_2 \sin^2\phi \sin^2\chi + e_3 \cos^2\phi)^n \times \sin\phi \, d\phi \, d\chi,$$

$$\left\langle \left(\frac{\partial u}{\partial x}\right) \right\rangle = 0,$$

$$\left\langle \left(\frac{\partial u}{\partial x}\right)^2 \right\rangle = \frac{2(e_1^2 + e_2^2 + e_3^2)}{15},$$

$$\left\langle \left(\frac{\partial u}{\partial x}\right)^3 \right\rangle = \frac{8(e_1 e_2 e_3)}{35},$$

$$\left\langle \left(\frac{\partial u}{\partial x}\right)^4 \right\rangle = \frac{8(e_1^4 + e_2^4 + e_3^4)}{105},$$

- *Result; moments of velocity gradient and vorticity pdfs as functions of order 2*p, p≥ 2, and Taylor Re*

$$F_{2p} = \hat{F}_{2p} R_\lambda^{p/2-3/4}, \quad S_{2p+1} = -\hat{S}_{2p+1} R_\lambda^{p/2-3/4}$$

$$G_{2p} = \hat{G}_{2p} R_\lambda^{p/2-3/4}$$

Velocity-gradient statistics; flatness, p = 2

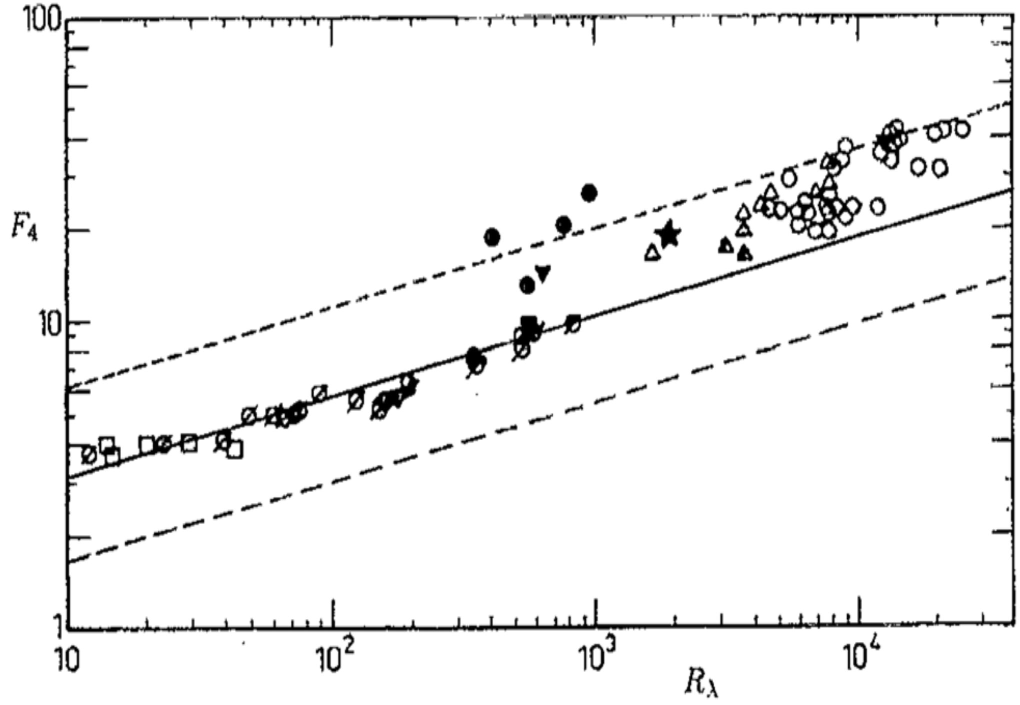

FIG. 4. Flatness factor F_4 vs R_λ. ---: $\phi=0.35$; ——: $\phi=0.475$; – – –: $\phi=0.7$. Symbols are a compilation of experimental data, Van Atta and Antonia[19] (reproduced with permission).

Longitudinal velocity structure functions

- Longitudinal velocity structure function of order m

$$B_m(r) = \overline{\overline{(u'_p - u_p)^m}}$$

- 2C-3P models; 5-dimensional integral as a function of separation r
- Monte-Carlo numerical integration
- Results for stretched-spiral vortex (PF, 1996)
- Agreement with experiment poor for large m

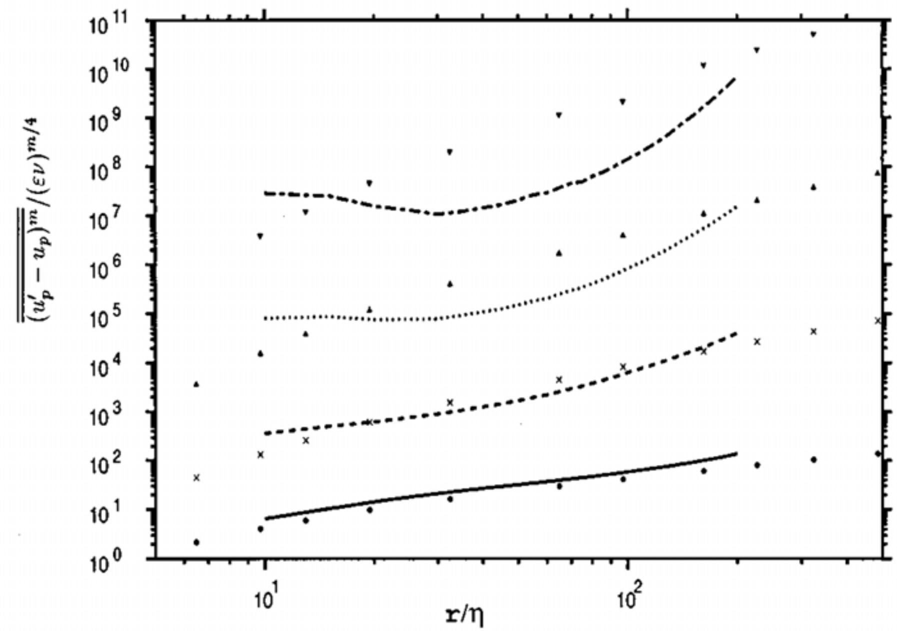

FIG. 4. Longitudinal velocity structure functions $\overline{\overline{(u'_p - u_p)^m}}/(\epsilon\nu)^{m/4}$ for the stretched-spiral vortex versus r/η, Monte Carlo, $R_\lambda=500$. — $m=2$, --- $m=4$, ··· $m=6$, -·- $m=8$: Symbols—experiment, Tabeling (Ref. 11), $R_\lambda=507$. Circles $m=2$, crosses $m=4$, up-triangles $m=6$, down-triangles $m=8$.

Structure-based models of turbulence small scales

- Velocity/vorticity field based on assumed vortex structure; HSV, Burgers vortex, SSV
  - *Requires solutions (approximate?) to Euler/NS*
  - *Complex integrations for statistics*

- Stretched-spiral vortex (Lundgren, 1982)
  - *Unifies Kolmogorov, Obukov-Corrsin/Batchelor, Lumley spectra*
  - *Good results for velocity-gradient/vorticity statistics (1-point)*
  - *Firm experimental/DNS evidence; open question?*

- Problems:
  - *Poor results for higher-order velocity structure functions (2-point)*
  - *Contains internal parameters (e.g. circulation etc.) not easily related to outer flow variables*

- Basis for subgrid-scale modeling?

Small-scale turbulence; theory, phenomenology and applications

Stretched vortices as basis for SGS modeling

D.I. Pullin

Graduate Aeronautical Laboratories

California Institute of Technology

Cargèse, August 13-26, 2007

Ashish Misra, Tobias Voelkl

Overview

- Motivation; why LES?
- Expectations of LES. Some present models.
- Stretched-vortex sub-grid scale model
  - *Structure-based SGS model (2C-3P)*
  - *SGS stresses*
  - *SGS vortex orientations*
- Example Applications
  - *Decaying incompressible turbulence*
  - *Channel flow at moderate Re_\tau*
- Subgrid-flux model for passive scalar
  - *Overholt-Pope test*

Why LES?

Table 2. Characteristics of some representative channel-flow simulations.

Re_τ	L_x/δ	L_z/δ	Points	Year
180	12	6	5 M	1987 [11]
590	6	3	40 M	1997 [12]
550	25	12	600 M	2001 [13]
950	25	9	4 G	2003 [14]
1 900	3	1.5	450 M	2003 [14]
10 000	12	6	900 T	2015?

- Jimenez (JOT, 2003)

Large-Eddy Simulation

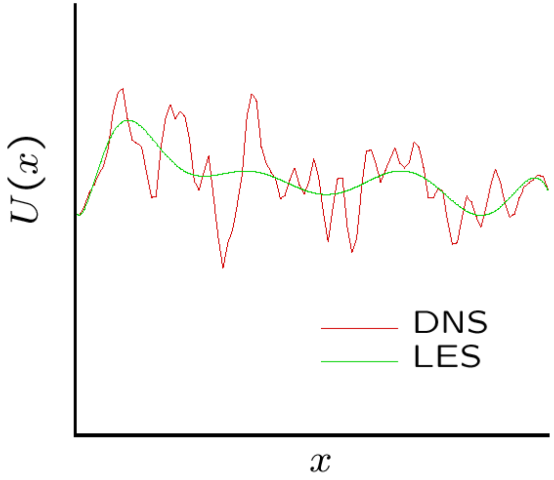

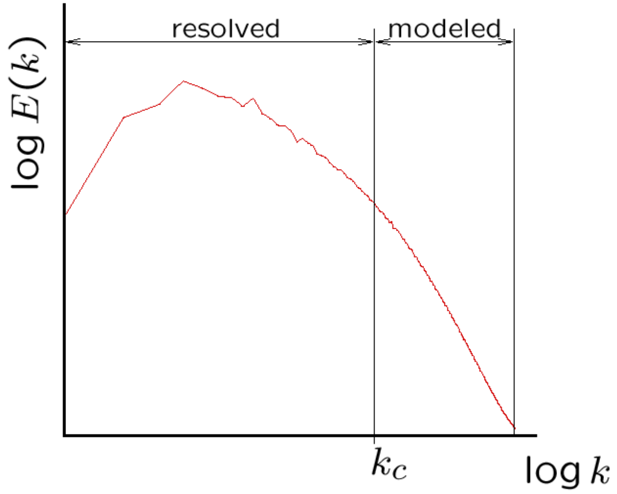

physical space: fine-scale fluctuations not resolved, their influence is modeled.

spectral space: resolved range, $k < k_c$ (cutoff wavenumber k_c), subgrid range $k > k_c$.

LES and SGS modeling

- LES equations

$$\frac{\partial \tilde{U}_i}{\partial t} + \frac{\partial}{\partial x_j}\left(\tilde{U}_i \tilde{U}_j\right) = -\frac{\partial \tilde{P}}{\partial x_i} - \frac{\partial T_{ij}}{\partial x_j} + \nu \frac{\partial^2 \tilde{U}_i}{\partial x_j \partial x_j} + F_i$$

  Large-eddy simulation (LES) makes modeling assumptions;

- $T_{ij} = \widetilde{U_i U_j} - \tilde{U}_i \tilde{U}_j$; Subgrid stresses are replaced by some model T_{ij}: subgrid stress (SGS) model:

  $T_{ij} = T_{ij}[\widehat{U}_j, \partial \widehat{U}_i / \partial x_j, ...]$

- $\tilde{U}_j \rightarrow \widehat{U}_j$; Filtered field $\tilde{U}_j$ is modeled by a computed under-resolved field $\widehat{U}_j$.

What can (should) we expect from LES?

- Robustness for different flows at large Re
- One-point statistics (velocity, density, concentration)
- Two-point statistics across full wavenumber range?
- Predictive for turbulent mixing
- Estimates for full turbulent fields
  - *Not just the 'filtered' part*
  - *Multiscale LES*
- Knowledge of Reynolds number; what is it?
- Fast convergence to DNS
  - *In some cases DNS is not available*
  - *DNS not possible for compressible turbulence containing strong shocks*

SGS models

- Smagorinsky
- Dynamic Smagorinsky (CTR, Germano)
- Eddy-viscosity structure function (Lesieur)
- Scale-similarity (Bardina)
- MILES (Boris,Grinstein))
- Approximate deconvolution model (Leonard, Adams)
- Optimal LES (Adrian, Moser)
- Stretched-vortex subgrid model

Explicit SGS model; stretched-vortex model

512^3 DNS (scale 4)

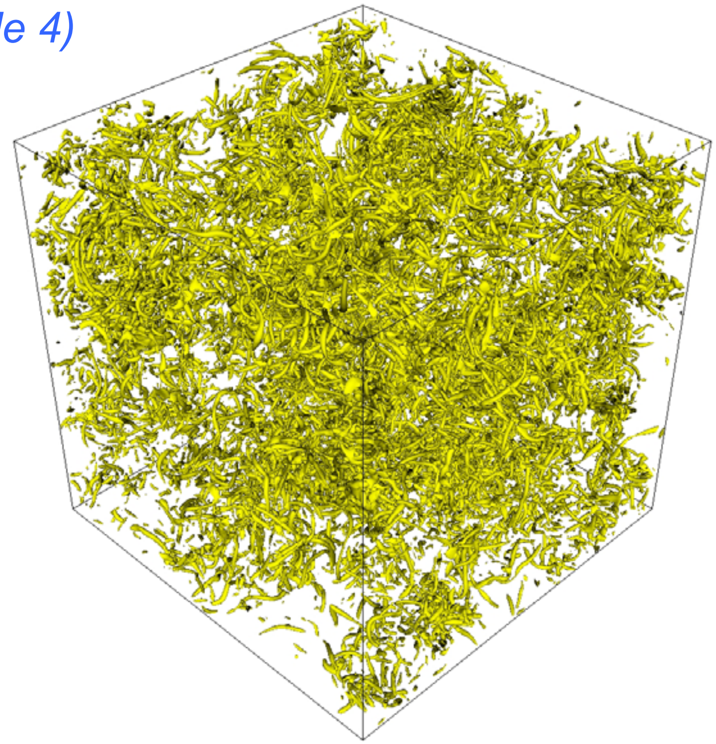

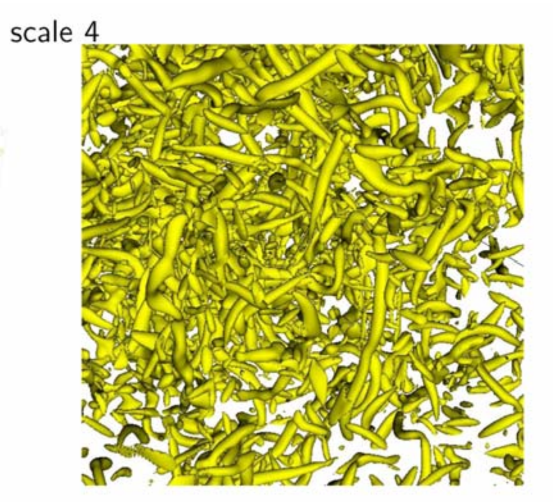

- *Small scales of turbulence Intense vorticity in form of ``worms''*

  Ashurst, Jimenez et al (1993)

- *Can this be used as a basis of a stucture-based sub-grid scale model?*

Explicit SGS model; stretched-vortex model

- Structure-based approach
- Subgrid motion represented by nearly axisymmetric vortex tube within each cell
- Local solution of NS equations for stretched spiral vortex
  - *Lundgren (1982), Pullin & Lundgren (2001)*
- Subgrid transport:

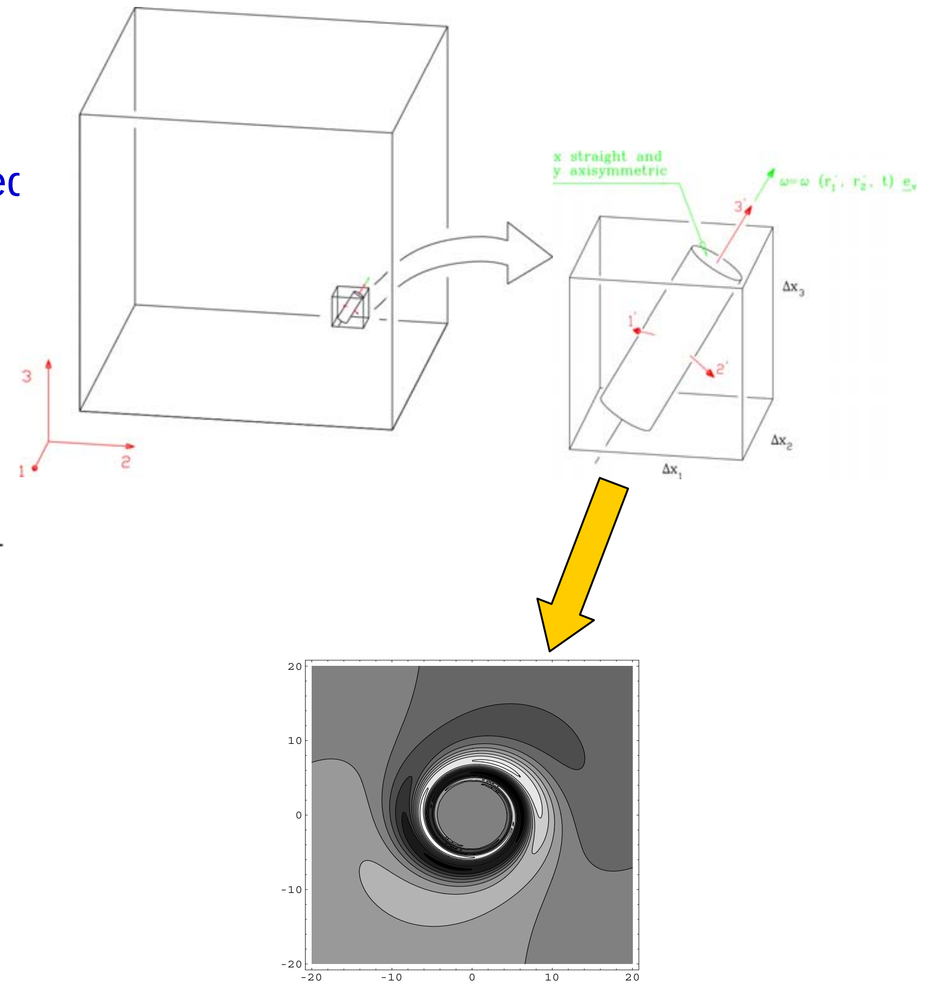

$$
\begin{aligned}
\tau_{ij} &= \overline{\rho}\tilde{K}(\delta_{ij} - e_i^v e_j^v) \\
q_i^T &= -\overline{\rho}\frac{\triangle_c}{2}\tilde{K}^{1/2}(\delta_{ij} - e_i^v e_j^v)\frac{\partial(\tilde{c}_p\tilde{T})}{\partial x_j} \\
q_i^\psi &= -\overline{\rho}\frac{\triangle_c}{2}\tilde{K}^{1/2}(\delta_{ij} - e_i^v e_j^v)\frac{\partial\tilde{\psi}}{\partial x_j} \\
\tilde{K} &= \int_{k_c}^{\infty} E(k)dk, \qquad k_c = \pi/\Delta_c
\end{aligned}
$$

Model parameters

- Subgrid energy spectrum (Lundgren, 1982)

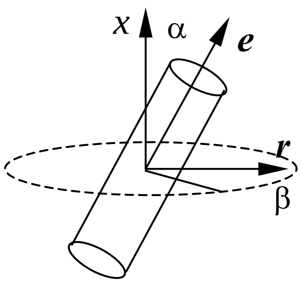

$$E(k) = \mathcal{K}_0 \epsilon^{2/3} k^{-5/3} \exp[-2k^2\nu/(3|\tilde{a}|)]$$

$$\tilde{a} = \tilde{S}_{ij} e_i^v e_j^v, \qquad \tilde{S}_{ij} = \frac{1}{2}\left(\frac{\partial \tilde{u}_i}{\partial x_j} + \frac{\partial \tilde{u}_j}{\partial x_i}\right)$$

- Parameters obtained from resolved-scale velocity structure-functions

$$\mathcal{K}_0 \epsilon^{2/3} = \frac{\overline{\mathcal{F}_2}(\triangle)}{\triangle^{2/3}\mathrm{A}}, \qquad \mathrm{A} = 4\int_0^\pi s^{-5/3}(1 - s^{-1}\sin s)ds \approx 1.90695$$

$$\overline{\mathcal{F}_2}(\triangle) = \frac{1}{6}\sum_{j=1}^{3}\left(\delta \tilde{u}_1^{+\,2} + \delta \tilde{u}_2^{+\,2} + \delta \tilde{u}_3^{+\,2} + \delta \tilde{u}_1^{-\,2} + \delta \tilde{u}_2^{-\,2} + \delta \tilde{u}_3^{-\,2}\right)_j,$$

- Subgrid vortex orientation, ***e***
  - λ *: fraction aligned with principal extensional eigenvector of resolved rate-of-strain tensor (corresponding eigenvalue,* λ_3*)*
  - (1- λ) *: fraction aligned with resolved vorticity vector,* $\boldsymbol{\omega}$ (*Misra & Pullin 1997*)

$$\lambda = \frac{\lambda_3}{\lambda_3 + \|\boldsymbol{\omega}\|}$$

Decay of homogeneous turbulence

- 32^3 LES of decaying turbulence; R_\lambda = 70 (PF, 1997)
- Data; Comte-Bellot & Corssin (1971)

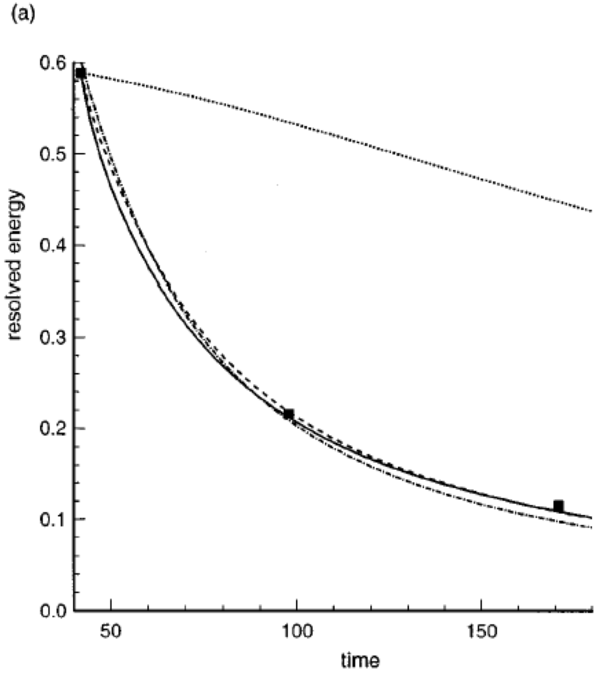

Resolved-scale energy

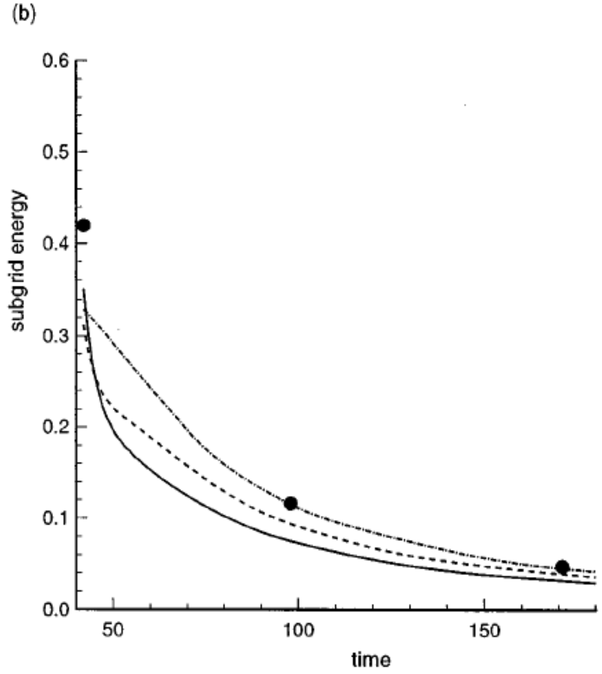

Subgrid-scale-scale energy

Decay of homogeneous turbulence

- 32^3 LES of decaying turbulence; R_\lambda = 70 (PF, 1997)
- Data; Comte-Bellot & Corssin (1971)

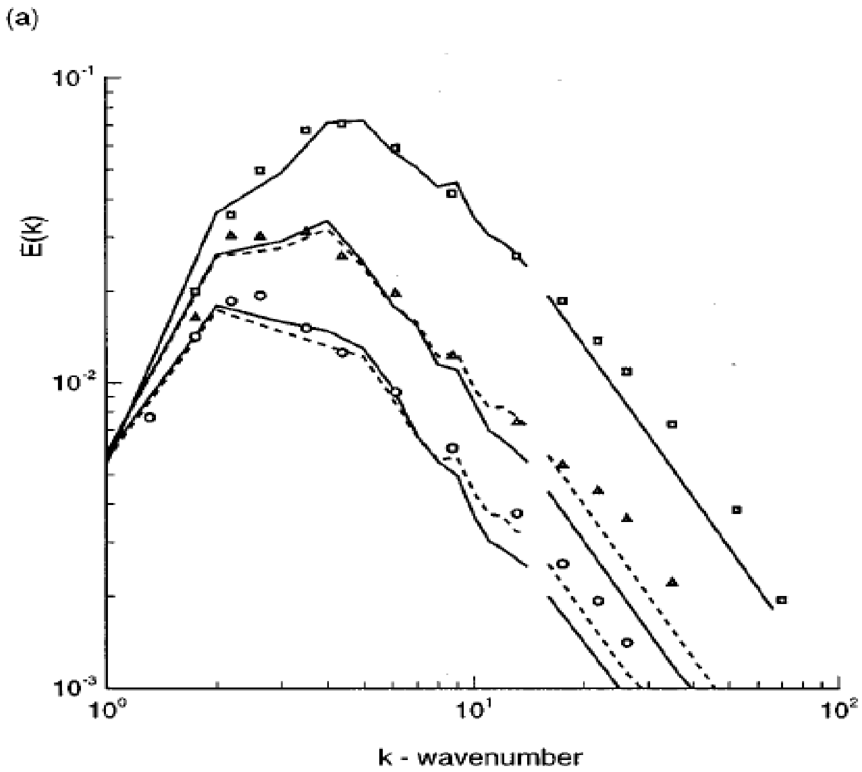

Velocity (energy) spectrum

LES of turbulent channel flow

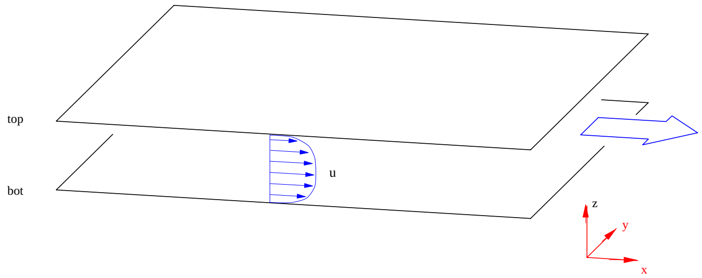

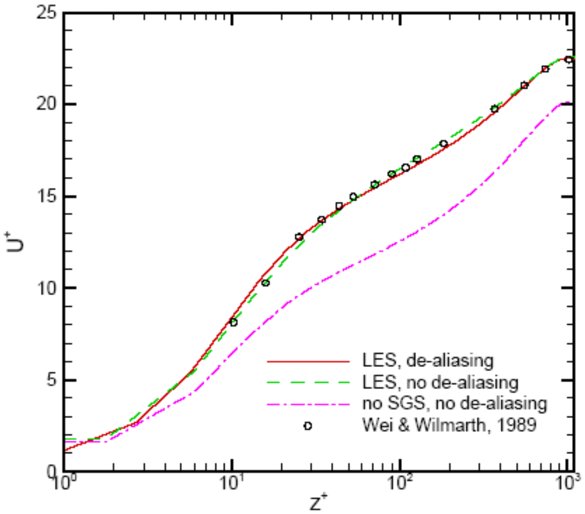

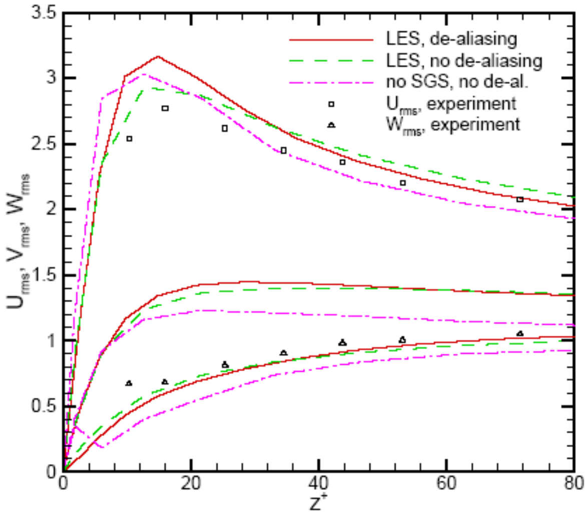

Domain size: $2.5\pi\delta \times \pi\delta \times 2\delta$,
effective resolution: $48 \times 64 \times 65$.

LES of turbulent channel flow

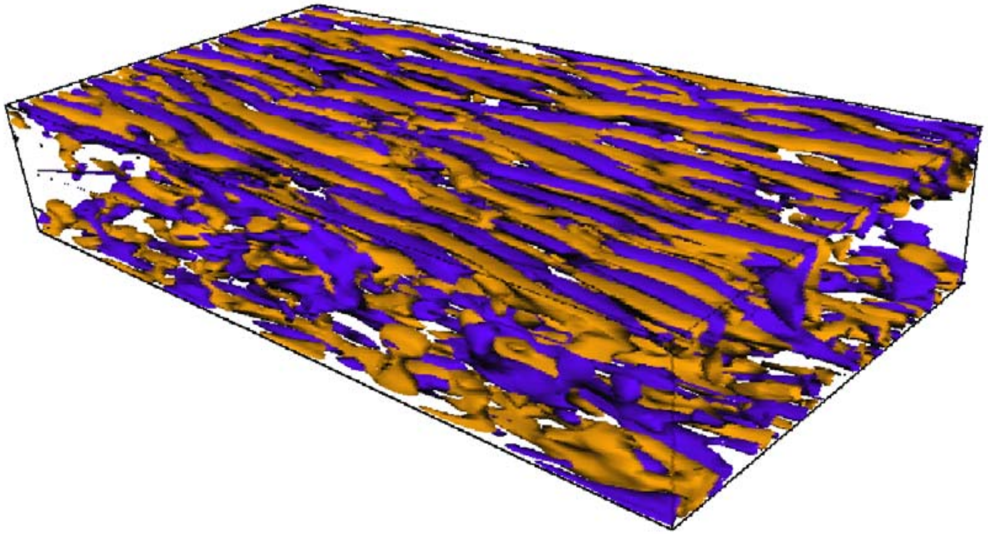

$Re_\tau = 180$, $\omega_z = 15u_\tau/h$ (purple)
and $\omega_z = -15u_\tau/h$ (yellow)

Rotating channel flow

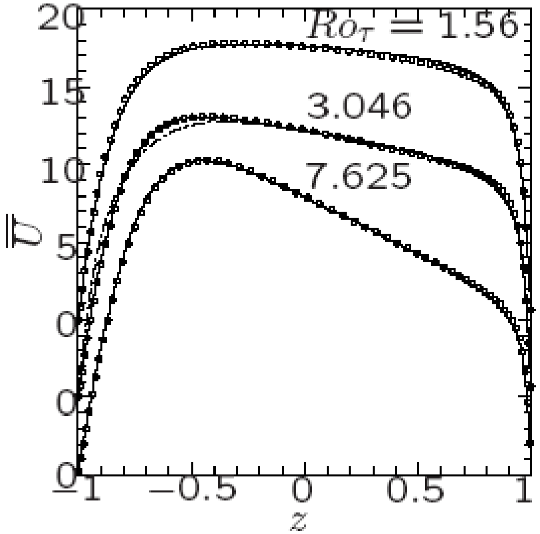

Resolution: $48 \times 64 \times 43$ (DNS: $128 \times 128 \times 128$)

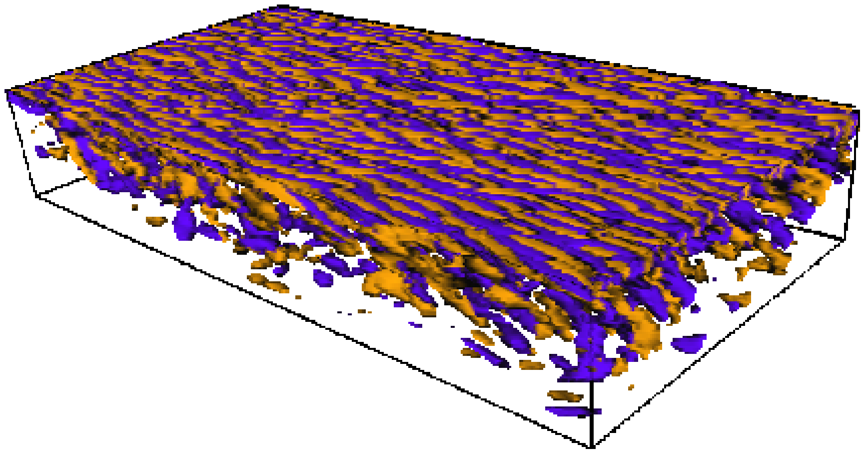

$Ro_\tau = 7.625$, $\omega_z = \pm 15 u_\tau / h$

SGS model for subgrid flux of a passive scalar

- Filtered equation for a passive scalar ϕ is

$$\frac{\partial \tilde{\phi}}{\partial t} + \frac{\partial}{\partial x_j}\left(\tilde{\phi}\tilde{U}_j\right) = -\frac{\partial g_j}{\partial x_j} + D\frac{\partial^2 \tilde{\phi}}{\partial x_j \partial x_j}$$

$$g_j = \widetilde{\phi U_j} - \tilde{\phi}\tilde{U}_j$$

g_j is the subgrid flux of ϕ by the turbulent velocity field.

- We model g_j by the winding of $\tilde{\phi}$ field by an *axisymmetric* model subgrid vortex

SGS model for subgrid flux of a passive scalar

- Subgrid velocity field. Scalar convection equation

$$u_\theta = r\,\Omega(r), \qquad u_r = u_{x'_3} = 0, \qquad \frac{\partial \phi}{\partial t} + \Omega(r)\,\frac{\partial \phi}{\partial \theta} = 0$$

$$\phi(r,\theta,t) = r\cos[\theta - \Omega\,t]\left(\frac{\partial \tilde{\phi}}{\partial x'_1}\right) + r\sin[\theta - \Omega\,t]\left(\frac{\partial \tilde{\phi}}{\partial x'_2}\right) + \text{background}$$

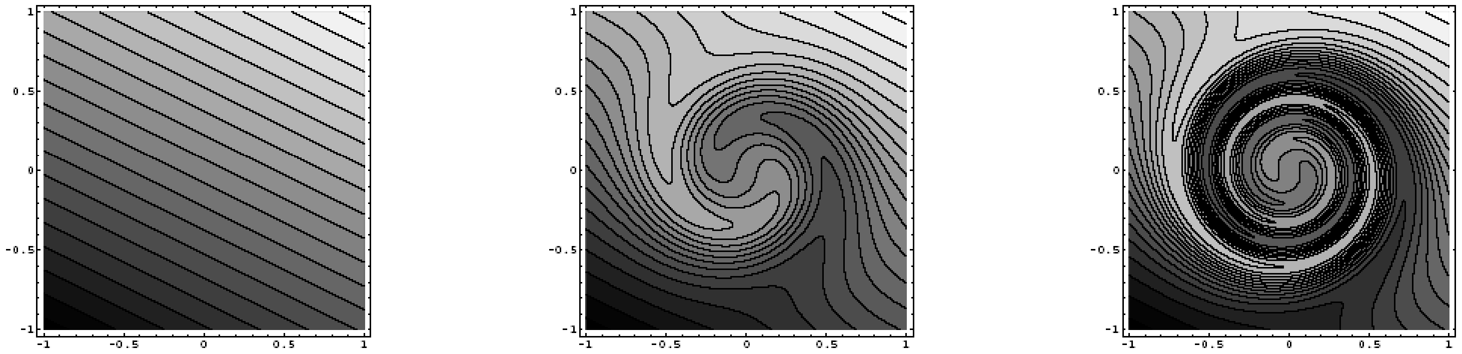

SGS model for subgrid flux of a passive scalar

- Average over cylinder, $R_1 = \Delta$, stiring time T and pdf of Γ

$$g_1' + i\, g_2' = \frac{1}{\pi R_1^2 T} \int_{-\infty}^{\infty} \int_0^{2\pi} \int_0^{R_1} \int_0^{T} \phi(r,\theta,t)\, i\, u_\theta\, \mathrm{e}^{i\theta}\, p(\Gamma)\, d\theta\, r dr\, dt\, d\Gamma$$

- In laboratory co-ordinates

$$g_j = -\frac{1}{2} K\, T\, (\delta_{jp} - e_j^v\, e_p^v)\, \frac{\partial \tilde{\phi}}{\partial x_p}, \qquad K = \frac{1}{R_1^2} \int_0^{R_1} r^3\, \Omega^2(r)\, dr$$

- Assume $T = \gamma \Delta x / K^{1/2}$. Argument based on scalar, velocity structure functions then gives

$$\gamma = \frac{2}{\pi\, \beta} \left(\frac{2}{3\mathcal{K}_0} \right)^{1/2}, \quad \mathcal{K}_0 = 1.67, \quad \beta = 0.67 \rightarrow \gamma = 0.74$$

SGS model for subgrid flux of a passive scalar

- Scalar flux subgrid model - tensor diffusivity

$$
\begin{aligned}
g_i &= -\frac{\gamma\,\pi}{2\,k_c} K^{\frac{1}{2}} (\delta_{ip} - e_i^v\, e_p^v)\, \frac{\partial \tilde{\phi}}{\partial x_p} \\
\text{SGS} \quad T_{ij} &= K\,(\delta_{ij} - e_i^v e_j^v)
\end{aligned}
$$

- Model parameter $\gamma = 1$ (present demonstration)

- Model appropriate for $Sc = \nu/D = O(1)$

- Model suggests scalar gradient is orthogonal to small scale vorticity (Ruetsch & Ferziger, DNS, 1997).

Passive scalar with imposed mean scalar gradient in forced homogeneous turbulence

- Forced turbulence in $(2\pi)^3$ box (32^3). $\tilde{\phi} = \alpha_1 x_1 + \hat{\phi}$

$$\frac{1}{2}\frac{\partial}{\partial t}\left\langle \hat{\phi}^2 \right\rangle + \alpha_1 \left\langle \hat{\phi}\, \tilde{U}_1 \right\rangle = \left\langle g_i \frac{\partial \hat{\phi}}{\partial x_i} \right\rangle - D \left\langle \left(\frac{\partial \hat{\phi}}{\partial x_i} \right)^2 \right\rangle$$

- α_1 is preserved by the evolution

- Statistical steady state for $\left\langle \hat{\phi}^2 \right\rangle$

- DNS, $R_\lambda = 27-180$ [Overholt and Pope, **Phys Fluids**, 1996]

Passive scalar with imposed mean scalar gradient in forced homogeneous turbulence

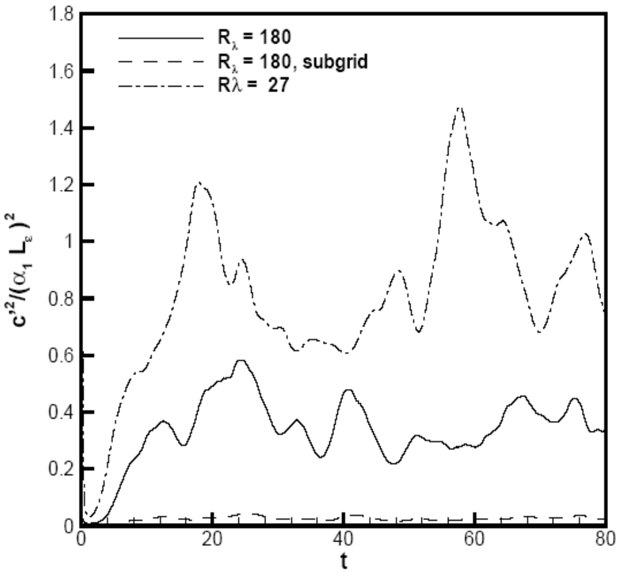

Scalar variance $<\phi'^2>/(\alpha_1 L_\epsilon)^2$ versus t. $Sc = 0.7$
$L_\epsilon = u'^3/\epsilon$, $T_L = L/u' \approx 2.2$

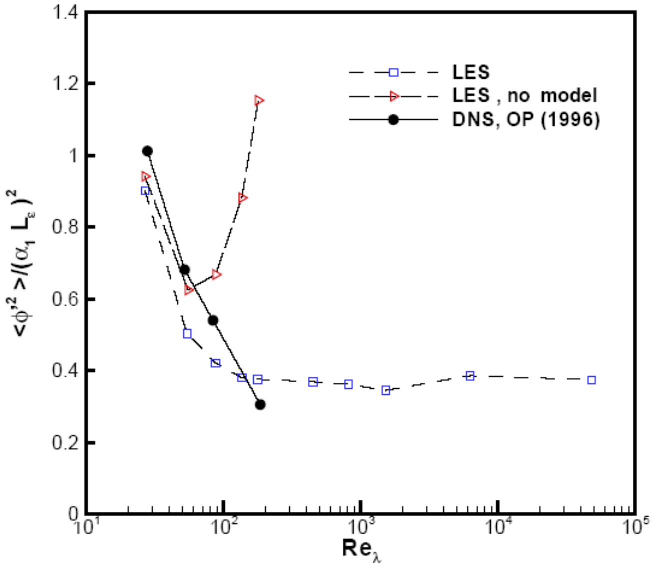

Scalar variance, 32^3 LES compared to
DNS - Overholt & Pope (1996), $32^3 - 256^3$. $Sc = 0.7$.

Stretched-vortices for SGS modeling

- Structure-based sub-grid-scale model for LES
- Uses stretched-spiral vortex as subgrid vorticity element
- 2-point SGS statistics known (spectrum, structure function)
- Uses second order velocity structure functions to dynamically determine model parameters
- Need model for SGS vortex orientations
- Good performance for standard LES tests; decaying turbulence and channel flow at moderate Reynolds number
- Problems:
  - *Each new/different SGS physics problem requires new analysis*
  - *Contains internal parameters (e.g. circulation etc.) not easily related to outer flow variables. Not needed for simple SGS momentum/scalar flux modeling but may be important for more complex SGS physics.*
- Promise; may admit SGS extension of some turbulence statistics, i.e. multi-scale modeling.

Small-scale turbulence; theory, phenomenology and applications

Large-eddy simulation with stretched-vortex SGS model

D.I. Pullin

Graduate Aeronautical Laboratories

California Institute of Technology

Cargèse, August 13-26, 2007

Carlos Pantano, David Hill, Ralf Deiterding, Daniel Chung

Ravi samtaney, Branko Kosovic

Overview

- LES of compressible, shock-driven turbulence
  - *Extension of SGS model to compressible flow*
  - *Issues of numerical methodology*
  - *Adaptive Mesh Refinement (AMR)*

- LES of Richtmyer-Meshkov instability with re-shock
  - *Growth of mixing layer thickness*
  - *Resolved-scale turbulence statistics*
  - *Multi-scale modeling; subgrid extension of turbulence statistics*
  - *Effect of magnetic field*
  - *Cylindrical RM instability*

- Near-wall SGS modeling
  - *No large eddies near the wall*
  - *Local inner scaling and near-wall modeling*
  - *Virtual-wall model*
  - *LES of channel flow at large Re_\tau*

LES of compressible turbulence. LES and strong shocks (D. Hill, C. Pantano, R. Deiterding).

- SGS models need extension to deal with compressible flow
- Standard LES methodology not well suited to LES of shock-driven turbulence
  - *Numerical methods for shock-capturing and LES `orthogonal'.*
    - *LES with explicit SGS model requires dissipation-free numerical scheme*
    - *Shock-capturing numerical schemes are essentially SGS models for shocks; they are generally extremely numerically dissipative even away from shocks.*
- Owing to its largely hyperbolic character, gas-dynamic turbulence can benefit greatly from Adaptive-Mesh-Refinement (AMR) technology

SAMR and AMROC (R. Deiterding)

- Structured Adaptive Mesh Refinement (SAMR)
- Adaptive Mesh Refinement Object Oriented C++ (AMROC)
- Berger & Colella's algorithm for conservation laws of the form:

$$\frac{\partial \boldsymbol{q}}{\partial t} + \frac{\partial}{\partial x_k} \boldsymbol{f}^k(\boldsymbol{q}) = 0,$$

- Hierarchical data structure contains the solution vector and fluxes
- On each patch, a standard Cartesian fluid solver is applied to march the solution (e.g. WENO/TCD)
- Boundary conditions and synchronization between patches is accomplished by filling ghost cells with interpolated data.
  - *ghost cell interpolation is an approximation for non-linear systems of equations*

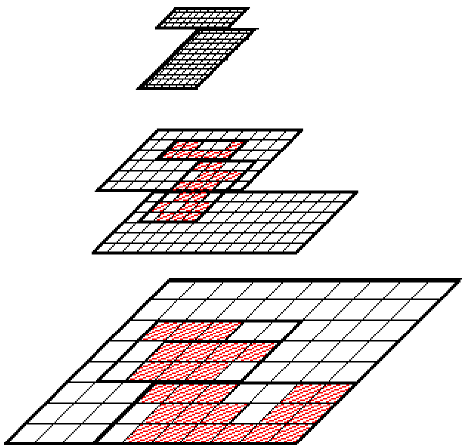

Figure 1. AMR hierarchy.

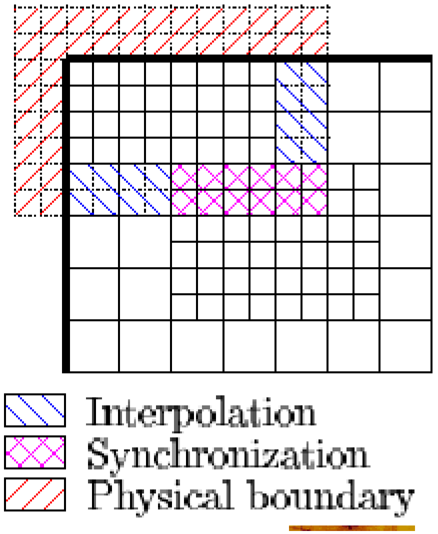

LES of compressible turbulence. LES and strong shocks (D. Hill). Hybrid WENO-TCDS algorithm:

- Numerical methods for shock-capturing and LES `orthogonal'.
- Our solution: hybrid technique: blending Weighted Essentially Non-Oscillatory (WENO) scheme with Tuned Centered-Difference (TCD) stencil.
- WENO in regions of very-large density ratio (Shocks)
  - *But WENO is not suitable for LES in smooth regions away from shocks.*
  - *Upwinding strategy is too dissipative*
- TCD stencil in smooth regions away from shocks
  - *Low numerical dissipation (centered method)*
  - *optimized for minimum resolved-scale discretization error in LES (Ghosal, 1996)*
  - *5- or 7-point stencil trades off formal order of accuracy for small dispersion errors*
- Target WENO stencil = TCD stencil
- In practice, target TCD stencil not always achieved; switch is used based on acceptable WENO smoothness measure
- Hybrid method designed for LES in presence of strong shocks

Test I; decay of compressible homogeneous turbulence

- 256^3 DNS of compressible decaying turbulence. Fully resolved (R. Samtaney)
- 10-th order compact Pade scheme
- R_lambda ~70, M_t = 0.49 (shocklets in turbulence)

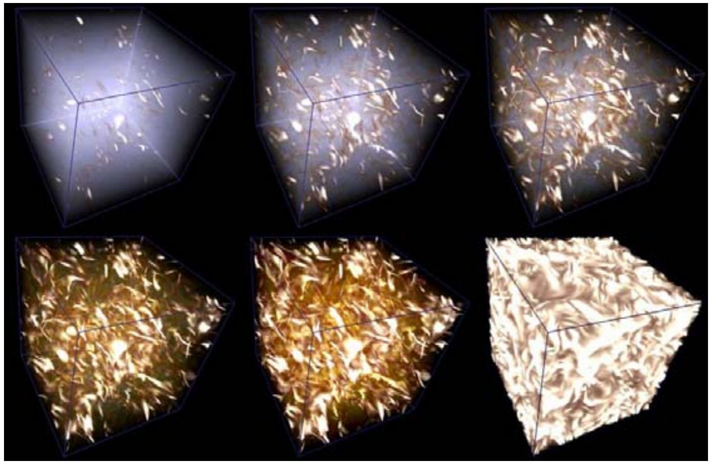

isosurfaces of |vorticity| (different levels)

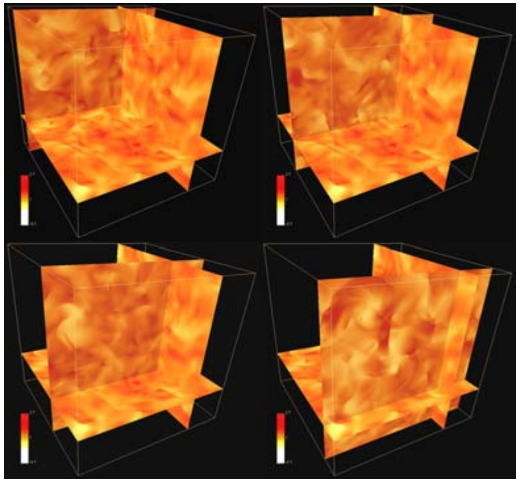

Density slices

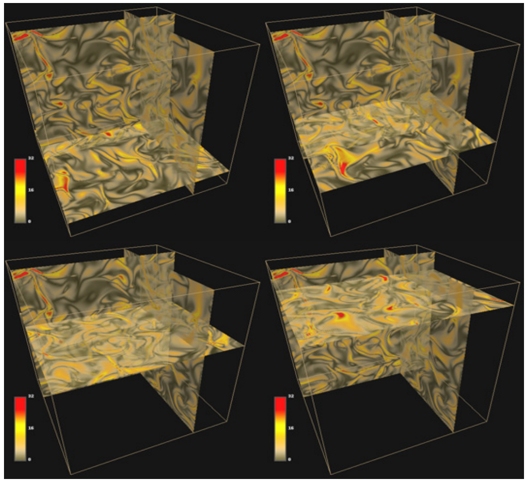

Vorticity slices

Test I; decay of compressible homogeneous turbulence

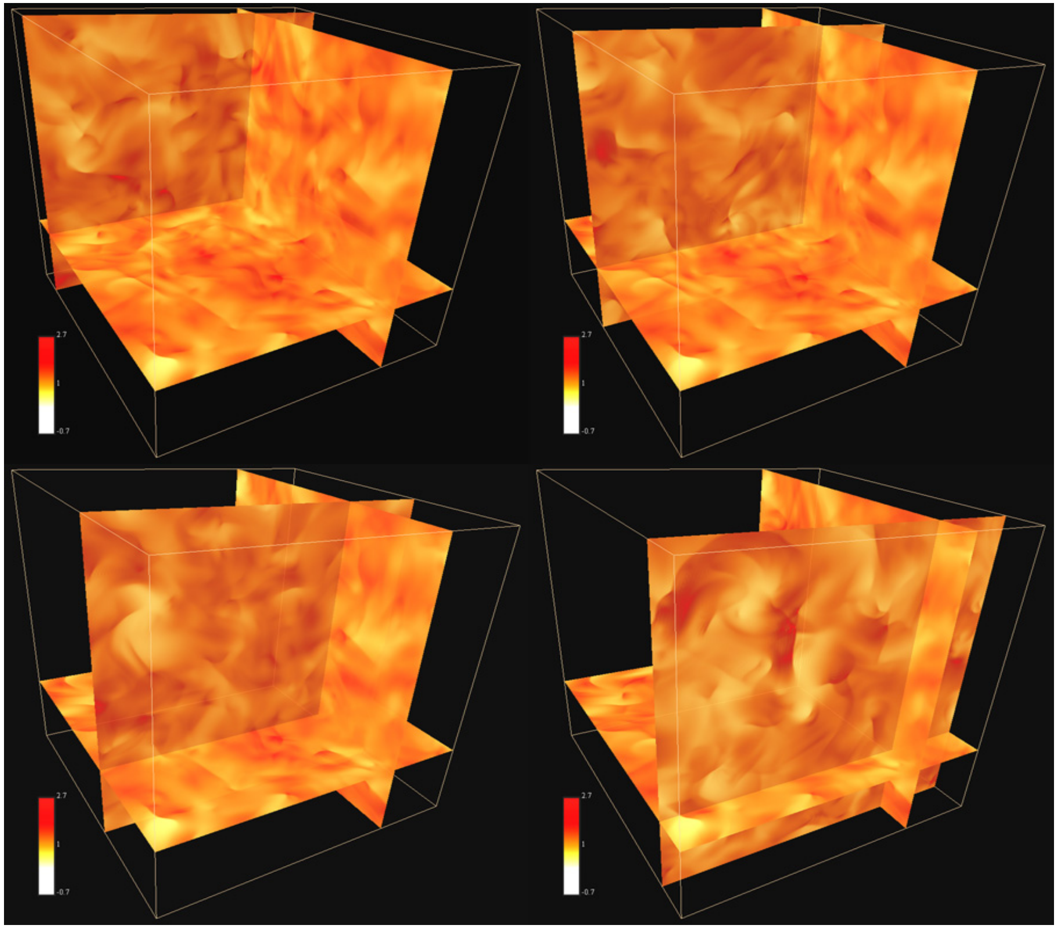

Density slices. Shocklets (weak shocks) evident

DNS and LES of decaying compressible turbulence; decay of TKE

- M_t =0.488, R_lambda = 70.
- Black; 256^3 DNS (10-th order Pade)
- Other; 32^3 LES
- Stretched-vortex SGS model

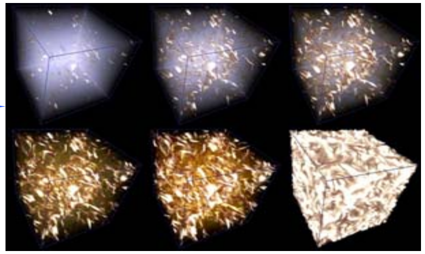

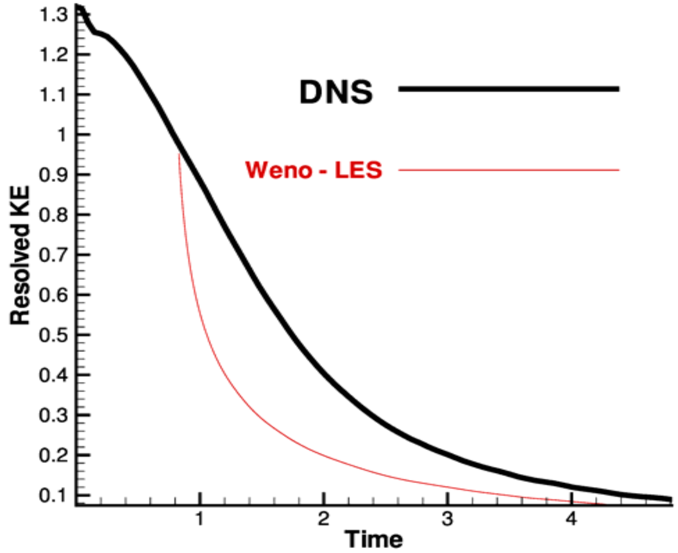

WENO scheme

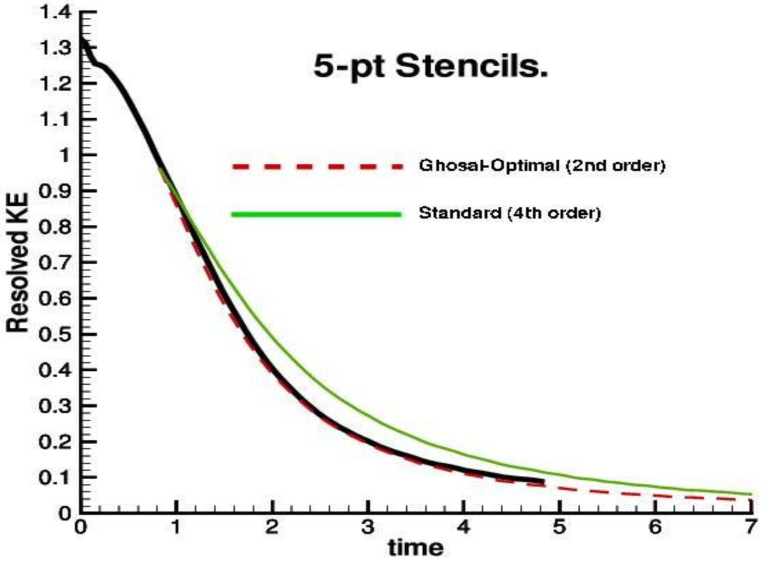

Hybrid WENO-TCD scheme

Test II: Riemann 1D Wave Exact solution of 1D Euler

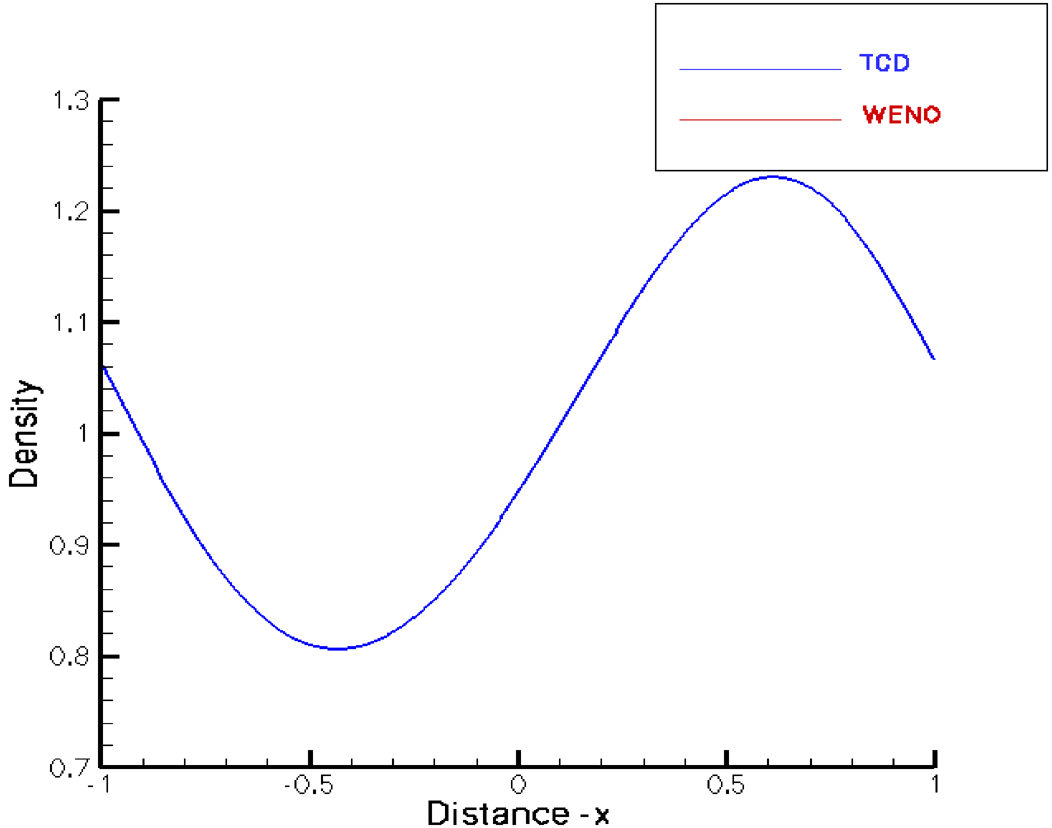

Hybrid WENO-TCD scheme

Richtmyer-Meshkov (R-M) Instability

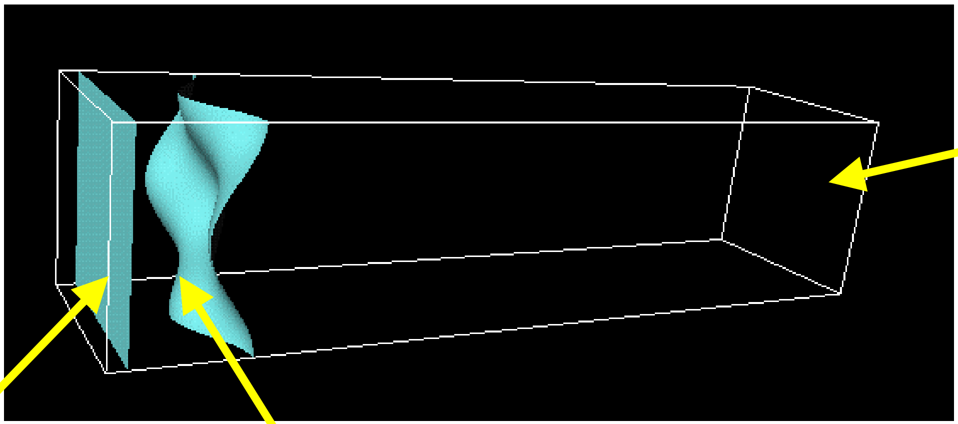

Shock reflects off end

Incident shock

interface

Misalignment of contact and shock

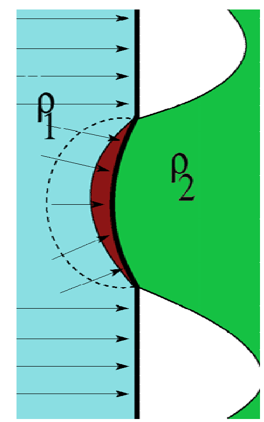

Self-stretching and dilitation

Barotropic vorticity Generation

$$\frac{\partial \varpi}{\partial t} + u \bullet \nabla \varpi = \varpi \bullet \nabla u - \varpi \nabla \bullet u + \frac{1}{\rho^2} \nabla(\rho) \times \nabla(p)$$

Advection

Richtmyer-Meshkov (R-M) Instability

- Astrophysics: A role in the description of the explosion of supernovae (Smarr 1981, Arnett 1989.)
  - *Supernova 1987A* *R. McCray (JILA) Images from HST*

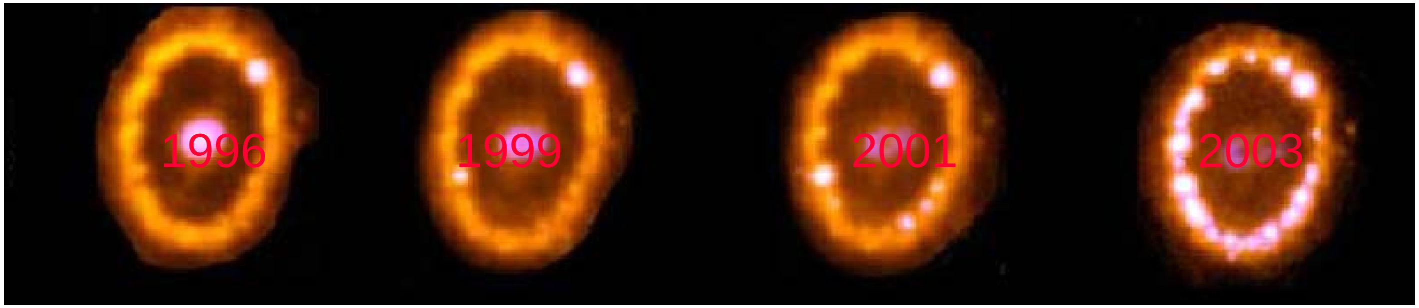

- A role in Inertial confinement fusion design (Lund 1997)
  - *Laser pulse drives pressure waves*
- National lab applications
- Canonical example of shock-turbulence interaction

Flow Description

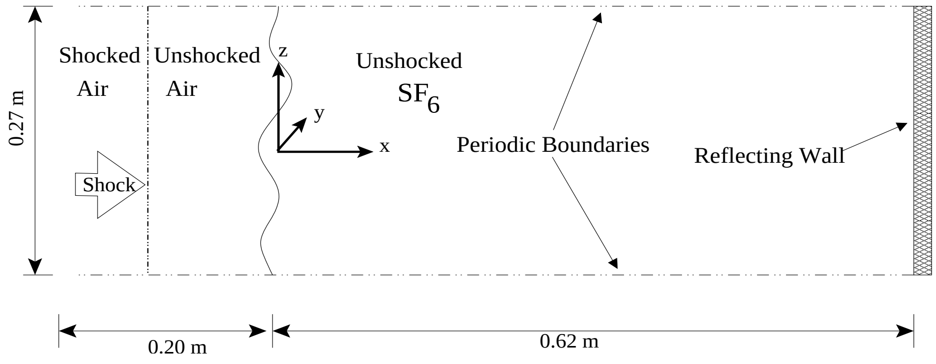

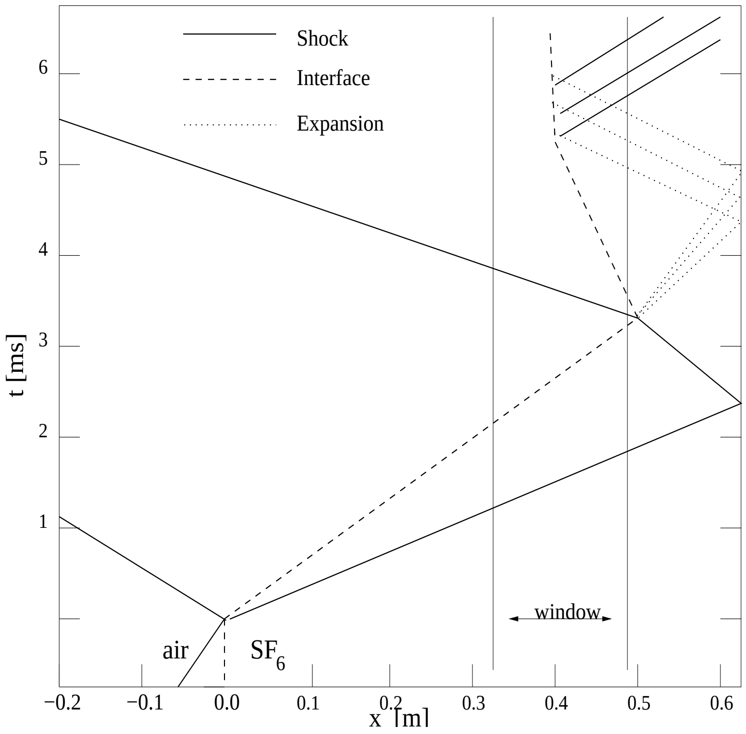

	II[b]	VI[b]	VII[b]
Incident Mach number	1.24	1.50	1.98
Pressure (kPa)	40	23	8
Length, membrane to end wall (cm)	110	62	49
Instantaneous velocity (ms^{-1})	72	150	287
Shocked growth rate (ms^{-1})	2.1	4.2	7.5
Reshocked growth rate (ms^{-1})	17.0	37.2	74.4
Shocked observation times (ms)	4.7-6.7	2.2-3.2	1.7-2.5
Reshocked observation times (ms)	15.5-16.5	4.0-5.5	1.7-2.5

Table 1: The test conditions and growth rates of the interface thickness from Vetter & Sturtevant (1995).

Shock tube, flow conditions (Vetter & Sturtevant 1995) and 1-D wave diagram

Computational runs: unigrid

- Unigrid simulations
- QSC supercomputer (Los Alamos)

	II^b	VI^b	VI^e	VII^b
Incident Mach number	1.24	1.50	1.50	1.98
Computational grid	616x128^2	388x128^2	776x256^2	327x128^2
Computational resolution:$\triangle x$ (cm)	0.21	0.21	0.105	0.21
Simulation time (ms)	16.62	6.35	12.0	2.57
CPU hours	3,982	972	38,400	544

Table 1: The computational cost in CPU hours for each of the runs. Simulation VI^e is a higher resolution version of VI^b computed to about twice the experimental time.

LES of planar Richtmyer-Meshkov instability

- Vetter & Sturtevant (1995) RMI with reshock off end wall
- Air/SF_6, Mach=1.5
- 3 levels of refinement

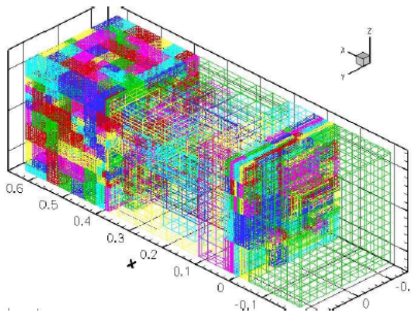

Mesh at one time

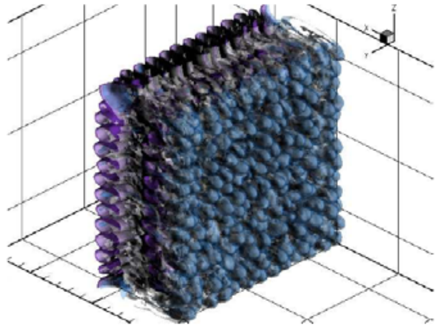

Interface at one time

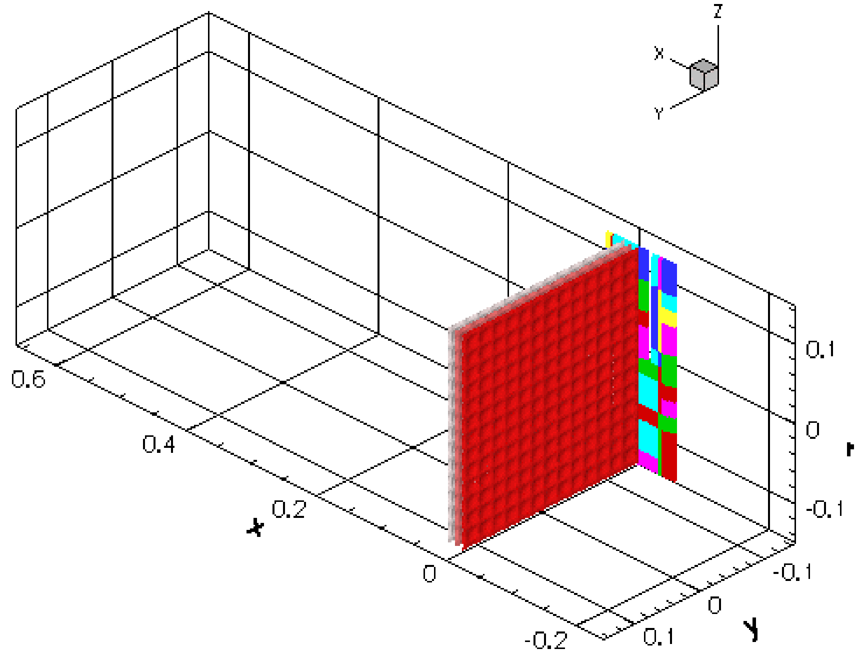

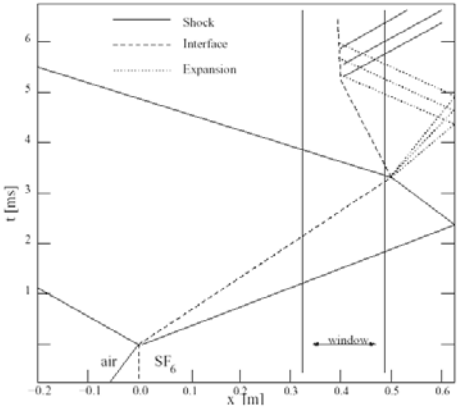

Wave diagram

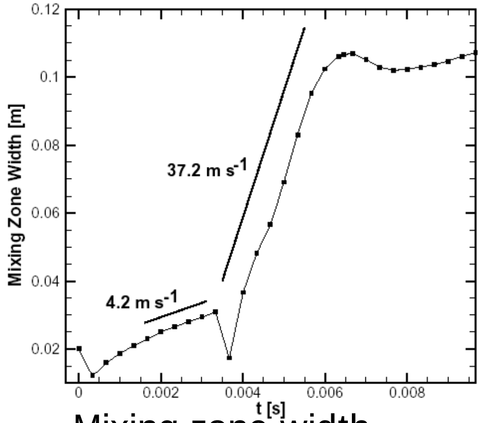

Mixing zone width

Growth of turbulent mixing zone

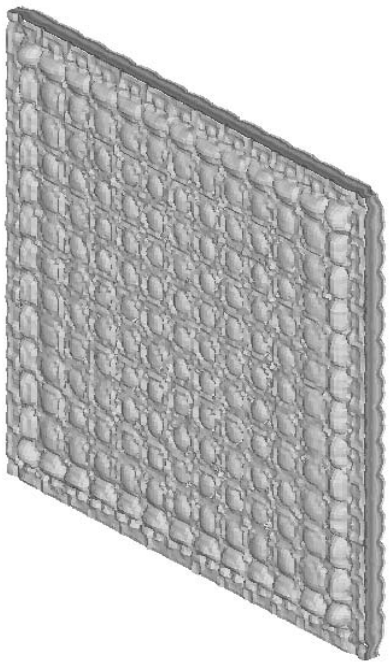

T = 0. ms

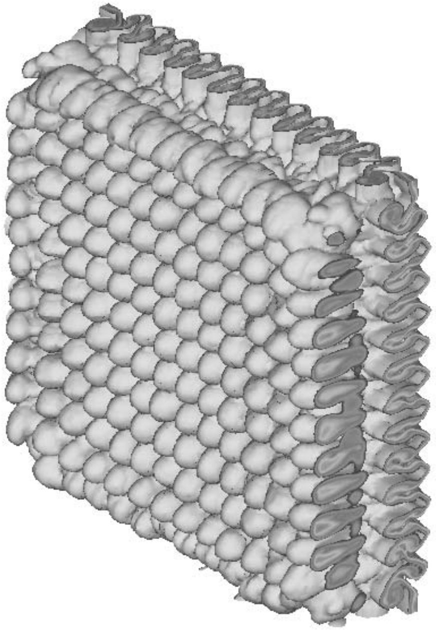

T = 3.6 ms

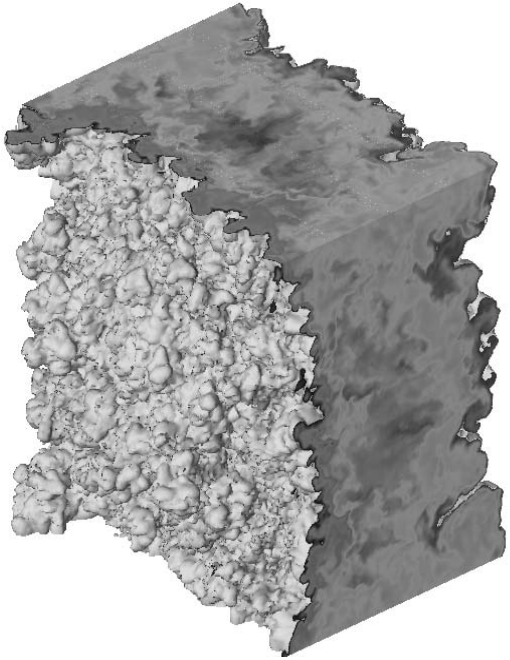

T = 10.0 ms

Growth of turbulent mixing zone

y-z plane-averaged mixing-layer width
compared with Vetter & Sturtevant (1995)

$$\begin{aligned}\langle f(x,t)\rangle &= \frac{1}{\mathcal{A}}\int\int f(x,y,z,t)\,dy\,dz\\ \delta_{\mathrm{MZ}}(t) &= 4\int_{\mathrm{tube}}(1-\langle\psi\rangle)\langle\psi\rangle\,dx\end{aligned}$$

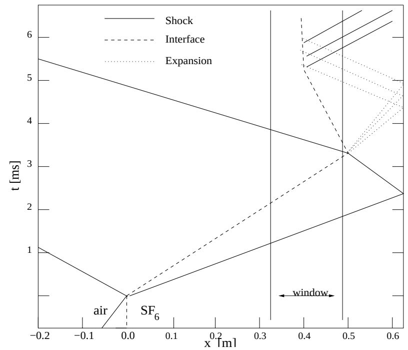

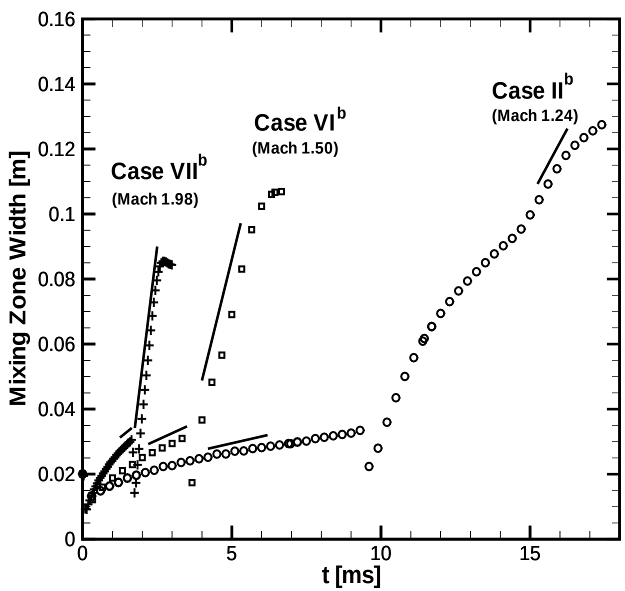

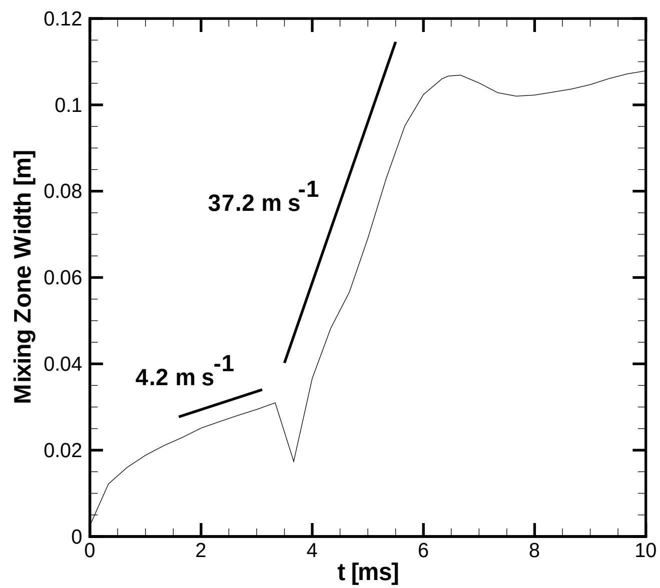

Case VIe; 776x256x256

Kinetic energy in mixing layer

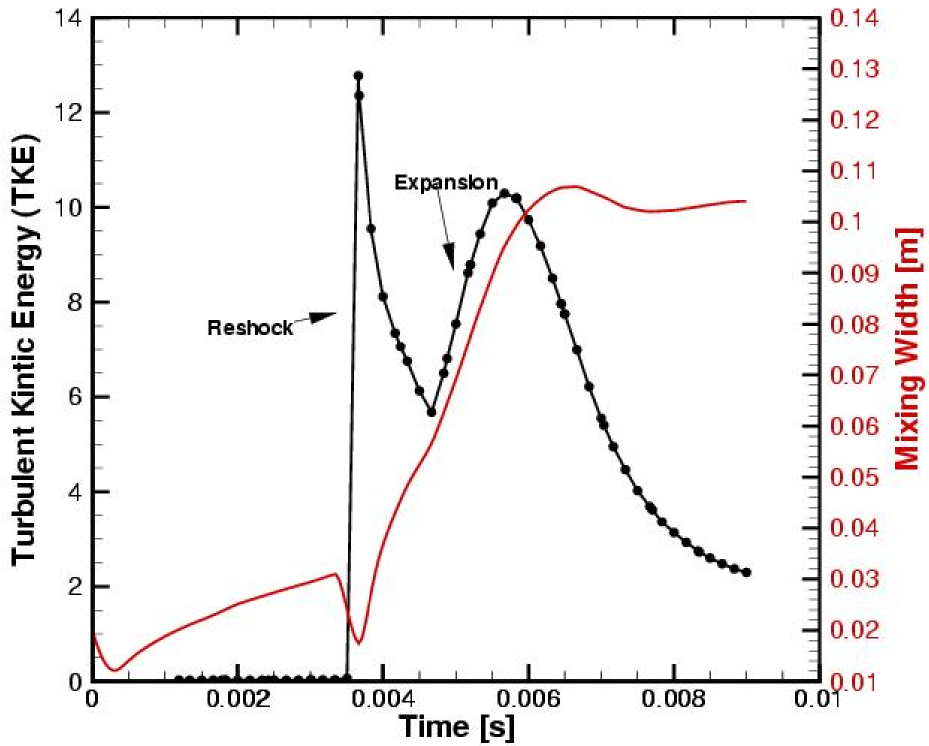

Turbulence statistics

$$\langle \tilde{K}_{res} \rangle = \frac{1}{2}\left(\frac{\langle \overline{\rho}\tilde{u}_k\tilde{u}_k \rangle}{\langle \overline{\rho} \rangle} - \frac{\langle \overline{\rho}\tilde{u}_k \rangle \langle \overline{\rho}\tilde{u}_k \rangle}{\langle \overline{\rho} \rangle^2} \right), \qquad \langle \tilde{K}_{sgs} \rangle = \frac{\langle \tau_{kk} \rangle}{2\langle \overline{\rho} \rangle}$$

$$\langle \epsilon_{res} \rangle = \frac{\langle \sigma'_{ij}\tilde{S}'_{ij} \rangle}{\langle \overline{\rho} \rangle}, \qquad \langle \epsilon_{sgs} \rangle = -\frac{\langle \tau'_{ij}\tilde{S}'_{ij} \rangle}{\langle \overline{\rho} \rangle}$$

$$K = \langle \tilde{K}_{res} \rangle + \langle \tilde{K}_{sgs} \rangle, \qquad u' = \sqrt{\frac{2K}{3}}, \qquad M_t = \frac{u'}{\langle c \rangle}$$

$$\mathrm{Re}_T = \frac{u'\ell}{\langle \nu \rangle}, \qquad \ell = \frac{u'^3}{\epsilon}$$

$$\eta = \left(\frac{< \nu >^3}{< \epsilon_{res} > + < \epsilon_{sgs} >} \right)^{1/4}$$

y-z plane-averaged quantities after reshock (10 ms)

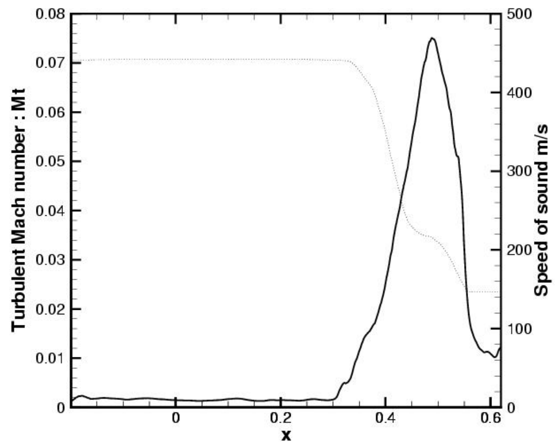

Turbulent (rms) Mach number and sound speed

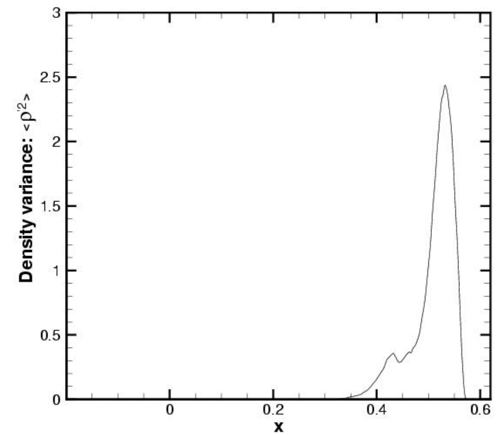

Density variance

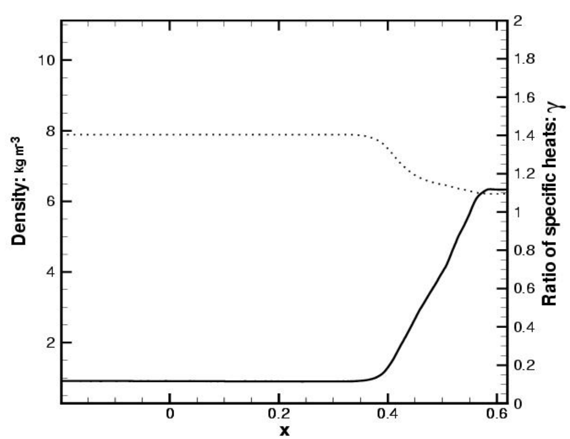

Density and gamma)

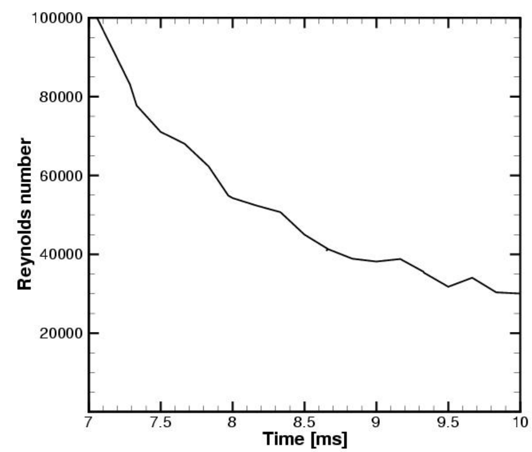

Decay of Reynolds number

y-z plane-averaged quantities after reshock

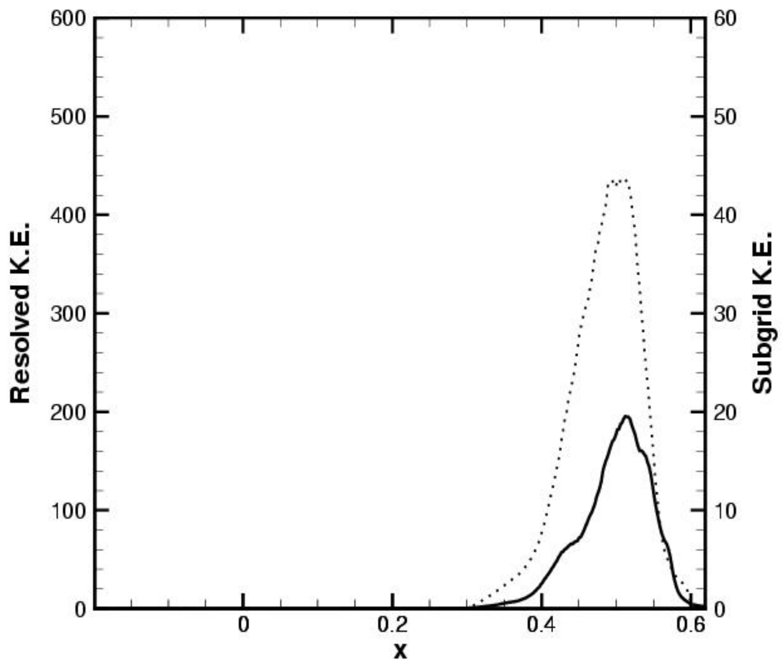

Resolved and subgrid scale TKE

t = 10ms (after reshock)

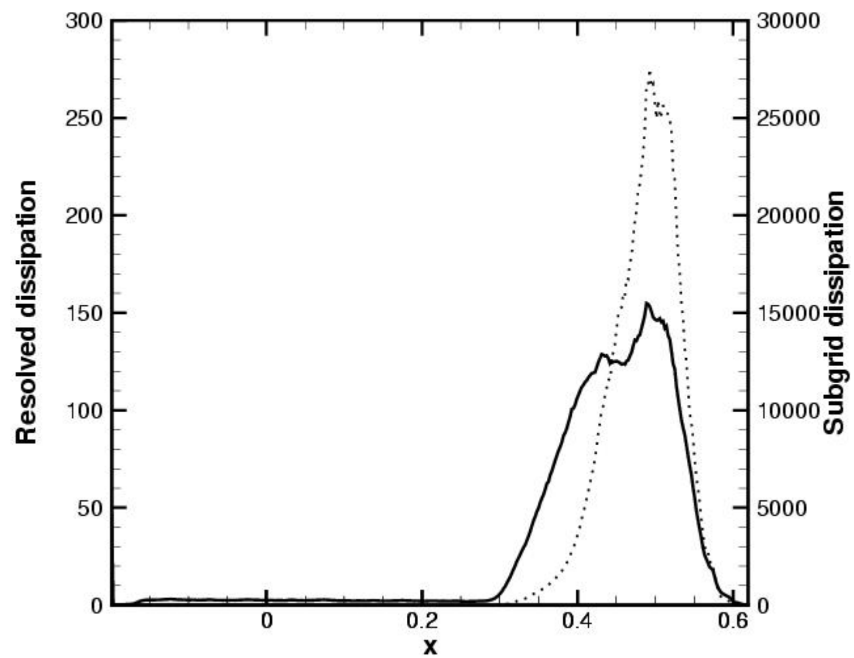

Resolved and subgrid scale dissipation

t = 10ms (after reshock)

Solid; resolved. Dashed; subgrid

Resolved-scale radial spectra in y-z plane

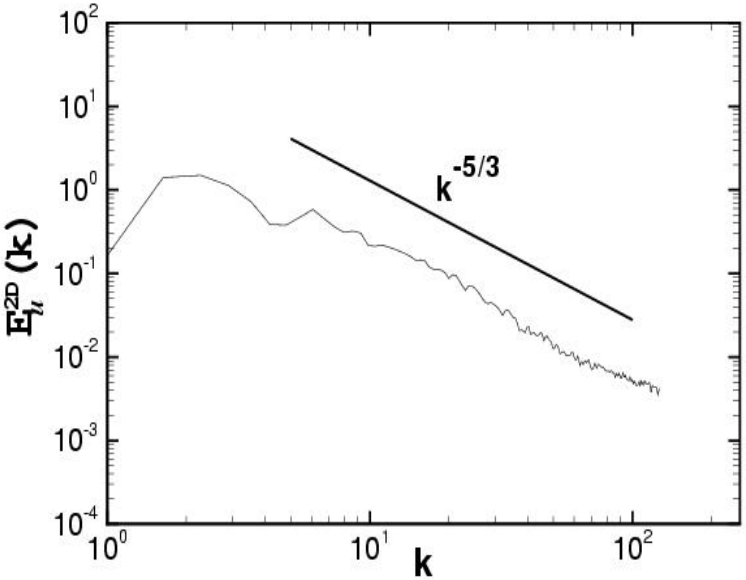

Radial spectrum of x-velocity, center of mixing layer

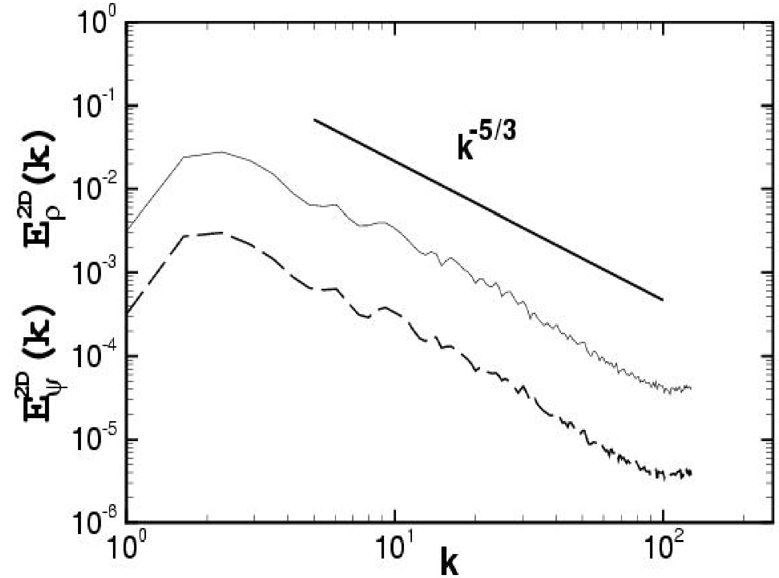

Radial spectrum of density (solid) and mixture fraction, center of mixing layer

Subgrid continuation

- Stretched-spiral vortex SGS model used for subgrid continuation
  - *Contains description of local anisotropy*
  - *Computation of local and plane-averaged Kolmorogov scale η*
  - *Parameters computed from LES (structure functions)*

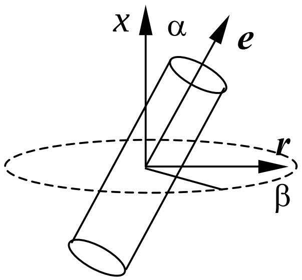

$$E(k) = \mathcal{K}_0 \epsilon^{2/3} k^{-5/3} \exp[-2k^2\nu/(3|\tilde{a}|)]$$

$$\tilde{a} = \tilde{S}_{ij} e_i^v e_j^v, \qquad \tilde{S}_{ij} = \frac{1}{2}\left(\frac{\partial \tilde{u}_i}{\partial x_j} + \frac{\partial \tilde{u}_j}{\partial x_i}\right)$$

$$E_{qq}^{2D}(k_r, \alpha_0) = \frac{2k_r}{\pi} \int_{k_r}^{|k_r/\cos\alpha_o|} \frac{E(\kappa)}{(\kappa^2 - k_r^2)^{1/2}(k_r^2 - \kappa^2\cos^2\alpha_o)^{1/2}} d\kappa.$$

$$E_{33}^{2D}(k_r, \alpha_0) = \frac{2k_r}{\pi} \int_{k_r}^{|k_r/\cos\alpha_o|} \frac{(k_r^2 - \kappa^2\cos^2\alpha_o)^{1/2} E(\kappa)}{\kappa^2(\kappa^2 - k_r^2)^{1/2}} d\kappa.$$

Subgrid continuation of radial velocity spectra

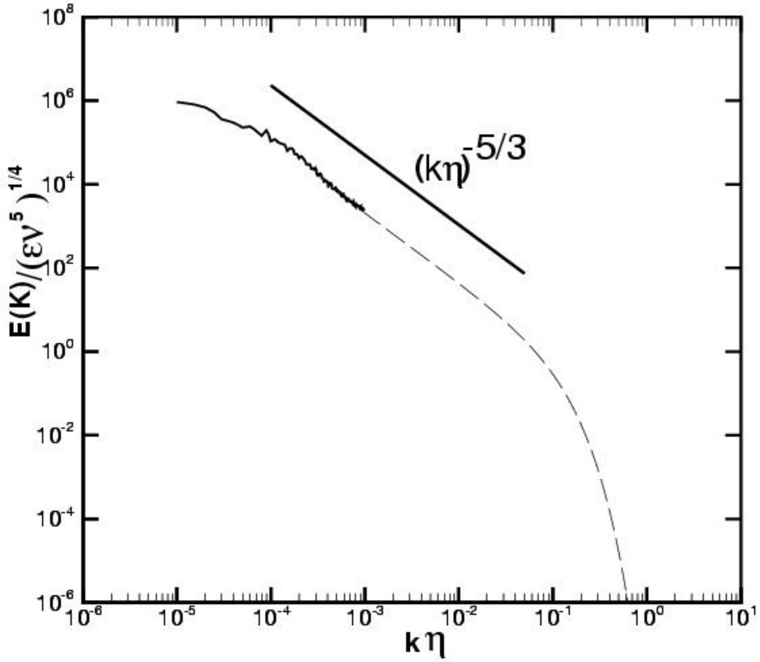

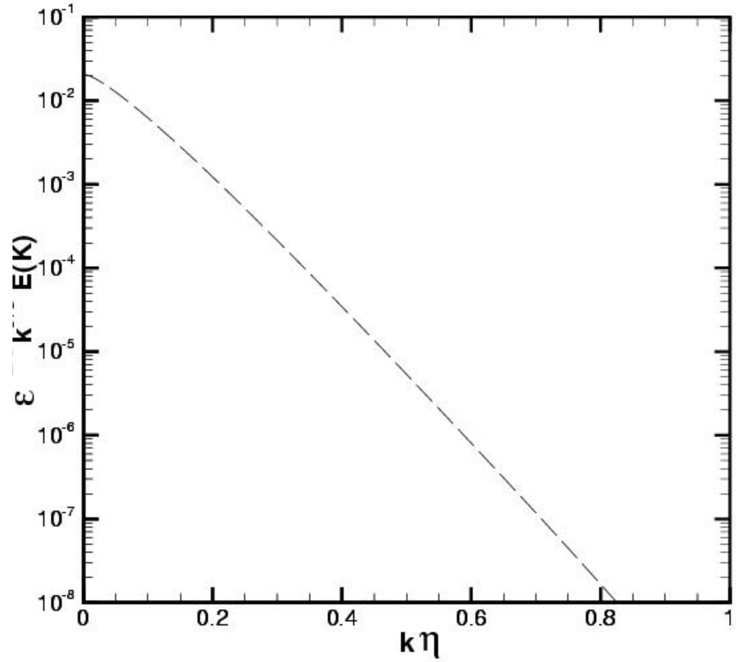

- Radial (in k-space) velocity spectrum on center plane of mixing layer
  - *Resolved-scale spectrum (solid)*
  - *Subgrid continuation (dashed)*
  - *Parameters computed from LES (structure functions)*
- Subgrid velocity spectrum in dissipation range
  - *Log-linear scale*
  - *Note exponential roll-off*

Subgrid continuation of radial velocity spectra.
Anisotropy of in-plane and normal velocity spectra

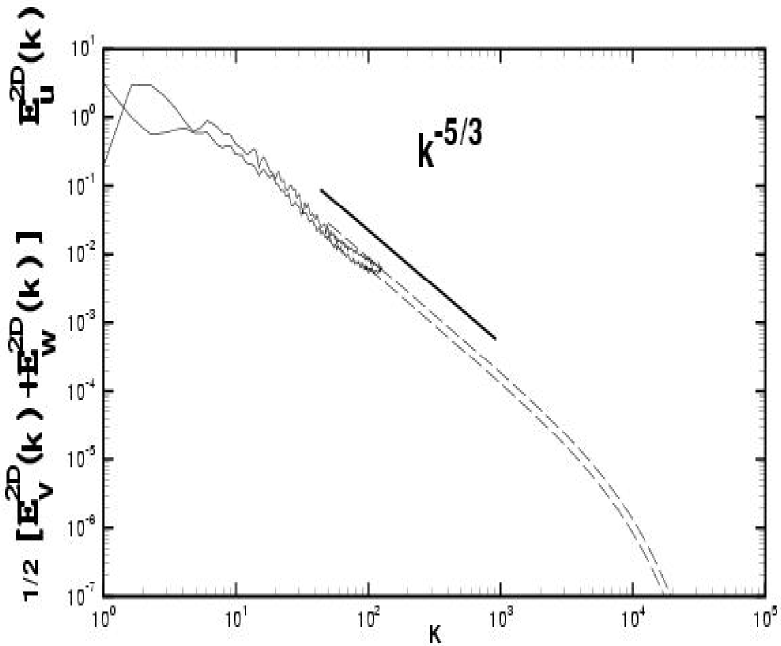

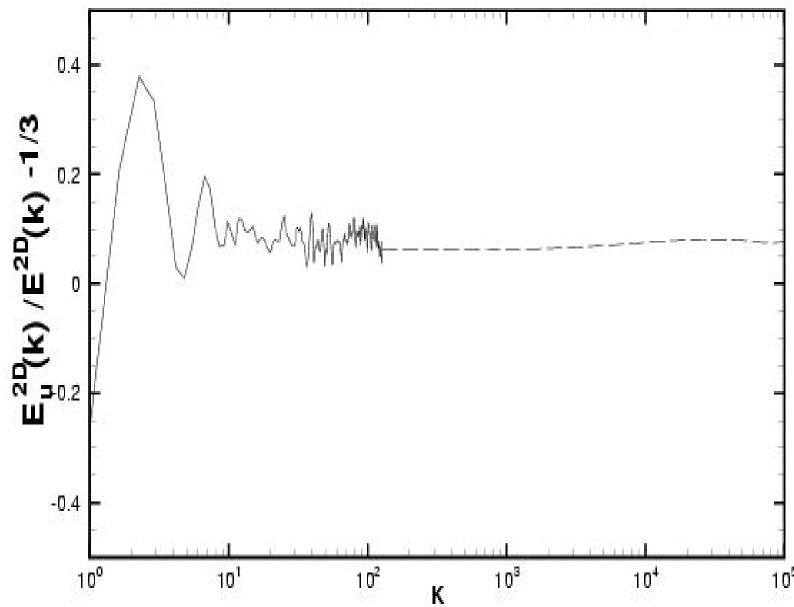

- Radial spectrum of u (top) and u+w (below)
  - *Resolved-scale spectrum (solid)*
  - *Subgrid continuation (dashed)*

- Measure of anisotropy for radial velocity spectra
  - *Resolved-scale spectrum (solid)*
  - *Subgrid continuation (dashed)*

Subgrid continuation of scalar spectum in y-z plane

Scalar spectrum for stretched-spiral vortex

Pullin & Lundgren (2000)

$$E_\psi(k) = \mathcal{K}_\psi \left(k^{-5/3} \exp\left(-\frac{(4\nu + 2D)k^2}{3\tilde{a}}\right) + \frac{8}{5\pi}\left(\frac{2\Gamma}{\tilde{a}}\right)^{1/3} k^{-1} \exp\left(-\frac{2Dk^2}{3\tilde{a}}\right) \right)$$

$$\tilde{\mathcal{F}}_2^\psi(\triangle) = 4\mathcal{K}_\psi \triangle^{2/3} \int_0^\pi \left(s^{-5/3} + \frac{8}{5\pi}\left(\frac{2\Gamma}{\tilde{a}\triangle^2}\right)^{1/3} s^{-1} \right)\left(1 - \frac{\sin s}{s}\right) ds$$

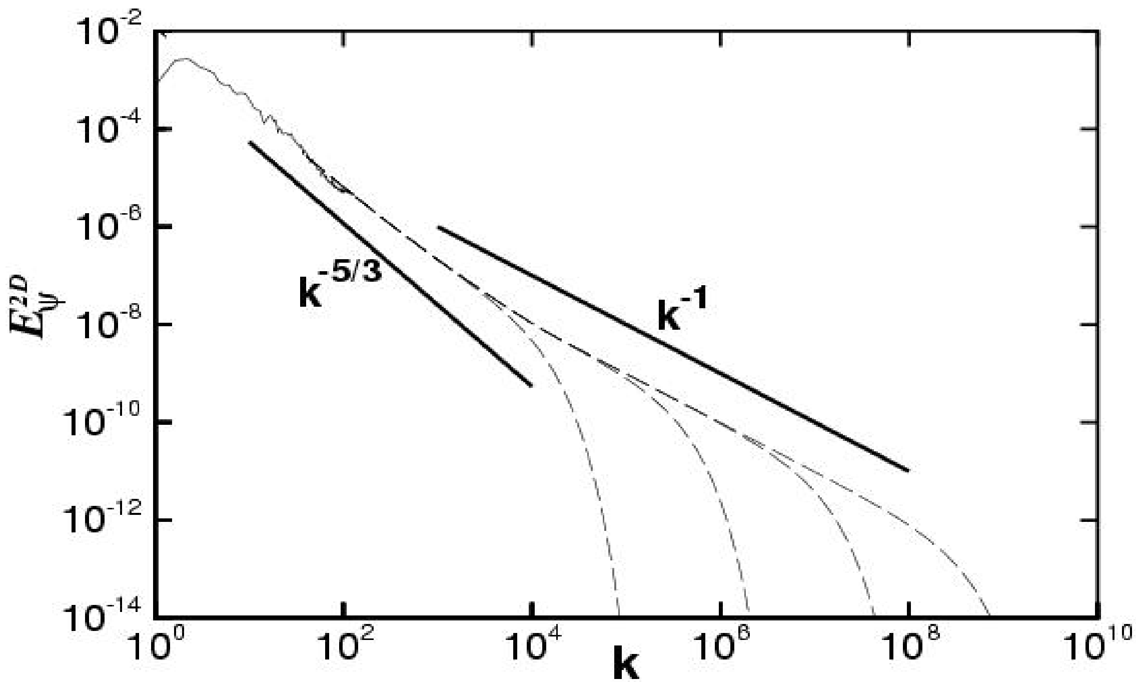

Resolved-scale and continued scalar spectrum in center y-z plane, t = 10ms. Left to right, Sc = 1, 1000, 1000,000

Favre P.D.F. P(ψ) of mixture fraction (resolved scales)

t = 3 ms

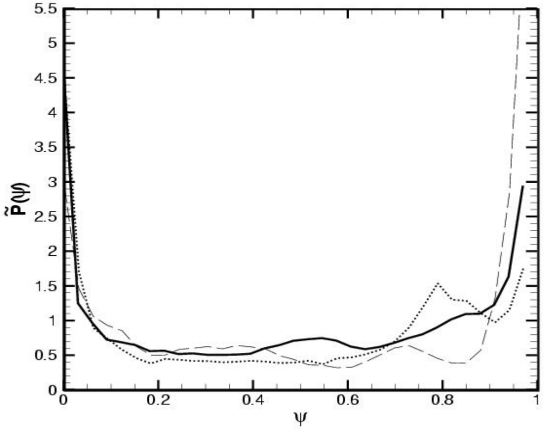

t = 3.6 ms

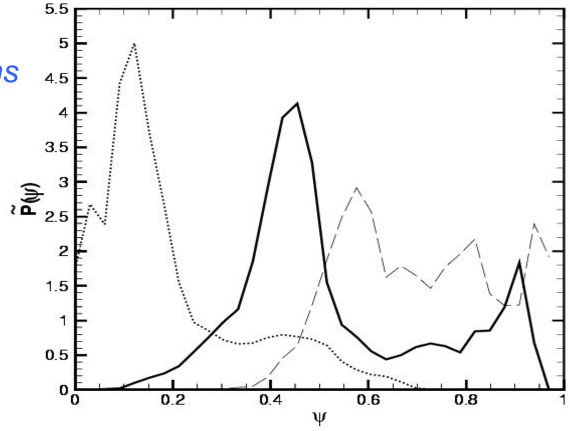

t = 7 ms

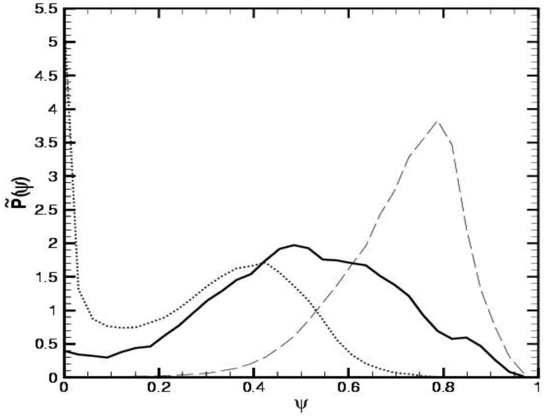

t = 10 ms

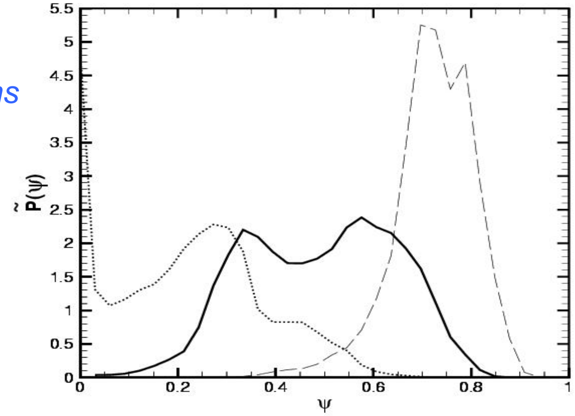

P.D.F. of mixture fraction with subgrid correction

$$\tilde{\mathcal{P}}_{sgs}(\psi,\tilde{\psi},\sigma_\psi^2;\boldsymbol{x},t) = \tilde{\mathcal{P}}_{sgs}(\psi|\tilde{\psi},\sigma_\psi^2)\tilde{\mathcal{P}}_{sgs}(\tilde{\psi},\sigma_\psi^2;\boldsymbol{x},t)$$

$$\tilde{\mathcal{P}}_{sgs}(\psi;\boldsymbol{x},t) = \int\int \tilde{\mathcal{P}}_{sgs}(\psi|\tilde{\psi},\sigma_\psi^2)\tilde{\mathcal{P}}_{sgs}(\tilde{\psi},\sigma_\psi^2;\boldsymbol{x},t)\, d\tilde{\psi} d\sigma_\psi^2$$

$$\tilde{\mathrm{P}}(\psi;\boldsymbol{x},t) \simeq \frac{\langle\overline{\rho}\tilde{\mathcal{P}}_{sgs}(\psi;\boldsymbol{x},t)\rangle}{\langle\overline{\rho}(\boldsymbol{x},t)\rangle}$$

$$\tilde{\mathcal{P}}_{sgs}(\psi;\boldsymbol{x},t) = \frac{\Gamma(a+b)}{\Gamma(a)\Gamma(b)}\psi^{a-1}(1-\psi)^{b-1}$$

$$a = \tilde{\psi}[\tilde{\psi}(1-\tilde{\psi})\sigma_\psi^{-2} - 1], \qquad b = a(\tilde{\psi}^{-1} - 1)$$

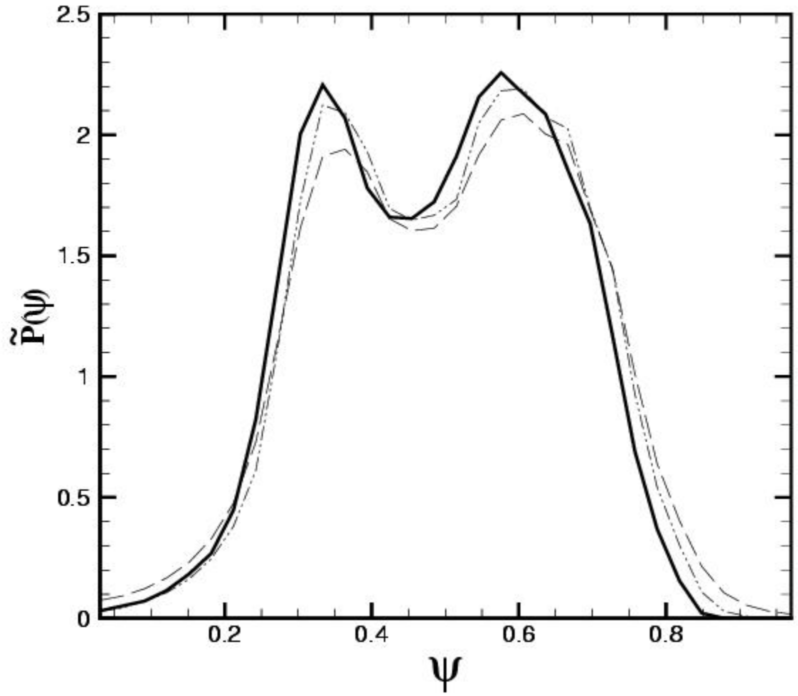

P.D.F of mixture fraction in center y-z plane, t = 10ms. Resolved-scale and Sc = 1, 1000,000

Suppression of RM instability by Magnetic Field
(V. Wheatley, R. Samtaney)

- Suppression due to change in shock refraction process at interface when $B \neq 0$ (Wheatley, Pullin & Samtaney, JFM 2004)
- Linear initial-value problem for impulsive acceleration of interface in presence of magnetic field solved exactly

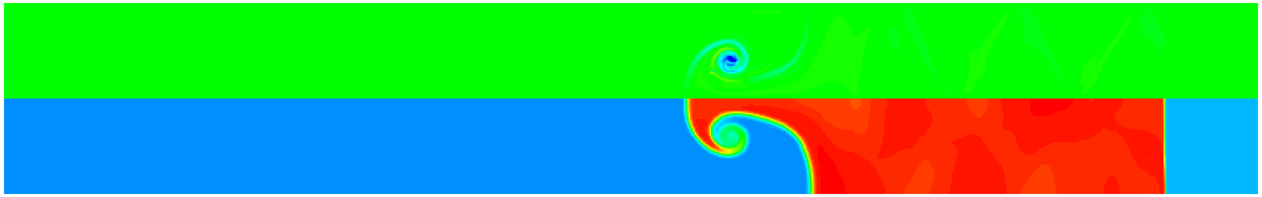

Vorticity (top) and ρ (bottom) at t =1.8 , B = 0, interface unstable

Vorticity (top) and ρ (bottom) at t =1.8, $B \neq 0$, instability suppressed

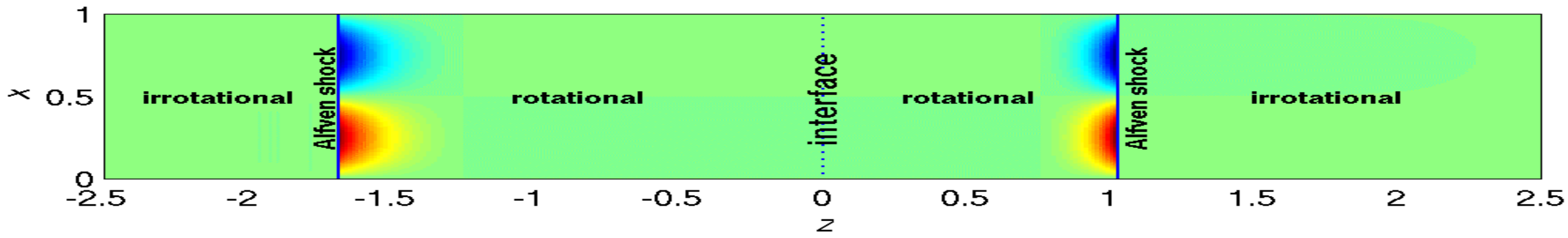

Analysis: Solution Features

Solution consists of:

- Inner region of rotational flow
- 2 small amplitude Alfvén shocks that carry circulation
- 2 outer irrotational regions

Notes:

- *w**(0, *t*) is interfacial growth rate
- this decays to zero as Alfvén shocks propagate away

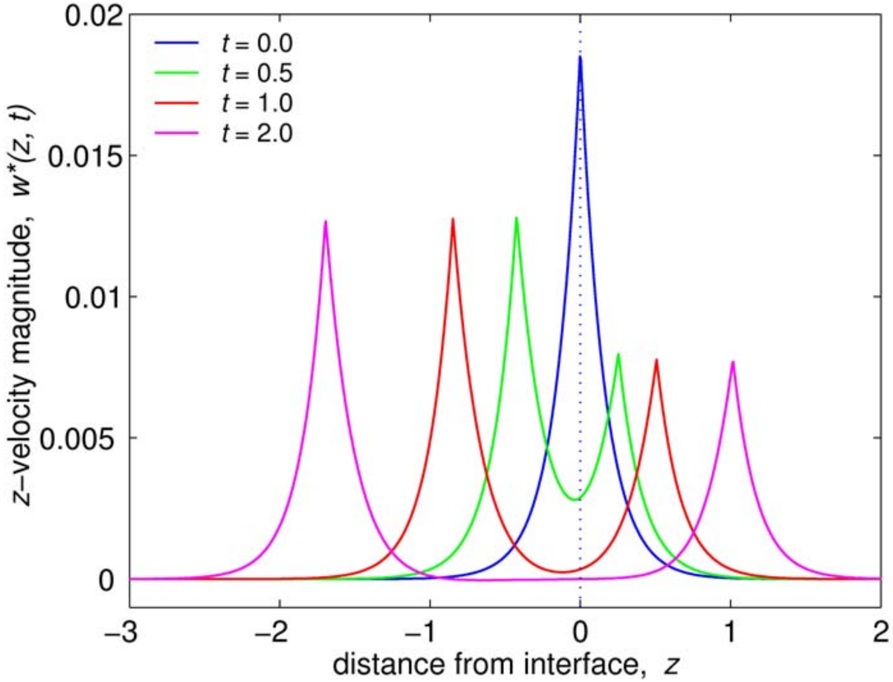

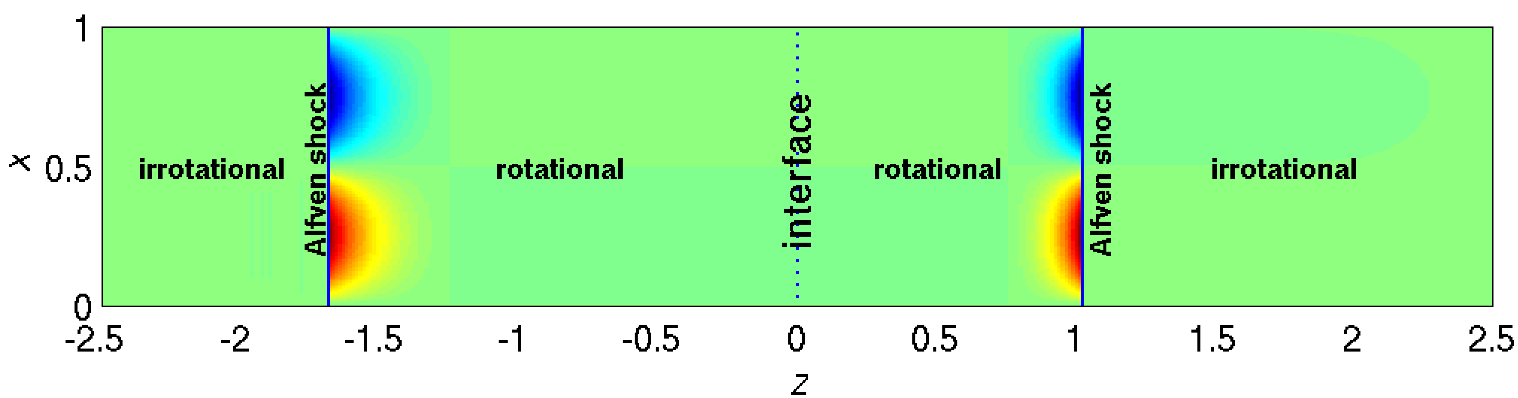

Cylindrical RMI: Flow Description

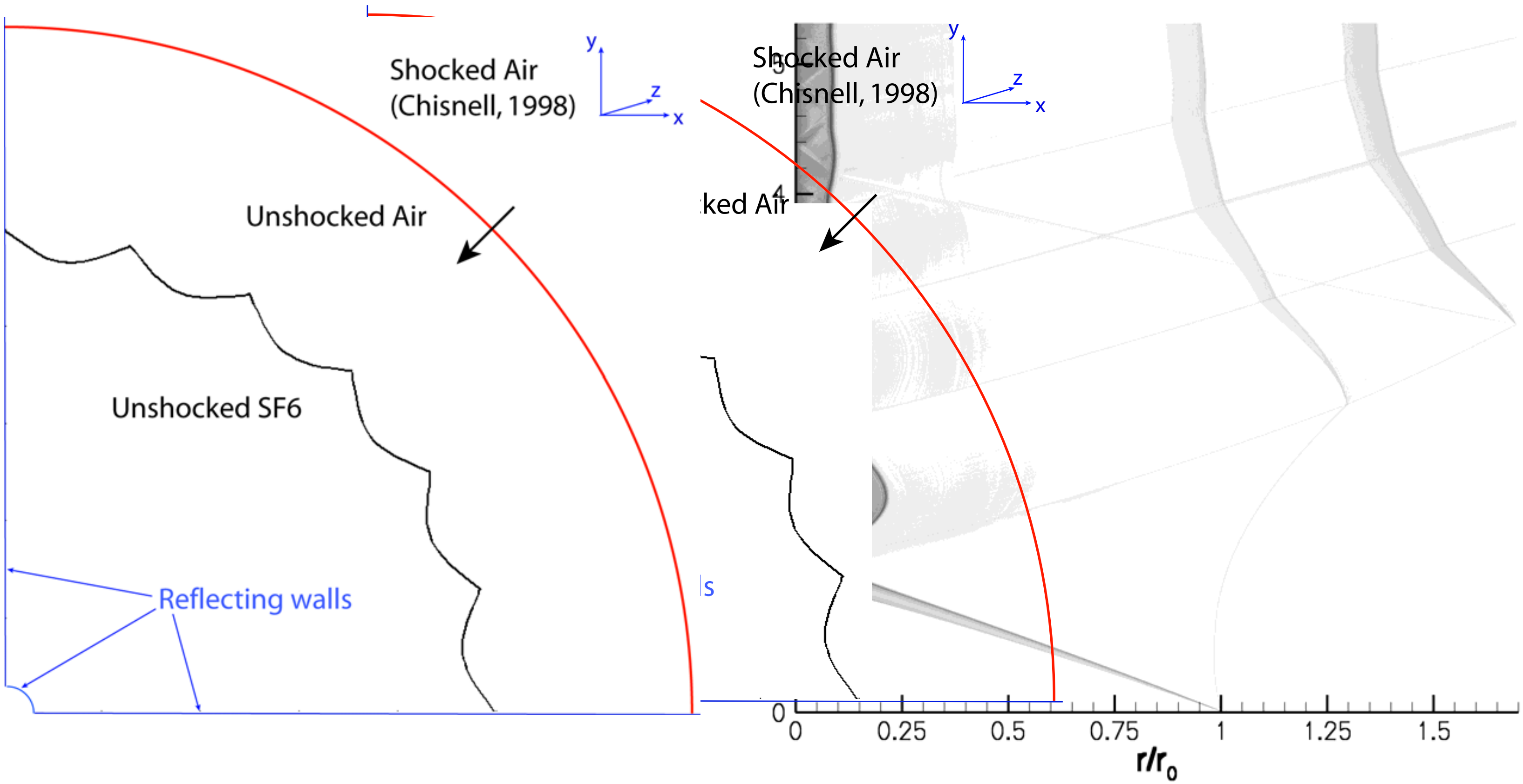

Flow conditions and 1-D wave diagram (*r*,*t*)

Cylindrical RMI; M_0=1.3, 90 degree wedge (M. Lombardini)

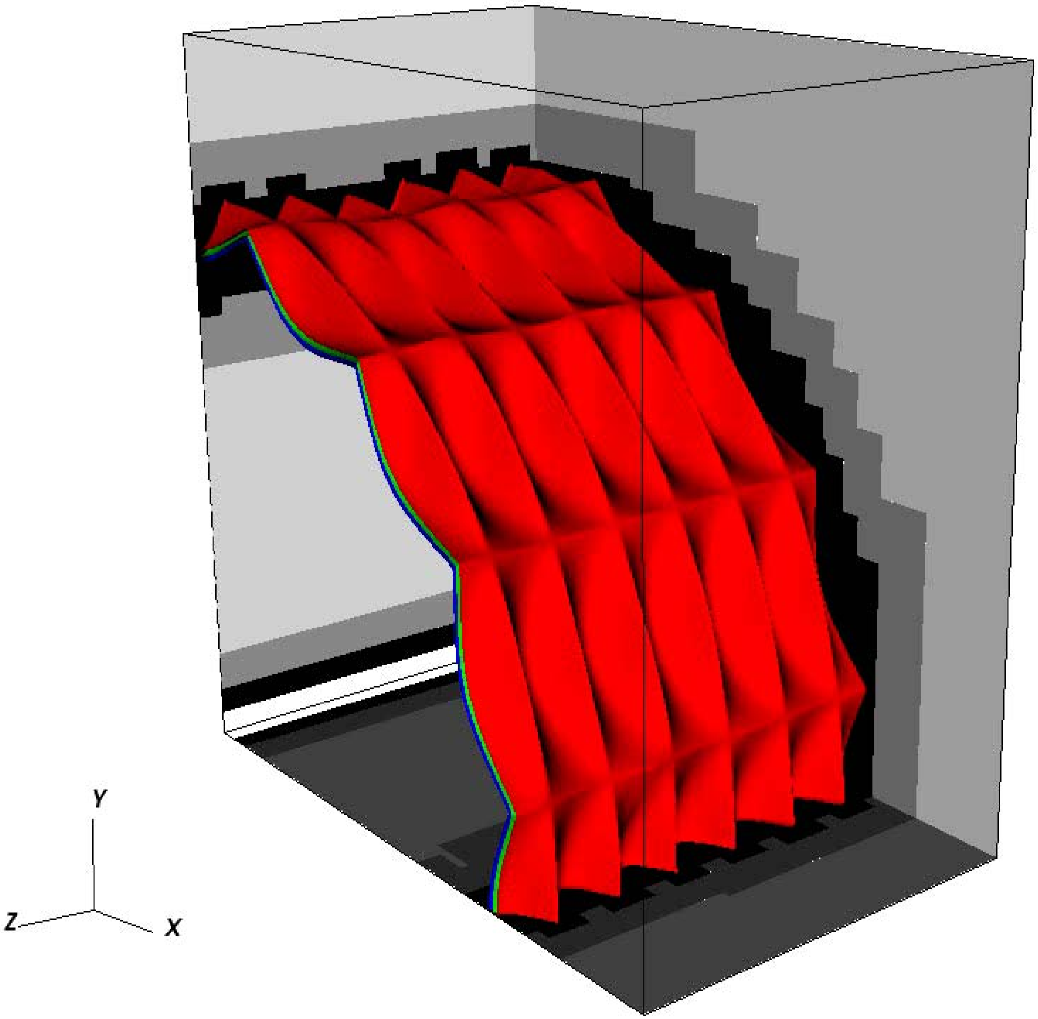

- WENO-TCD with LES (SV model)
- Adaptive Mesh Refinement (AMROC) Ghost Fluid Method (inner and outer cylindrical boundaries)
- Initial conditions:
  - *M_0 = 1.3 or 2.0 or 3.0*
  - *Air/SF_6 (Atwood number = 2/3)*
  - *"egg-carton" + smaller symmetry breaking perturbation with random phase*
  - *Chisnell's converging flow behind the shock wave*
- Resolution:
  - *Base grid 83 x 83 x 51*
  - *2 additional levels of refinement*
  - *Equivalent refined resolution 332 x 332 x 204*

Passive scalar contours & adaptive levels of refinement

Growth of turbulent mixing zone (M_0=2.0)

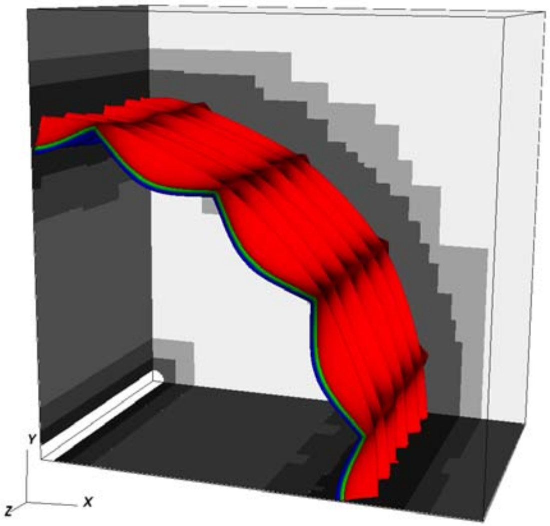

t = 0. ms

Initial condition

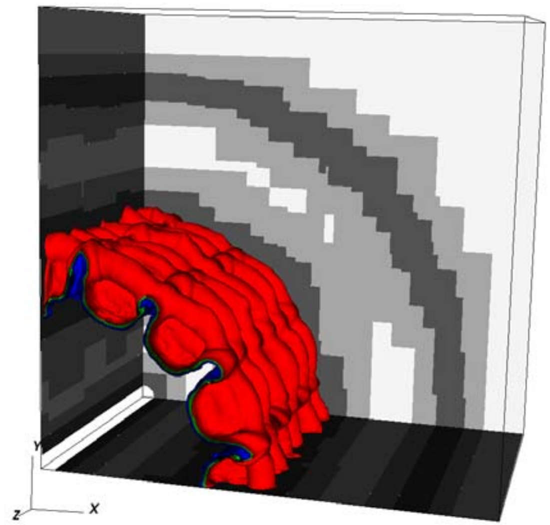

t = 1.45 ms

After first shock interaction

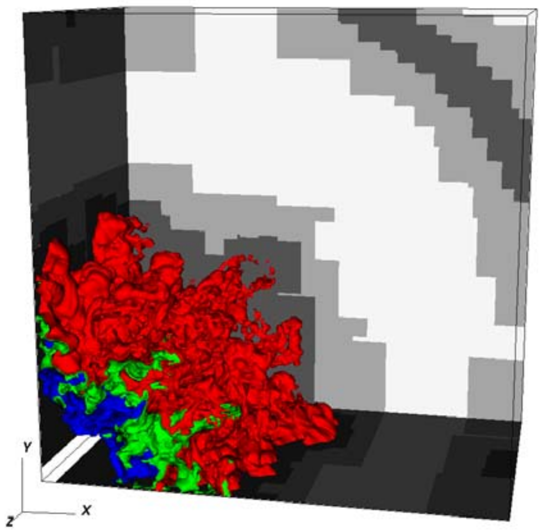

t = 5.13 ms

After first reschock

Turbulent channel flow

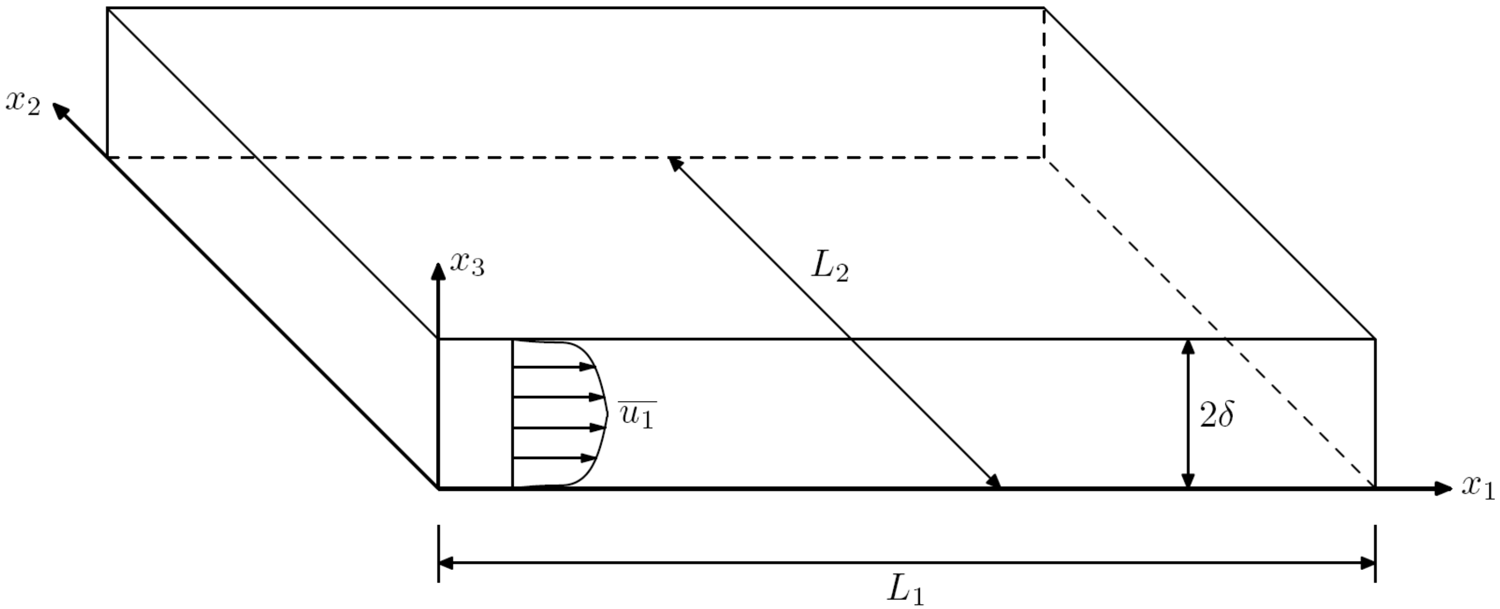

$$-\delta \overline{\frac{\partial p}{\partial x_1}} = \nu \left(\frac{\partial \overline{u_1}}{\partial x_3} \right)_{\text{wall}} \equiv u_\tau^2, \qquad \mathrm{Re}_\tau = u_\tau \delta / \nu$$

Previous work

A physical-space version of the stretched-vortex subgrid-stress model for large-eddy simulation

Tobias Voelkl and D. I. Pullin
Graduate Aeronautical Laboratories 301-46, California Institute of Technology, Pasadena, California 91125

Daniel C. Chan
GE Corporate Research and Development Center, Room KW-C118, One Research Circle, Niskayuna, New York 12309

(Received 15 July 1999; accepted 14 March 2000)

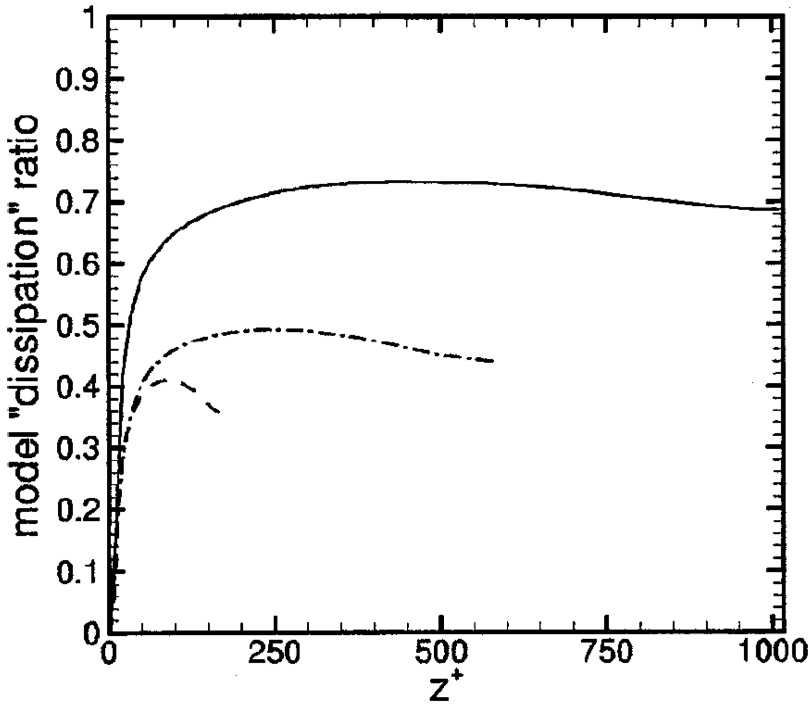

FIG. 8. Model "dissipation" ratio $\varepsilon_{sgs}/(\tilde{\epsilon}_{visc}+\varepsilon_{sgs})$, —: $Re_\tau=1017$; -·-: $Re_\tau=590$, ---: $Re_\tau=180$.

No large eddies near wall

Ten questions concerning the large-eddy simulation of turbulent flows

Stephen B Pope
Sibley School of Mechanical and Aerospace Engineering, Cornell University, Ithaca, NY 14853, USA
E-mail: pope@mae.cornell.edu

New Journal of Physics **6** (2004) 35
Received 3 December 2003
Published 16 March 2004
Online at http://www.njp.org/ (DOI: 10.1088/1367-2630/6/1/035)

A second example is high Reynolds number near-wall flows, the simplest specific case being the turbulent boundary layer on a smooth wall. The wall shear stress—all-important in aerodynamic applications—arises from momentum transfer from the outer flow through the boundary layer to the wall. In the viscous near-wall region, the momentum transfer is effected by the near-wall structures, the length scale of which scales with the tiny viscous length scale. As Bradshaw has succinctly put it: in the viscous near-wall region *there are no large eddies*. But, as has been appreciated at least since Chapman [15], the near-wall motions cannot be resolved in high-Reynolds number LES, but must instead be modelled (to avoid impracticable computational requirements that increase as a power of Reynolds number, as in DNS).

Near-wall filtering

Streamwise and spanwise Gaussian filter

$$\widetilde{Q}\left(x_1, x_2, x_3, t\right) \equiv \int_{-\infty}^{\infty} \int_{-\infty}^{\infty} Q\left(x_1', x_2', x_3, t\right) G_1\left(x_1, x_1'; \Delta_1\right) G_2\left(x_2, x_2'; \Delta_2\right)\, dx_1'\, dx_2'$$

$$\Delta_1, \Delta_2 \gg \nu / u_\tau$$

Wall-normal top-hat filter

$$\langle Q \rangle \left(x_1, x_2, t\right) \equiv \frac{1}{h} \int_0^h \widetilde{Q}\left(x_1, x_2, x_3', t\right)\, dx_3'$$

$$\nu / u_\tau = \delta / \mathrm{Re}_\tau \ll h \ll \delta$$

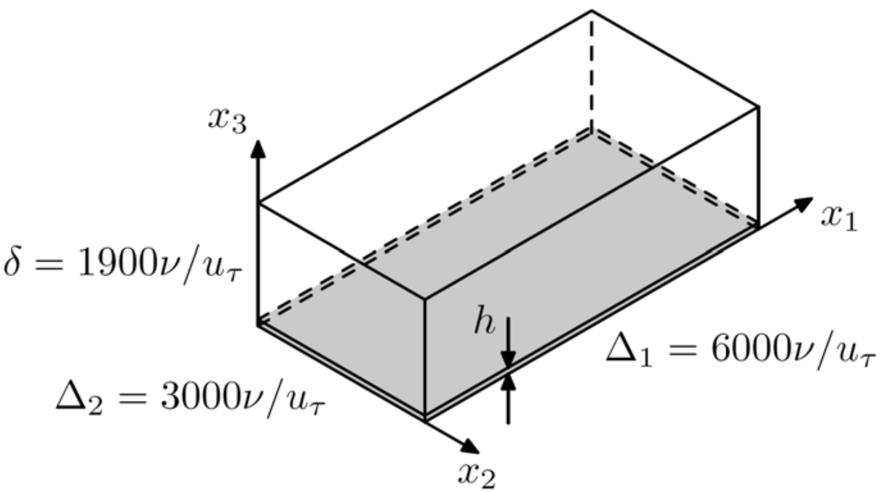

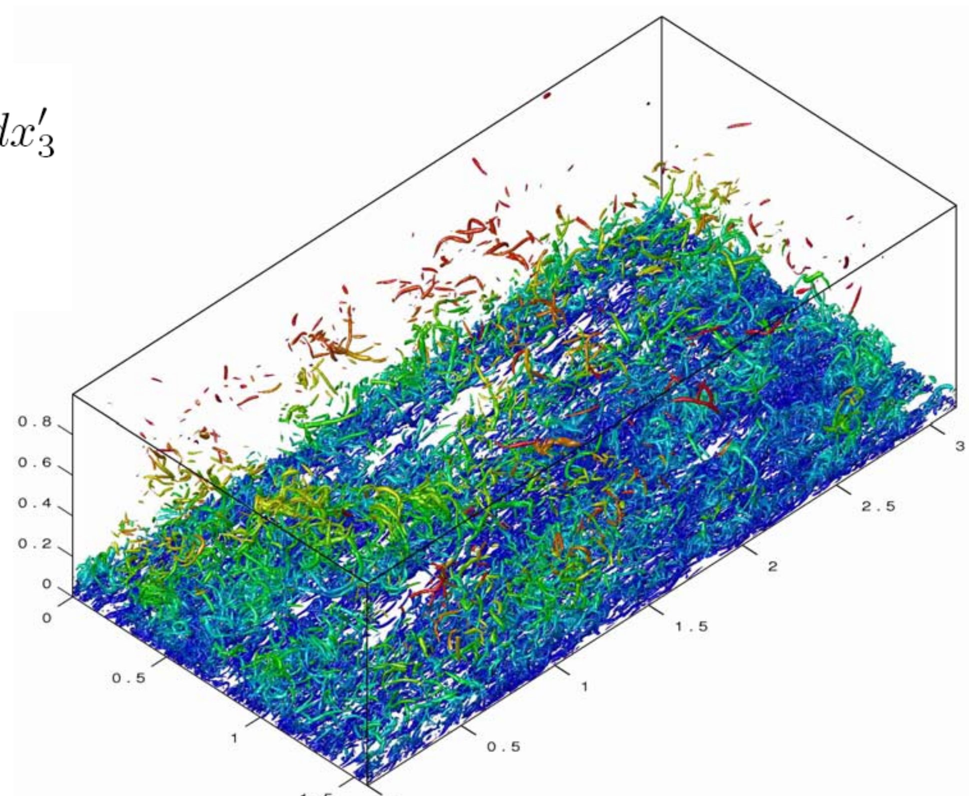

http://torroja.dmt.upm.es/ftp/channels/

Local inner scaling

Filtered streamwise momentum equation

$$\frac{\partial \langle u_1 \rangle}{\partial t} = \left(-\frac{1}{h}\widetilde{u_3 u_1} - \frac{\partial \widetilde{p}}{\partial x_1} + \frac{\nu}{h}\left[\frac{\partial \widetilde{u_1}}{\partial x_3} - u_0' \right] \right)_{x_3=h}$$

$$u_0'\left(x_1, x_2, t\right) \equiv \left(\frac{\partial \widetilde{u_1}}{\partial x_3} \right)_{x_3=0} = \widetilde{u_\tau}^2\left(x_1, x_2, t\right)/\nu$$

$$\Downarrow$$

Law of the wall in a local sense

$$\widetilde{u_1}^+ = F\left(x_3^+\right) \quad \Longleftrightarrow \quad \frac{\widetilde{u_1}\left(x_1, x_2, x_3, t\right)}{\left(\nu u_0'\right)^{1/2}} = F\left(\frac{x_3}{\left(\nu / u_0'\right)^{1/2}} \right)$$

$$\frac{\partial \langle u_1 \rangle}{\partial t} = \frac{\left(\widetilde{u_1}\right)_{x_3=h}}{2\, u_0'} \frac{\partial u_0'}{\partial t}$$

$$\Downarrow$$

Local shear stress equation

$$\frac{\partial u_0'}{\partial t} = \frac{2\, u_0'}{\left(\widetilde{u_1}\right)_{x_3=h}} \left(-\frac{1}{h}\widetilde{u_3 u_1} - \frac{\partial \widetilde{p}}{\partial x_1} + \frac{\nu}{h}\left[\frac{\partial \widetilde{u_1}}{\partial x_3} - u_0' \right] \right)_{x_3=h}$$

Fluctuating virtual-wall BC

$$\widetilde{u_1}^+(x_1, x_2, h_0, t) = F\left(h_0^+\right) = h_0^+, \quad h_0^+ \le 10$$

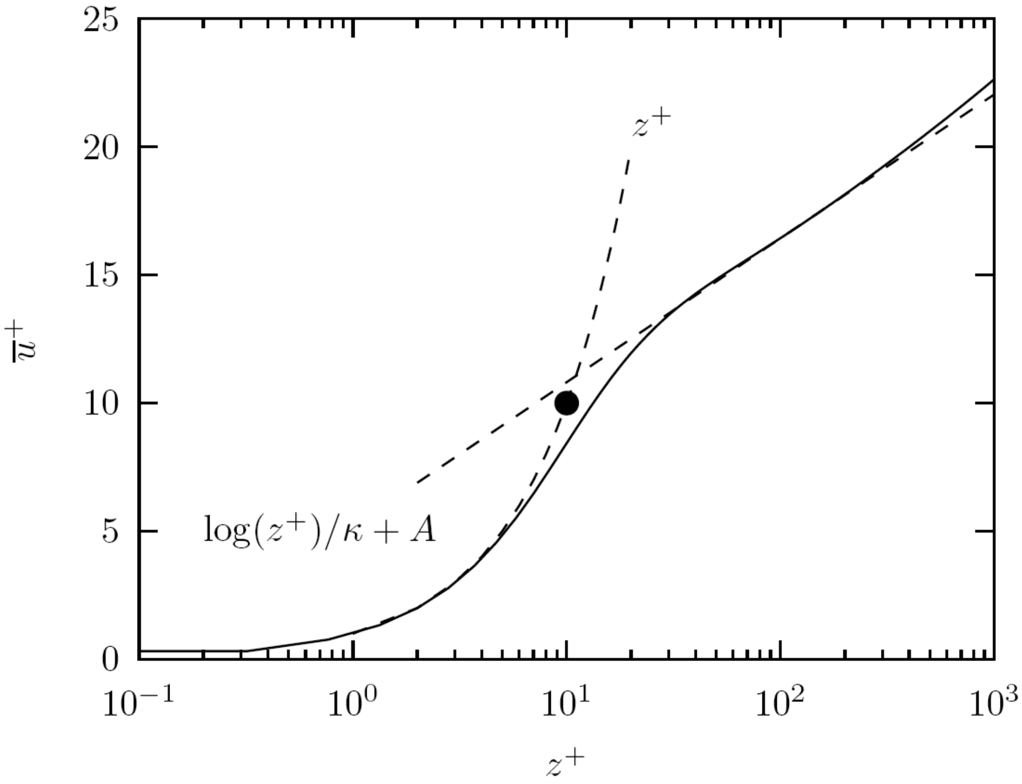

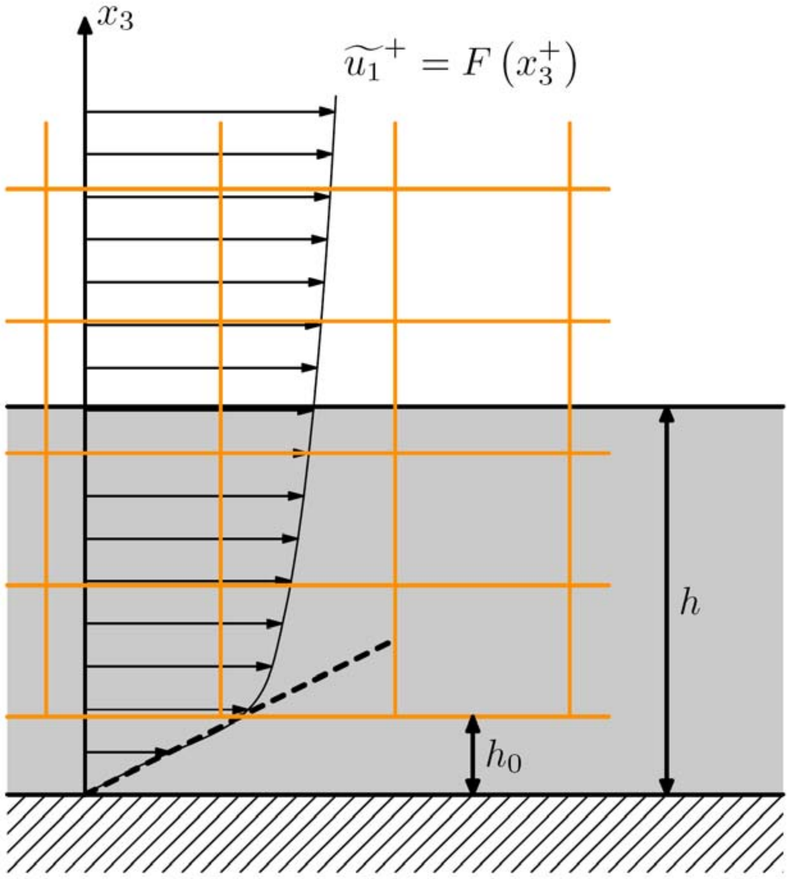

Extended stretched-vortex SGS model

LES decomposition

$$u_i\left(\mathbf{x},t\right)=\widetilde{U_i}\left(\mathbf{x},t\right)+U_i\left(\mathbf{x},t\right)$$

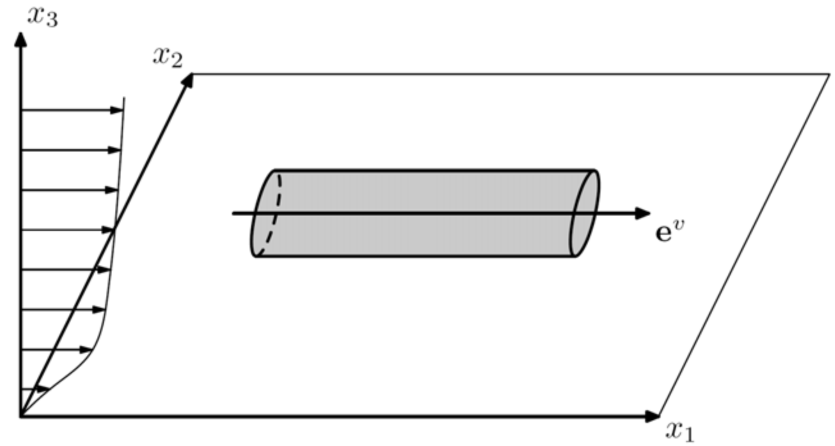

Dynamic alignment of subgrid vortices

$$\frac{\partial e_i^v}{\partial t}=e_j^v\frac{\partial\widetilde{U_i}}{\partial x_j}-e_i^v e_k^v e_j^v\frac{\partial\widetilde{U_k}}{\partial x_j}$$

Additional stresses from subgrid stretched-vortex wrapping axial velocity.

Pullin, D. I. & Lundgren, T. S. 2001 Axial motion and scalar transport in stretched spiral vortices. Phys. Fluids 13 (9), 2553-2563.

$$\begin{aligned}T_{ij}&=\widetilde{U_iU_j}+\widetilde{U_i\widetilde{U_j}}+\widetilde{\widetilde{U_i}U_j}\\&=K\left(\delta_{ij}-e_i^ve_j^v\right)-\gamma\frac{1}{2}\Delta_cK^{1/2}\left(e_j^ve_k^v\frac{\partial\widetilde{U_k}}{\partial x_l}\left(\delta_{li}-e_l^ve_i^v\right)+e_i^ve_k^v\frac{\partial\widetilde{U_k}}{\partial x_l}\left(\delta_{lj}-e_l^ve_j^v\right)\right)\end{aligned}$$

$$\left(e_1^v,e_2^v,e_3^v\right)=\left(1,0,0\right)\quad\Rightarrow\quad T_{13}=-\gamma\frac{1}{2}\Delta_cK^{1/2}\frac{\partial\widetilde{U_1}}{\partial x_3}$$

LES coupled to wall closure

1) Time march local shear stress equation.

$$\frac{\partial u_0'}{\partial t} = \frac{2\,u_0'}{\left(\widetilde{u_1}\right)_{x_3=h}}\left(-\frac{1}{h}\widetilde{u_3 u_1} - \frac{\partial \widetilde{p}}{\partial x_1} + \frac{\nu}{h}\left[\frac{\partial \widetilde{u_1}}{\partial x_3} - u_0'\right]\right)_{x_3=h}$$

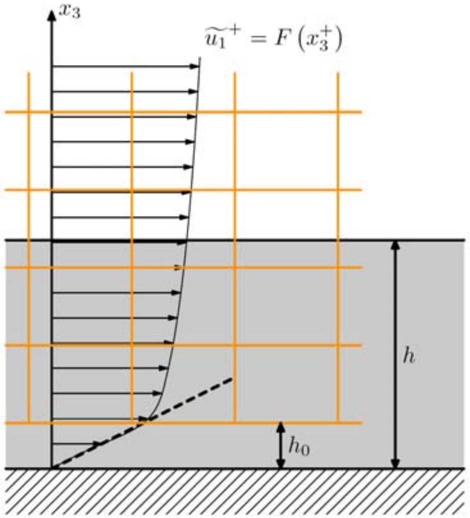

2) Obtain fluctuating slip BC from shear stress.

$$\widetilde{u_1}^+\left(x_1, x_2, h_0, t\right) = F\left(h_0^+\right) = h_0^+, \quad h_0^+ \leq 10$$

3) Time march filtered N-S with extended SGS model.

$$\begin{aligned} T_{ij} &= \widetilde{U_i U_j} + \widetilde{U_i \widetilde{U_j}} + \widetilde{\widetilde{U_i} U_j} \\ &= K\left(\delta_{ij} - e_i^v e_j^v\right) - \gamma \frac{1}{2}\Delta_c K^{1/2}\left(e_j^v e_k^v \frac{\partial \widetilde{U_k}}{\partial x_l}\left(\delta_{li} - e_l^v e_i^v\right) + e_i^v e_k^v \frac{\partial \widetilde{U_k}}{\partial x_l}\left(\delta_{lj} - e_l^v e_j^v\right)\right) \end{aligned}$$

4) Time march dynamic subgrid vortex alignment model.

$$\frac{\partial e_i^v}{\partial t} = e_j^v \frac{\partial \widetilde{U_i}}{\partial x_j} - e_i^v e_k^v e_j^v \frac{\partial \widetilde{U_k}}{\partial x_j}$$

Results (Re_{tau} = 600 to 60k)

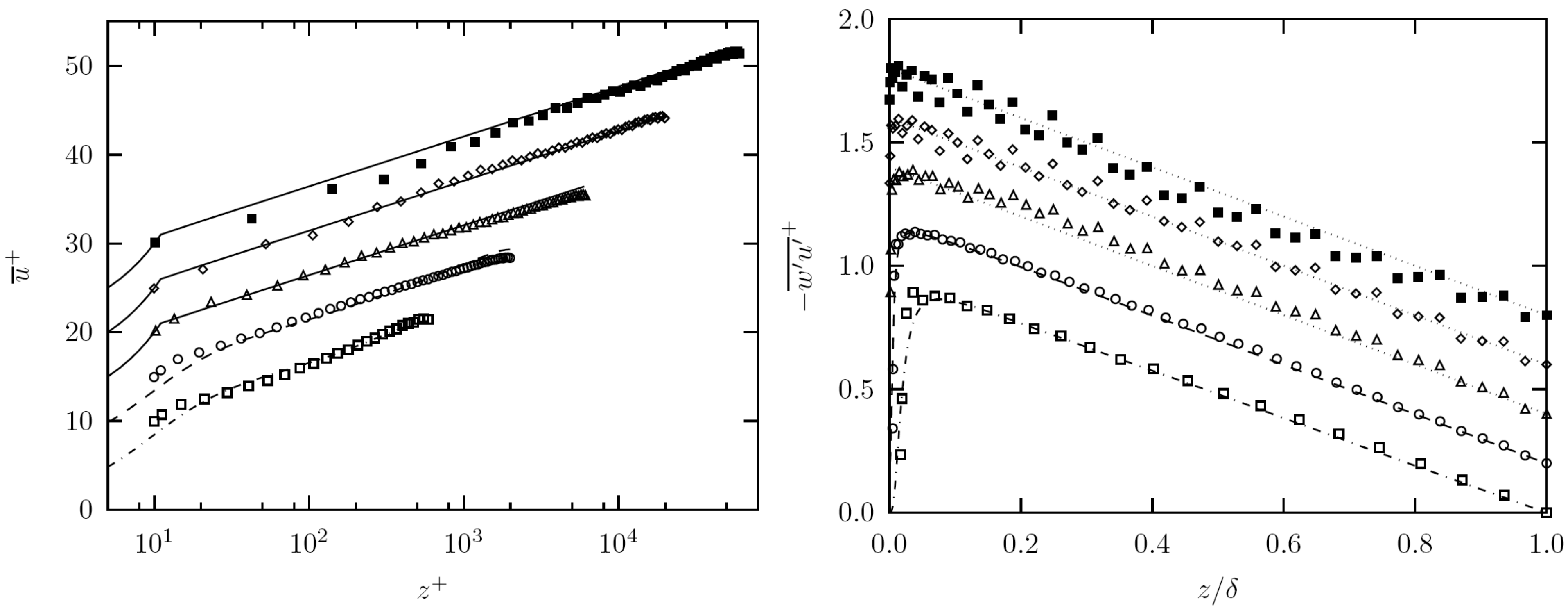

	$\mathrm{Re}_\tau = u_\tau\delta/\nu$	$\mathrm{Re} = u_{\mathrm{CL}}\delta/\nu$		$N_1 \times N_2 \times N_3$	$L_1 \times L_2$
———			$\log(z^+)/0.41 + 5.2$		
········			$1 - z/\delta$		
—·—	5.9×10^2	1.2×10^4	DNS (Moser *et al.*1999)	$384 \times 384 \times 257$	$2\pi\delta \times \pi\delta$
– – –	2.0×10^3	4.9×10^4	DNS (Hoyas & Jiménez 2006)	$6144 \times 4608 \times 633$	$8\pi\delta \times 3\pi\delta$
□	5.9×10^2	1.2×10^4	LES	$32 \times 32 \times 33$	$8\pi\delta \times 3\pi\delta$
○	2.0×10^3	4.9×10^4	LES	$64 \times 64 \times 65$	$8\pi\delta \times 3\pi\delta$
△	6.0×10^3	1.6×10^5	LES	$64 \times 64 \times 65$	$8\pi\delta \times 3\pi\delta$
◇	2.0×10^4	5.9×10^5	LES	$64 \times 64 \times 65$	$8\pi\delta \times 3\pi\delta$
■	6.0×10^4	1.9×10^6	LES	$64 \times 64 \times 65$	$8\pi\delta \times 3\pi\delta$

Reynolds stresses

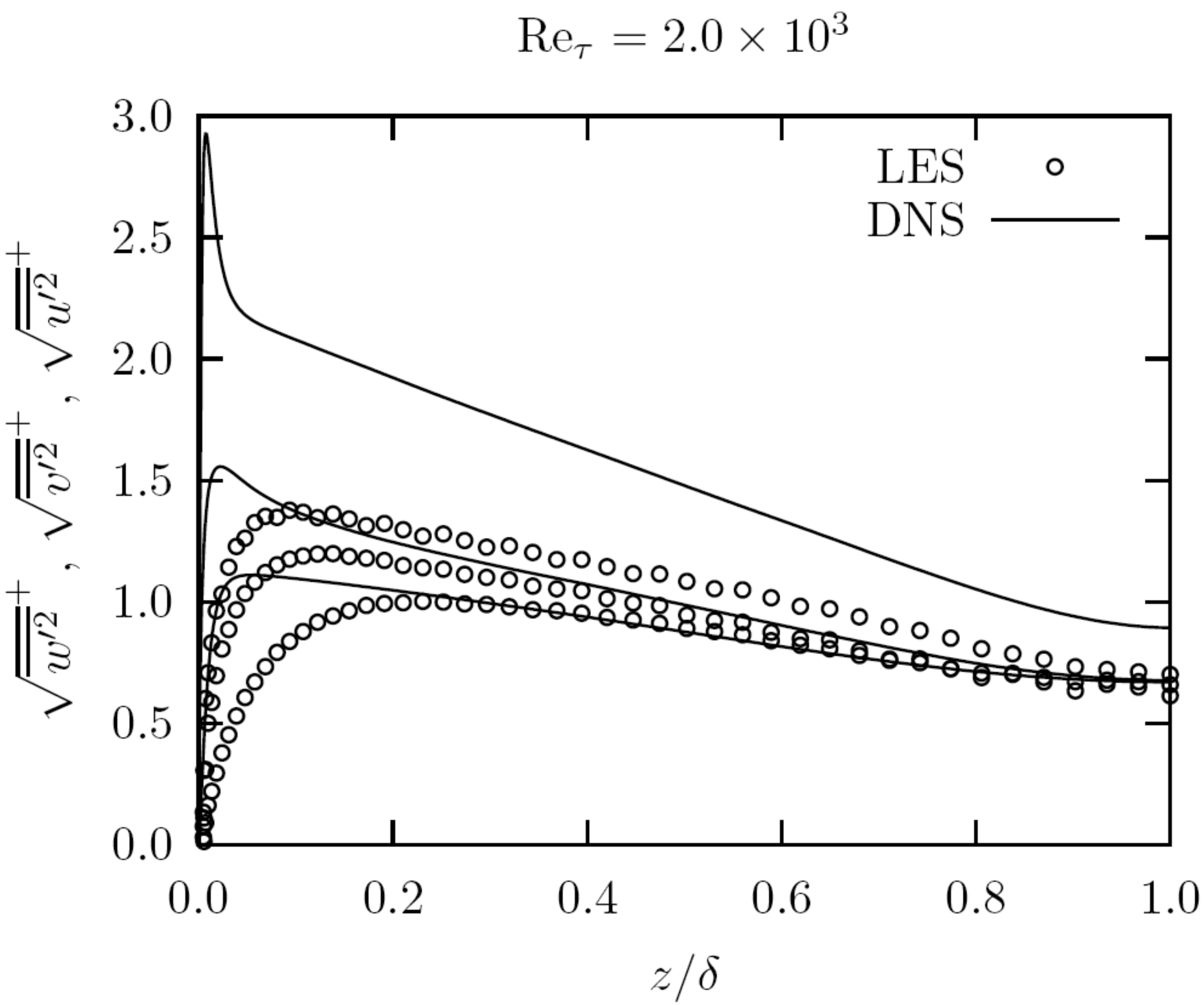

Future work

- Higher Reynolds number.
- Dynamic gamma from structure function matching.
- Application to flow over airfoil.
- Two-vortex SGS model to improve Reynolds stresses.
- Plug for related presentation:

LES of turbulent channel flow; virtual wall model

- LES of turbulent channel flow
- Turbulent flow between two parallel plates driven by pressure gradient
  - *Flow contains many features of complex wall-bounded flows*
  - *Viscous sublayer, stream-wise vortices, log layer*
- Stringent test of SGS/LES model for wall-bounded turbulence
- SGS model must accurately model turbulent transport processes
- Near-wall LES; frontier problem in present research
- Special ``virtual-wall'' near-wall SGS model
- Allow LES of wall bounded flows at large Re_tau =20,000; Re_U = 650,000
- Comparison with DNS;
- Re_tau = 590 (Moser et al, 1999
- Re_tau =2000(Hoyas et al, 2006)

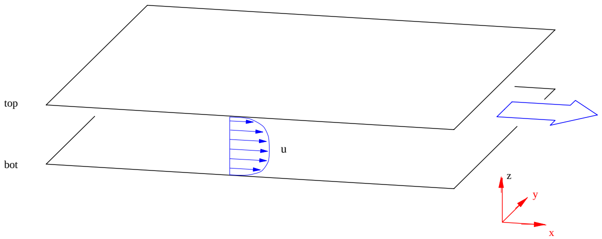

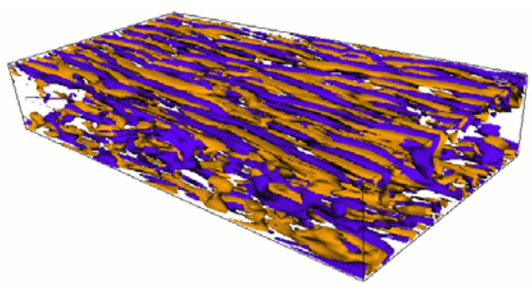

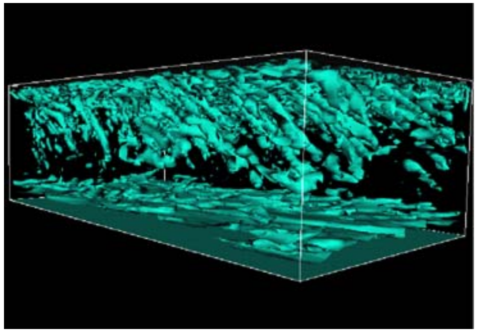

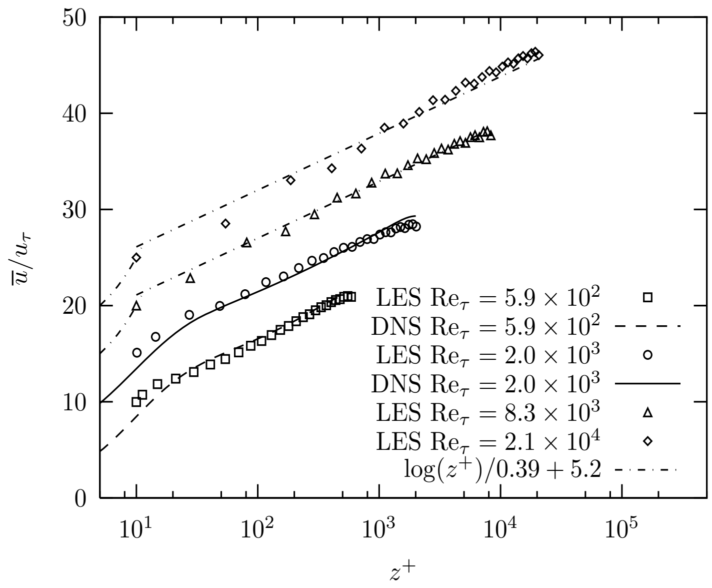

Summary

- LES methodology
  - *Two-component Favre-filtered Navier-Stokes equations*
  - *Stretched-vortex subgrid-scale (SGS) model; strucure based*

- Computational method: hybrid WENO-TCD
  - *Shock capturing low nunmerical dissipation*
  - *Verification*
    - *Decaying compressible turbulence*
    - *Riemann 1D wave (Exact Euler)*

- Large-eddy simulation of Richtmyer-Meshkov instability with reshock
  - *RM instability in plane channel with end wall; Air-SF6*
  - *Modeled on experiments of Vetter & Sturtevant (1995)*

- Traditional Statistics
  - *Mixing-layer growth*
  - *Turbulence statistics, velocity, density & scalar spectra*

- “Multi-scale modeling”
  - *Subgrid continuation statistics; spectra and anisotropy*
  - *Scalar p.d.f.s, including subgrid contribution*
  - *Effect of Schmidt number*

- Adaptive Mesh Refinement (AMROC)
  - *Berger & Colella’s algorithm for conservation laws*
  - *Hierarchical data structure*
  - *WENO-TCD and stretched-vortex SGS model implemented*

Conclusions

- Large-eddy simulation of plane Richtmyer-Meshkov instability with reshock
  - *Hybrid WENO-TCD scheme with SV SGS model*
  - *Air-SF6; modeled on experiments of Vetter & Sturtevant (1995)*
- Growth of mixing-layer width
  - *Initial linear growth of interface following first shock impact*
  - *Period of nonlinear bubble/spike growth*
  - *Reshock produces rapid transition to turbulent mixing layer*
  - *Strong mixing layer growth*
  - *Enhanced by interaction with reflected expansion*
  - *Eventual saturation of growth*
- Traditional Statistics
  - *Mixing-layer growth*
  - *turbulence statistics, velocity, density & scalar spectra*
- "Multi-scale modeling"
  - *SV SGS model provides basis for subgrid continuation statistics; spectra and anisotropy*
  - *Scalar p.d.f.s, including subgrid contribution*
  - *log-dependence of scalar p.d.f. on Schmidt number*

Reynolds number and integral length

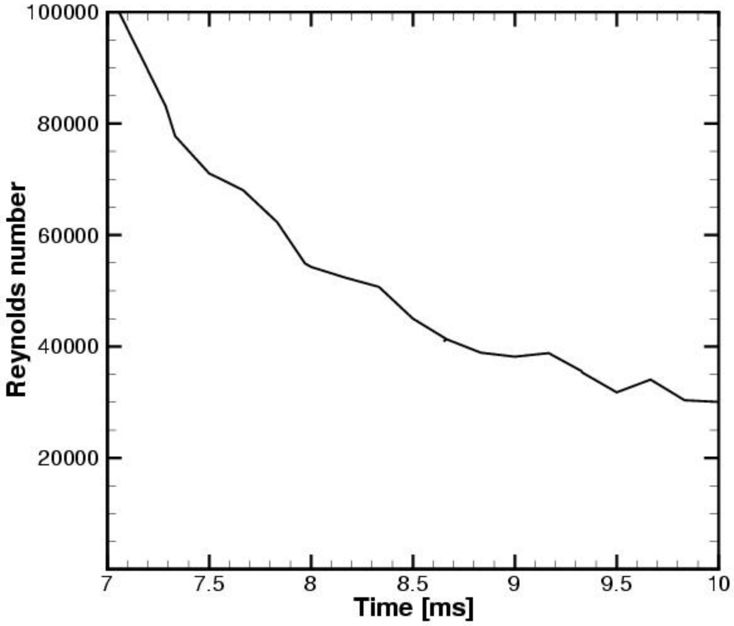

Decay on Reynolds number

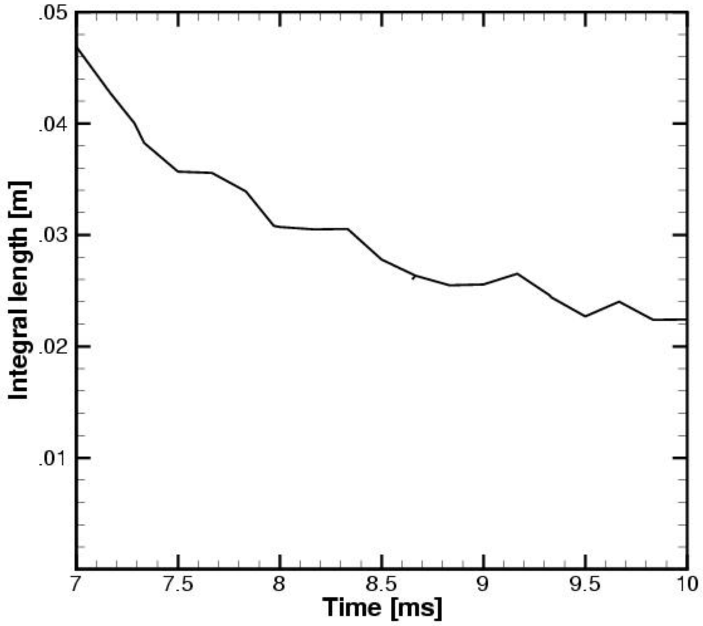

Decay of integral length

Scalar spectrum from stretched-spiral vortex

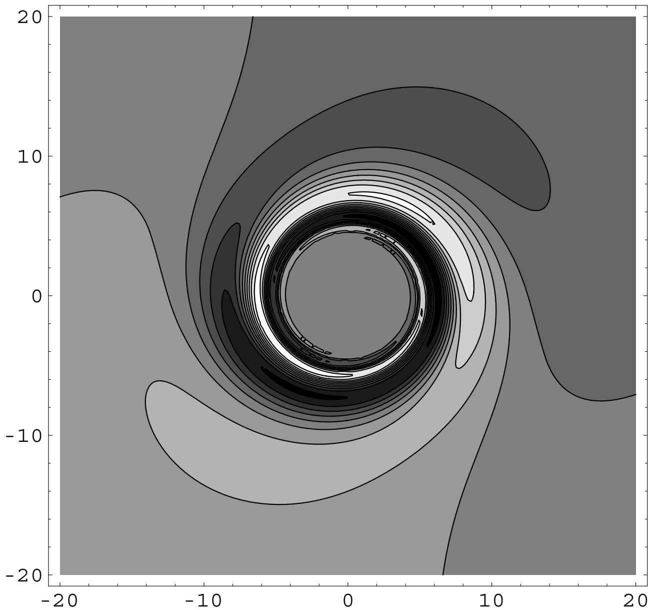

Schematic showing winding of scalar field by `subgrid vortex'. Contours of passive scalar

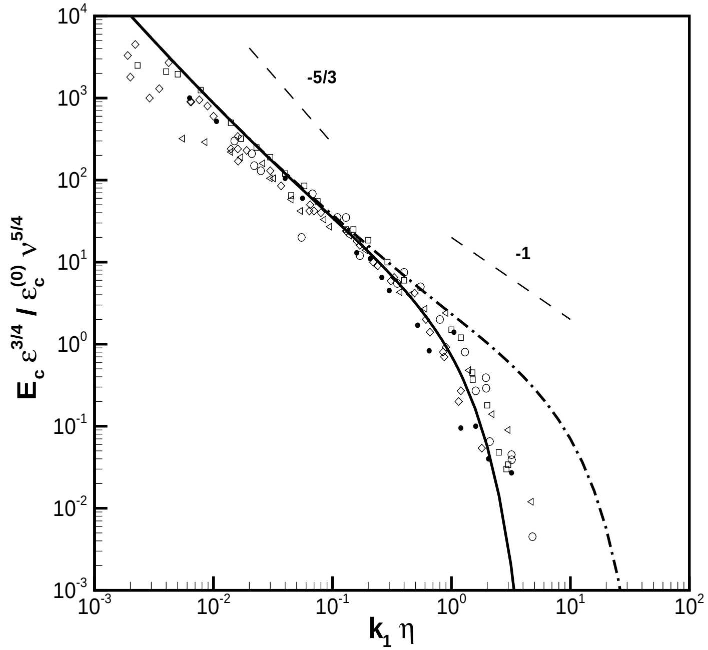

1-D scalar spectrum for homogeneous turbulence,Pullin & Lundgren (2001)

______ Sc = 7, ------- Sc = 700. Symbols, Data

(Gibson & Schwarz 1963)

Numerical algorithm (D. Hill, C. Pantano)

- WENO-TCD hybrid method (Hill & Pullin, JCP, 2004)
  - *Tuned-Centered Difference (TCD); away from shocks exploit smoothness of flow*
  - *Order of accuracy traded for minimization of one-step truncation error in LES equations (Ghosal, 1995)*
  - *5-point stencil -> 2-nd order accuracy*
  - *At shocks (only) revert to full WENO*
  - *Optimal WENO stencil matched to TCD stencil*
- Flux-based finite difference
  - *Naturally integrated in AMROC*
  - *Conservative, skew-symmetri*
- Skew-symmetric
  - *Energy conserving*
  - *Satisfies summation-by-parts*
- Tested in 1D, 2D, 3D
  - *Decaying compressible turbulence*
- No explicit filtering

Riemann 1D Wave

Exact solution of 1D Euler

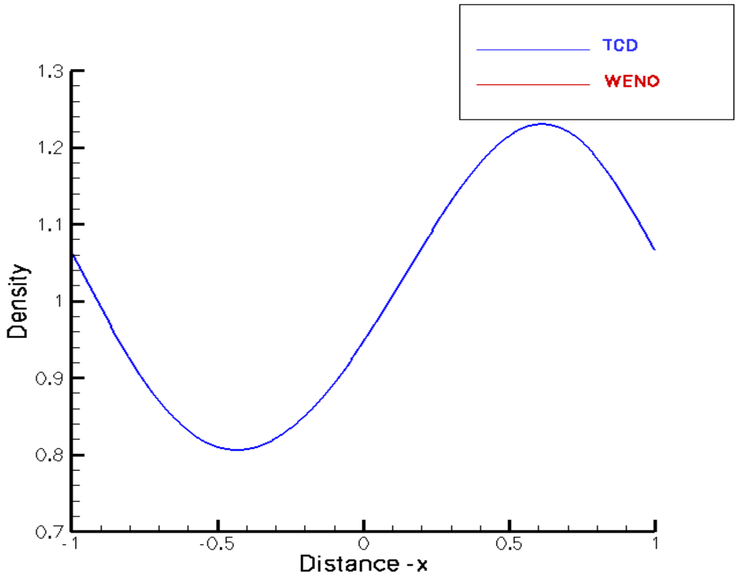

Idea: Improve K(k) for center-difference

- Finite-difference operator

$$\mathbf{D}f(x) = \frac{1}{\Delta x} \sum_{j=-3}^{j=3} d_j \left[f(x + j\,\Delta x) - f(x - j\,\Delta x) \right]$$

$$d_1 = \frac{2}{3}, \quad d_2 = -\frac{1}{12}, \quad d_3 = 0, \quad \to 5-pt,\ 4^{th}\text{order}$$

$$d_1 = \frac{3}{4}, \quad d_2 = -\frac{1}{10}, \quad d_3 = -1/2, \to 7-pt,\ 6^{th}\text{order}$$

- Tuned 5-point with parameter α

$$d_1 = \frac{1}{2} - 2\alpha, \quad d_2 = \alpha, \quad d_3 = 0, \to 5-pt,\ 2^{nd}\text{ order}$$

- Tuned 7-point with parameter α

$$d_1 = \frac{2}{3} + \alpha, \quad d_2 = -\frac{1}{12} - 4\alpha, \quad d_3 = \alpha, \to 7-pt,\ 4^{th}\text{ order}$$

Performance for LES of decaying turbulence

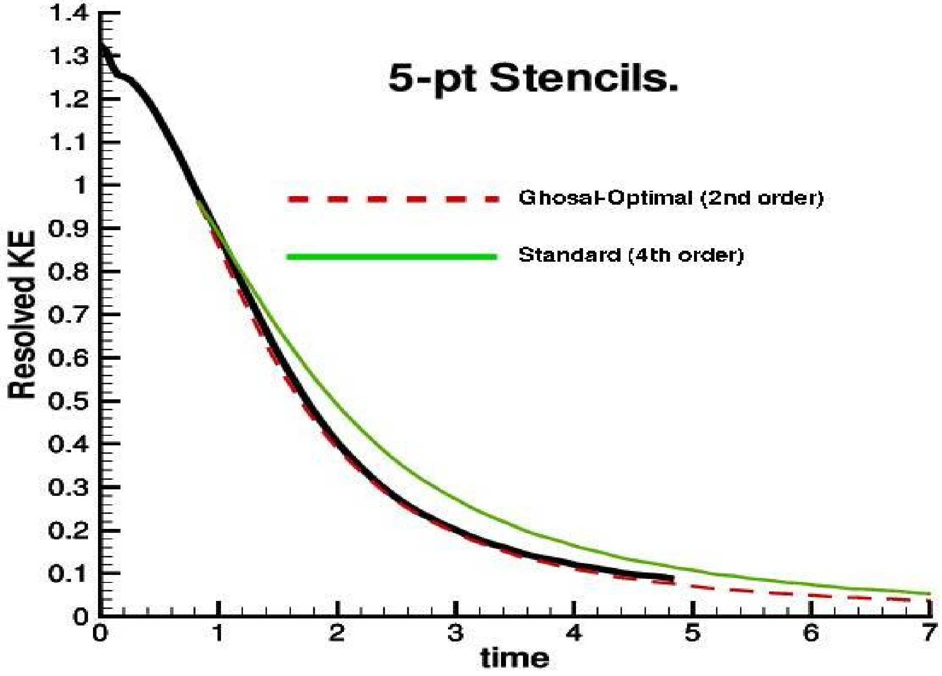

DNS and LES of Decaying compressible turbulence, M_t =0.488, R_lambda = 70.

Decay of total TKE. Black; 256^3 DNS (10-th order Pade)

Numerical algorithm (D. Hill, C. Pantano)

- WENO-TCD hybrid method (Hill & Pullin, JCP, 2004)
  - *Tuned-Centered Difference (TCD); away from shocks exploit smoothness of flow*
  - *Order of accuracy traded for minimization of one-step truncation error in LES equations (Ghosal, 1995)*
  - *5-point stencil -> 2-nd order accuracy*
  - *At shocks (only) revert to full WENO*
  - *Optimal WENO stencil matched to TCD stencil*
- Flux-based finite difference
  - *Naturally integrated in AMROC*
  - *Conservative, skew-symmetri*
- Skew-symmetric
  - *Energy conserving*
  - *Satisfies summation-by-parts*
- Tested in 1D, 2D, 3D
  - *Decaying compressible turbulence*
- No explicit filtering

Riemann 1D Wave

Exact solution of 1D Euler

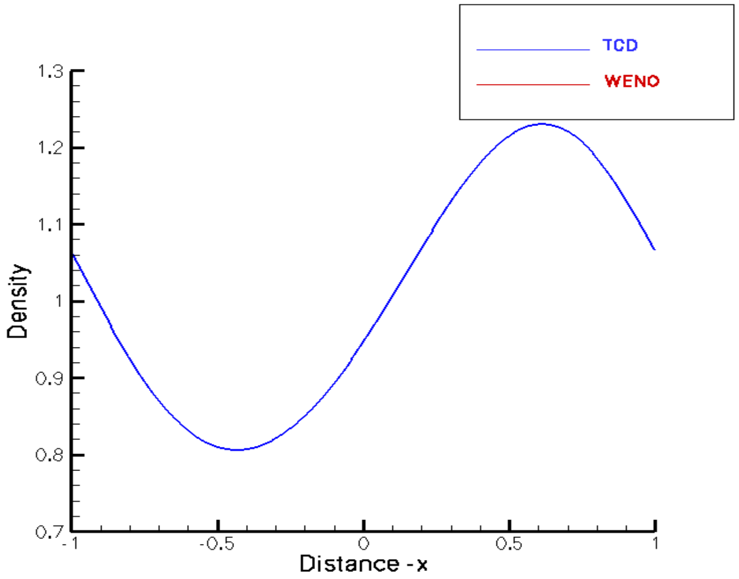

Conservation and time adaptation

- Hanging nodes exist because cells at different levels are logically conforming
- A special correction, fixup, must be applied to satisfy global conservation
- Fluxes at coarse cells next to fine cells are replaced by the sum of those fluxes at the fine cells

$$\delta \boldsymbol{F}^{1,l+1}_{i-\frac{1}{2},j} := \delta \boldsymbol{F}^{1,l+1}_{i-\frac{1}{2},j} + \frac{1}{r^2_{l+1}} \sum_{m=0}^{r_{l+1}-1} \boldsymbol{F}^{1,l+1}_{v+\frac{1}{2},w+m}(t + \kappa \Delta t_{l+1})$$

- This correction impacts the spatial as well as temporal integration scheme

$$\check{\boldsymbol{Q}}^{n+1}_{ij} := \boldsymbol{Q}^{n+1}_{ij} + \frac{\Delta t_l}{\Delta x_{1,l}} \delta \boldsymbol{F}^{1,l+1}_{i-\frac{1}{2},j}$$

- Ghost cell values of fine patches are obtained by linear time interpolation from the coarse patch solution

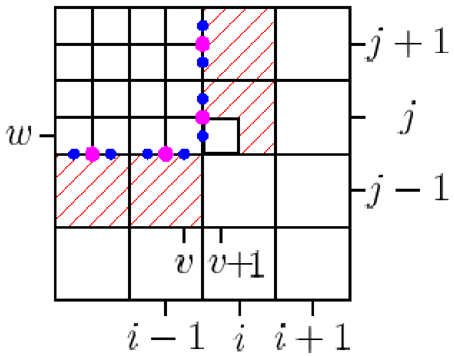

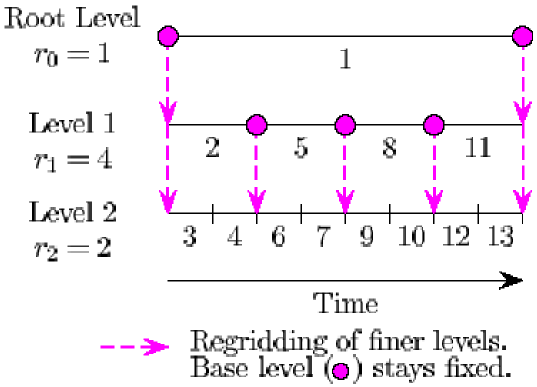

LES in the absence of strong shocks and density contacts

- The nonlinear term $\dfrac{\partial}{\partial x_i}\left(\rho u_i u_j\right)$ is responsible primarily for the energy cascade
- The most successful Eulerian methods are global
  - *Spectral*
  - *High-Order Pade*

- Good response across all (*spectral*) or most (*Pade*) of the resolved scales, I.e. modified wavenumber

$$\boldsymbol{F}(\partial / \partial x) = ik \qquad \boldsymbol{F}\left(D_x\right) = i\widehat{K}(k)$$

- Limitations of spectral methods:
  - *global nature results in (fatal?) ringing at discontinuities like shocks and contacts*
  - *Limited to simple geometries*

Conservation and time adaptation

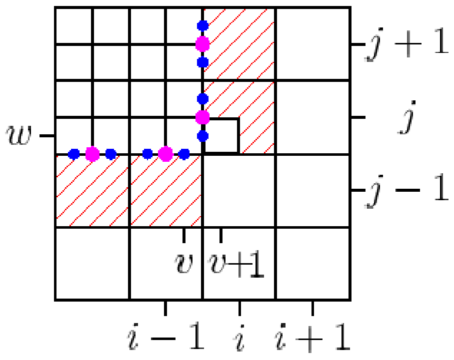

- Hanging nodes exist because cells at different levels are logically conforming
- A special correction, fixup, must be applied to satisfy global conservation
- Fluxes at coarse cells next to fine cells are replaced by the sum of those fluxes at the fine cells

$$\delta \boldsymbol{F}^{1,l+1}_{i-\frac{1}{2},j} := \delta \boldsymbol{F}^{1,l+1}_{i-\frac{1}{2},j} + \frac{1}{r^2_{l+1}} \sum_{m=0}^{r_{l+1}-1} \boldsymbol{F}^{1,l+1}_{v+\frac{1}{2},w+m}(t+\kappa\Delta t_{l+1})$$

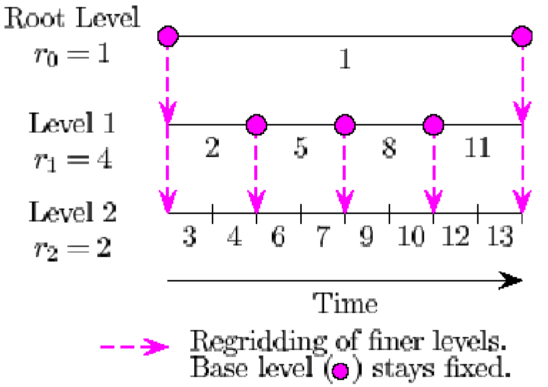

- This correction impacts the spatial as well as temporal integration scheme

$$\check{\boldsymbol{Q}}^{n+1}_{ij} := \boldsymbol{Q}^{n+1}_{ij} + \frac{\Delta t_l}{\Delta x_{1,l}} \, \delta \boldsymbol{F}^{1,l+1}_{i-\frac{1}{2},j}$$

- Ghost cell values of fine patches are obtained by linear time interpolation from the coarse patch solution

Idea: Improve K(k) for center-difference

- Finite-difference operator

$$\mathbf{D}f(x) = \frac{1}{\Delta x}\sum_{j=-3}^{j=3} d_j\,[f(x+j\,\Delta x) - f(x - j\,\Delta x)]$$

$$d_1 = \frac{2}{3},\quad d_2 = -\frac{1}{12},\quad d_3 = 0, \quad \rightarrow 5-pt,\; 4^{th}\text{order}$$

$$d_1 = \frac{3}{4},\quad d_2 = -\frac{1}{10},\quad d_3 = -1/2,\; \rightarrow 7-pt,\; 6^{th}\text{order}$$

- Tuned 5-point with parameter α

$$d_1 = \frac{1}{2} - 2\alpha,\quad d_2 = \alpha,\quad d_3 = 0,\; \rightarrow 5-pt,\; 2^{nd}\text{ order}$$

- Tuned 7-point with parameter α

$$d_1 = \frac{2}{3} + \alpha,\quad d_2 = -\frac{1}{12} - 4\alpha,\quad d_3 = \alpha,\; \rightarrow 7-pt,\; 4^{th}\text{ order}$$

Tuned Center-Difference Stencil (TCD)

- Error in resolved-scale energy spectrum produced by one step of Navier-Stokes equations using given discretization; Ghosal (1996)
- Asssume –
  - *Von-Karman energy spectrum*
  - *Joint normal velocty pdf*

- $\mathcal{E}^{(\mathrm{FD})}(\kappa, \tilde{\kappa}(\kappa, \alpha))$ is spectrum of truncation error for numerical method with modified wavenumber behavior $\tilde{\kappa}(\kappa, \alpha)$

- Define total discretization error;

$$\mathrm{E}_G(\alpha) = \int_0^{\frac{\pi}{\Delta x}} \mathcal{E}^{(\mathrm{FD})}(\kappa, \tilde{\kappa}(\kappa, \alpha)) d\kappa$$

Optimized 5-point TCD stencil (second order)

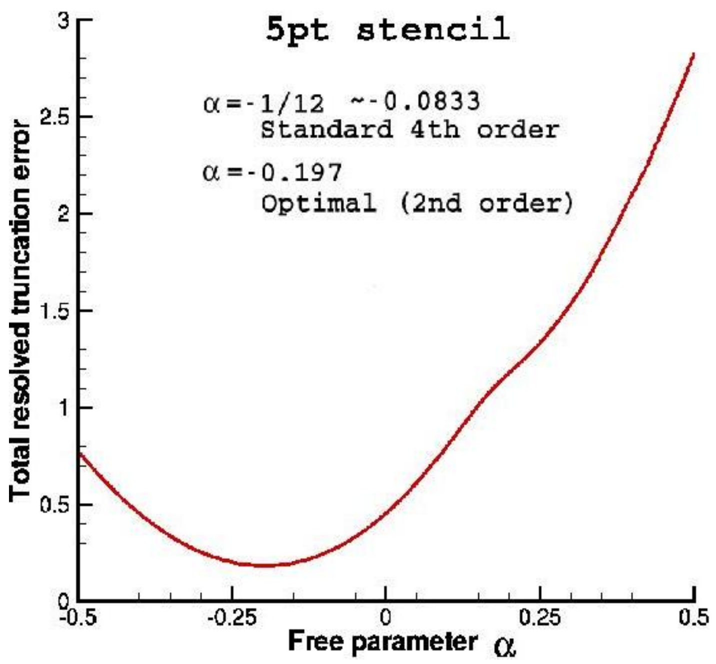

Truncation error

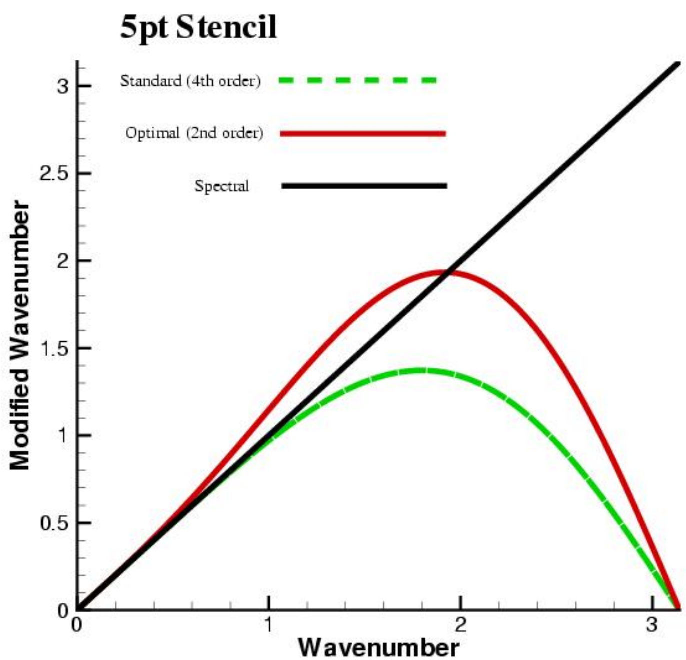

Modified wavenumber of minimal error stencil

Shock capturing solvers; WENO

- True shocks have a thickness on the mean free path order
- The shocks are not resolved: Euler equations are solved in conservative form
- Euler solver shocks are ‘captured’, I.e. smeared across a few cells – first-order accurate at shocks

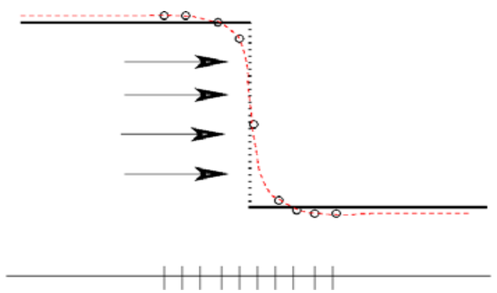

$$\frac{d\mathbf{q}}{dt} + \frac{\partial \mathbf{F}(\mathbf{q})}{\partial x} + \frac{\partial \mathbf{G}(\mathbf{q})}{\partial y} + \frac{\partial \mathbf{H}(\mathbf{q})}{\partial z} = 0$$

$$\mathbf{q} = \left(\rho, \rho u, \rho v, \rho w, E\right)^T$$

$$\mathbf{F}(\mathbf{q}) = \begin{pmatrix} \rho u \\ \rho u^2 + P \\ \rho u v \\ \rho u w \\ \rho u(E+P) \end{pmatrix}$$

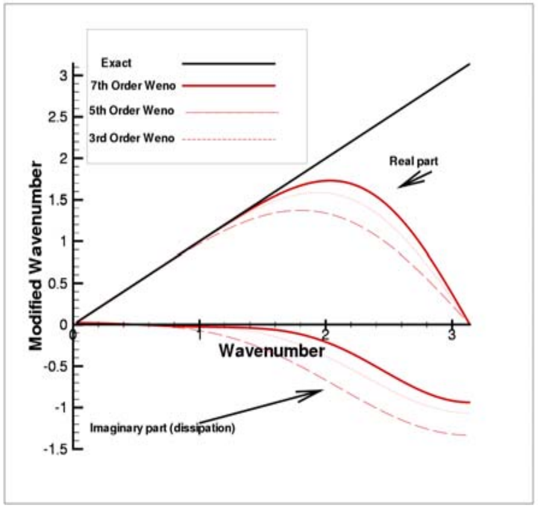

Weighted Essentially Non-Oscillatory (WENO) method (Osher)

Hybrid WENO-TCDS algorithm: LES and strong shocks (D. Hill)

- Hybrid technique: blending Weighted Essentially Non-Oscillatory (WENO) scheme with Tuned Centered-Difference (TCD) stencil.
- WENO in regions of very-large density ratio (Shocks)
  - *But WENO is not suitable for LES in smooth regions away from shocks.*
  - *Upwinding strategy is too dissipative*
- TCD stencil in smooth regions away from shocks
  - *Low numerical dissipation (centered method)*
  - *optimized for minimum resolved-scale discretization error in LES (Ghosal, 1996)*
  - *5- or 7-point stencil trades off formal order of accuracy for small dispersion errors*
- Target WENO stencil = TCD stencil
- In practice, target TCD stencil not always achieved; switch is used based on acceptable WENO smoothness measure
- Hybrid method designed for LES in presence of strong shocks

Cylindrical RM instability with AMROC (R.Deiterding)

- AMROC – Adaptive Mesh Refinement engine
- Exploratory 2D Richtmyer-Meshkov instability with reshock in wedge geometry
- Passage of the shock results in vorticity deposition by means of baroclinic generation
- Canonical model of phase 2 experiments
- Incident shock modeled by Chisnell (1998) approximation to Guderley solution for similarity shock
- Euler simulation
- Initial density interface ; sinusoidal perturbation corresponding to n = 24 on circle

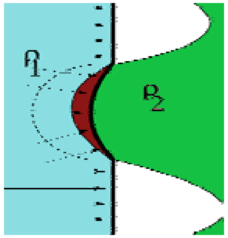

Schlieren

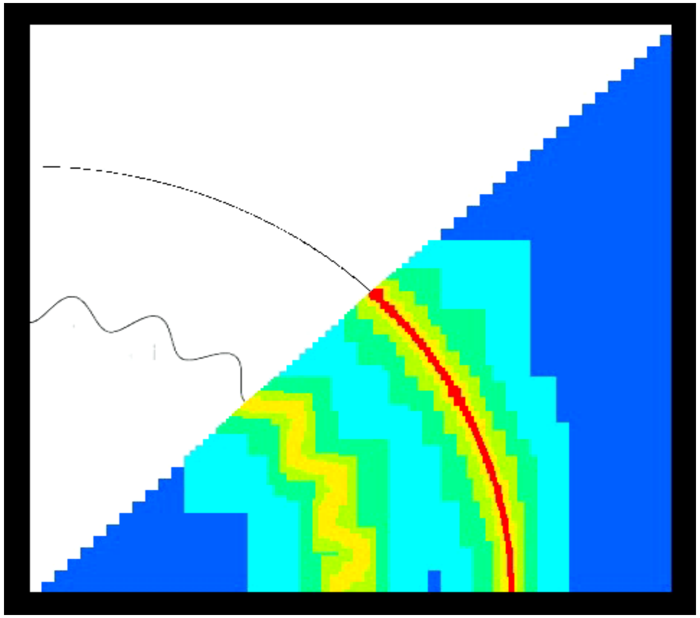

Refinement

Scalar

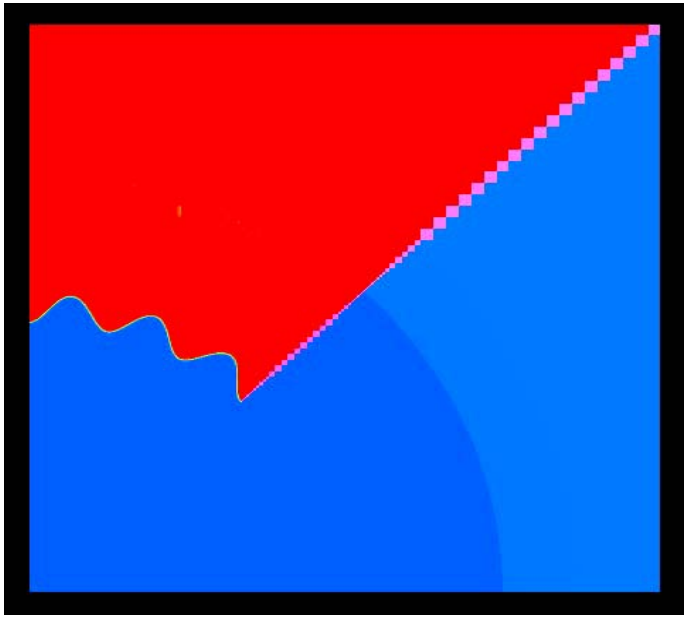

Pressure

Reacting Hydrogen Jet flame (C. Pantano)

- Planar hydrogen jet flame of Rehm & Clemens (1999), Mach=0.28
- 5 10^6 grid cells and 4 levels of refinement
- 128 processors at LLNL ALC, 50,000 cpu/hours
- Cantera chemistry solver by D. Goodwin for flamelet model

experiment

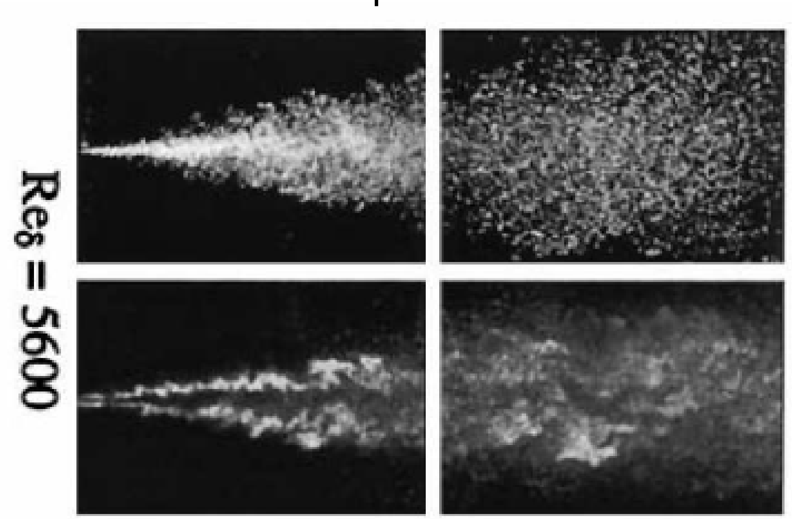

simulation